Institute of Soil Science and Land Evaluation
University of Hohenheim
Soil Biology
Prof. Dr. Ellen Kandeler

Biological Regulation of Subsoil C-cycling

Dissertation

Submitted in fulfilment of the requirements for the degree

“Doktor der Agrarwissenschaften”

(Dr. sc. agr. / Ph.D. in Agricultural Sciences)

to the

Faculty of Agricultural Sciences

presented by

Sebastian Preußer

Duisburg

2019

This thesis was accepted as a doctoral dissertation in fulfilment of the requirements for the degree “Doktor der Agrarwissenschaften” (Dr. sc. agr. / Ph.D. in Agricultural Sciences) by the Faculty of Agricultural Sciences at the University of Hohenheim, Germany on: 12.12.2018

Date of oral examination: 10.05.2019

Examination committee

Supervisor and Reviewer: Prof. Dr. Ellen Kandeler
Co-reviewer: Prof. Dr. Georg Guggenberger
Additional Examiner: Prof. Dr. Georg Cadisch
Head of Committee: Prof. Dr. Markus Rodehutscord

This thesis was conducted at the Institute of Soil Science and Land Evaluation of the University of Hohenheim and funded by the Deutsche Forschungsgemeinschaft (DFG) in the research group FOR 1806 SUBSOM “The Forgotten Part of Carbon Cycling: Organic Matter Storage and Turnover in Subsoils”.

Table of Contents

List of Figures I

List of Tables IV

List of Supplementary Material V

1 Summary 1

2 Zusammenfassung 4

3 General Introduction 7

3.1 Soil as carbon reservoir 7

3.2 Deep soil – source or sink for carbon? 8

3.3 Microbial biomass, community composition and activity with soil depth 11

3.4 Changing habitat conditions and microbial SOM decomposition 14

3.5 Stable isotopes in the research of soil carbon dynamics 16

4 Objectives 19

5 Microbial community response to changes in substrate availability and habitat conditions in a reciprocal subsoil transfer experiment 22

5.1 Introduction 24

5.2 Materials and methods 26

5.3 Results 34

5.4 Discussion 47

5.5 Conclusion 56

5.6 Acknowledgements 57

5.7 Supplementary materials 58

6 Fungi and bacteria respond differently to changing habitat conditions within a soil profile 64
6.1 Introduction 66
6.2 Materials and methods 70
6.3 Results 78
6.4 Discussion 88
6.5 Conclusion 95
6.6 Acknowledgements 96
6.7 Supplementary materials 97
7 Multiple exchange processes on mineral surfaces control the transport of dissolved organic matter through soil profiles 107
7.1 Introduction 109
7.2 Materials and methods 112
7.3 Results 124
7.4 Discussion 134
7.5 Conclusion 141
7.6 Acknowledgements 142
7.7 Supplementary materials 143
8 General Discussion 149
9 Final Conclusions and Perspectives 158
10 References 161
Curriculum vitae 180
Publications, Presentations and Supervisions 182
Acknowledgements 186
Eidesstattliche Erklärung 188

List of Figures

Figure 5.1 Exemplary front view of one of nine tree facing profile walls with six soil containers with six different treatments (SUB20 + 0% cellulose, SUB20 + 1% cellulose, SUB20 + 5% cellulose, SUB120 + 0% cellulose, SUB120 + 1% cellulose and SUB120 + 5% cellulose) randomly incorporated into both soil depths (20 cm and 120 cm). Due to the randomized distribution of the different containers in the two depths of each of the nine profile pits this is an exemplary incorporation pattern to illustrate the incorporation design. 29

Figure 5.2 Amount of extractable organic carbon (EOC) (a and c) and extractable total nitrogen (ETN) (b and d) in SUB20 and SUB120 samples under different translocation and cellulose addition treatments at the sampling dates July 2013, October 2013 and June 2014. Error bars indicate standard deviation (n=3). 35

Figure 5.3 Microbial biomass C (a and c) and relative incorporation of ^{13}C-cellulose-derived C into C_{mic} (b and d) in SUB20 and SUB120 samples under different translocation and cellulose addition treatments at the sampling dates July 2013, October 2013 and June 2014. Error bars indicate standard deviation (n=3). 37

Figure 5.4 Abundance of gram-positive bacteria ($PLFA_{gram+}$), gram-negative bacteria ($PLFA_{gram-}$) and fungi ($PLFA_{fungi}$) in SUB20 (a, b, c) and SUB120 (d, e, f) samples under different translocation and cellulose addition treatments at the sampling dates July 2013, October 2013 and June 2014. Error bars indicate standard deviation (n=3). 40

Figure 5.5 Relative incorporation of ^{13}C-cellulose-derived C into gram-positive bacteria ($PLFA_{gram+}$), gram-negative bacteria ($PLFA_{gram-}$) and fungi ($PLFA_{fungi}$) in SUB20 (a, b, c) and SUB120 (d, e, f) samples under different translocation and cellulose addition treatments at the sampling dates July 2013, October 2013 and June 2014. Error bars indicate standard deviation (n=3). 41

Figure 5.6 Amount of ergosterol in SUB20 (a) and SUB120 (b) samples under different translocation and cellulose addition treatments at the sampling dates July 2013, October 2013 and June 2014. Error bars indicate standard deviation (n=3). 43

Figure 5.7 Bacterial community structures indicated by relative abundance (%) of the different bacterial taxa in SUB20 (a, b, c) and SUB120 (d, e, f) samples under different translocation and cellulose addition treatments at the sampling dates July 2013, October 2013 and June 2014...... 45

Figure 6.1 Mean daily (a) soil temperatures (°C) and (b) soil water content (%) from June 1, 2014 to June 31, 2015 at six different soil depths (10 cm, 30 cm, 50 cm, 90 cm, 150 cm and 180 cm) at the field site. 71

Figure 6.2 Amount of extractable organic carbon (EOC, a and c) and microbial biomass C (C_{mic}, b and d) in TOP5 and SUB110 samples under different translocation and root addition treatments for the sampling dates September 2014, December 2014, March 2015 and June 2015. Error bars indicate standard error (n=3). The figure shows significant effects with respective P-values. A = root addition, T = translocation, D = sampling date.. 80

Figure 6.3 Relative incorporation (%) of ^{13}C-root-derived C into microbial biomass C ($^{13}C_{mic}$, a and b) and absolute amount of incorporated ^{13}C-root-derived C per g root addition (mg C g^{-1} added ^{13}C roots, c and d) in TOP5 and SUB110 samples under different translocation and root addition treatments for the sampling dates September 2014, December 2014, March 2015 and June 2015. Error bars indicate standard error (n=3). The figure shows significant effects with respective P-values. S = soil origin, A = root addition, T = translocation, D = sampling date..... 82

Figure 6.4 Abundance of gram-positive bacteria ($PLFA_{gram+}$), gram-negative bacteria ($PLFA_{gram-}$), and fungi ($PLFA_{fungi}$) in TOP5 (a, b, c) and SUB110 (d, e, f) samples under different translocation and root addition treatments for the sampling dates September 2014, December 2014, March 2015 and June 2015. Error bars indicate standard error (n=3). The figure shows significant effects with respective P-values. A = root addition, T = translocation, D = sampling date.. 85

Figure 6.5 Relative (%) (a - f) and absolute (mg C g^{-1} ^{13}C root addition) incorporation of ^{13}C-root-derived C into gram-positive bacteria ($PLFA_{gram+}$), gram-negative bacteria ($PLFA_{gram-}$) and fungi ($PLFA_{fungi}$) in TOP5 and SUB110 samples under different translocation and root addition treatments for the sampling dates September 2014, December 2014, March 2015 and June 2015. Error bars indicate standard error (n=3). The figure shows significant effects with respective P-values. S = soil origin, A = root addition, T = translocation, D = sampling date.. 86

Figure 7.1 Experimental setup of the column experiment. The arrows represent the direction of water flow. The dotted arrows represent sampling ports. 115

Figure 7.2 Mean DOC concentrations (mg L^{-1}) and standard deviations of the outflow solution per treatment and depth (4, 30, and 100 cm for the columns with sandy soil and 4, 12, and 26 cm for the columns with silty soil). Abbreviations: SaCG = sandy soil and OM-coated goethite, SaPG = sandy soil and pure goethite, SiCG = silty soil and OM-coated goethite, SiPG = silty soil and pure goethite. Different letters above the error bars indicate significant differences with p-values <0.05. 125

Figure 7.3 Total output DOC (mg) vs. total input DOC (mg) of all experimental treatments. Abbreviations: SaCG = sand and OM-coated goethite, SaPG = sand and pure goethite, SiCG = silt and OM-coated goethite, SiPG = silt and pure goethite. Values above the 1:1 line represent net leaching, whereas values below the 1:1 line represent net retention. Error bars indicate standard deviation. Filled symbols represent columns with OM-coated goethite whereas empty symbols represent columns with pure goethite. 125

Figure 7.4 Mean values of output specific UV-Vis absorbance (SUVA) at 280 nm (L mg C^{-1} cm^{-1}) vs. input SUVA at 280 nm of all experimental variations. Abbreviations: SaCG = sand and OM-coated goethite, SaPG = sand and pure goethite, SiCG = silt and OM-coated goethite, SiPG = silt and pure goethite. Values above the 1:1 line represent increasing SUVA values as a result of sorption / desorption processes, whereas values below the 1:1 line represent decreasing SUVA values. Error bars indicate standard deviation. 126

Figure 7.5 (A) $\delta^{13}C$ value of the outflow solution of the three cascade depths of the columns from both soils. (B) Mean proportion of OM derived from the coated goethite in the outflow solution of the three cascade depths of the columns from the sandy and the silty soils. Error bars indicate standard deviation. Different letters above the error bars indicate significant differences ($p < 0.05$). 127

Figure 7.6 Mean fraction of the newly sorbed solution-derived carbon (SDC; eq. 9) versus the remaining carbon of the initial carbon coating (GDC; eq. 8) on the goethite samples after the column experiment for the sandy soil (4, 30, and 100 cm) and the silty soil (4, 12, and 26 cm), the net carbon exchange (ΔC; eq. 10), and the mobilized carbon (MC; eq. 11) of the respective samples. Standard deviations are given in brackets. 128

Figure 7.7 SEM image of goethite superposing the NanoSIMS image of $^{12}C^{-}$ in red and $^{56}Fe^{16}O^{-}$ in blue. A) Sample from the 4-cm depth compartment of sandy soil; B) Sample from 30-cm depth compartment of sandy soil. Regions of carbon accumulation on the goethite surface identified as regions of interest (ROI) are encircled. The color represents the range of the atom% ^{13}C for the respective ROI: green marks OM with <1.4 atom% ^{13}C (high abundance of newly adsorbed organic matter; low ^{13}C enrichment), white marks OM with 1.4-2.4 atom% ^{13}C (intermediate abundance of newly adsorbed organic matter, intermediate ^{13}C enrichment), and brown marks OM with >2.4 atom% ^{13}C (low abundance of newly adsorbed organic matter, high ^{13}C enrichment). The white line surrounds the mineral surface. 130

Figure 7.8 Results from NanoSIMS measurements of the OM-coated goethite samples from the columns with sandy soil. A) Atom% ^{13}C of the ROIs of the OM-coated goethite before the experiment (G0) and from the three depth compartments with sandy soil after the experiment, as determined by NanoSIMS. For comparison the respective bulk atom% ^{13}C value as calculated from the IRMS measurements is shown as a black cross. The number of ROIs is given for each boxplot (n). B) Area of high (atom% ^{13}C > 2.4), intermediate (atom% ^{13}C 1.4-2.4) and low (atom% ^{13}C < 1.4) ^{13}C enrichment, relative to the total OM covered surface, as determined by NanoSIMS. 131

Figure 7.9 Microbial abundances of the sandy soil above and below the goethite layer (GL) as well as in the goethite itself sampled from the 4 cm, 30 cm, and 100 cm depth increments. A) Mean abundances of bacteria, fungi and archaea; B) Mean abundances of the bacterial taxa *Acidobacteria*, *Actinobacteria*, *Betaproteobacteria*, *Bacteroidetes*, *Firmicutes*, *Gemmatimonadetes*, and *Verrucomicrobia*. 132

List of Tables

Table 5.1 Soil parameters of the field site. 27

Table 5.2 Mean ratios of $PLFA_{fungi}$ / $PLFA_{bacteria}$. 39

Table 6.1 a: Substrate addition effect: Mean increase (%) of microbial biomass C (C_{mic}), $PLFA_{gram+}$, $PLFA_{gram-}$, $PLFA_{fun}$ and Ergosterol in TOP5 and SUB110 samples with root addition compared to samples without root addition in different incorporation depths.
b: Translocation effect: Mean increase/ decrease (%) of microbial biomass C (C_{mic}), $PLFA_{gram+}$, $PLFA_{gram-}$, $PLFA_{fun}$ and Ergosterol in TOP5 and SUB110 samples translocated to different incorporation depths based on the related non-translocated treatments with or without root addition, respectively.
c: Interaction effect of substrate addition and translocation: Mean increase / decrease (%) of microbial biomass C (C_{mic}), $PLFA_{gram+}$, $PLFA_{gram-}$, $PLFA_{fun}$ and Ergosterol in translocated TOP5 and SUB110 samples with root addition compared to the respective non-translocated samples without root addition. 81

Table 6.2 Fungi to bacteria ratios (18:2ω6 to bacterial PLFA) of TOP5 and SUB110 samples with and without root addition. 83

Table 7.1 Basic physical and chemical soil properties of the three sampling depths in each of the two soils before the experiment. 113

Table 7.2 Specific surface area (SSA), carbon (C) and nitrogen (N) content, C/N ratio, change of carbon concentration over the course of the experiment (ΔC), $\delta^{13}C$, proportion of C sorbed to the goethite derived from before the experiment (GDC), proportion of solution-derived C associated with goethite after the experiment (SDC), and previously bound OC that was either removed or replaced over the course of the experiment (MC). Results of the uncoated goethite before the experiment are shown (Gp), and the samples from the respective three depth compartments with sandy soil (GpSa1, GpSa2 GpSa3) and silty soil (GpSi1, GpSi2, GpSi3), the OM-coated goethite before the experiment (G0), and the respective three depth compartments with sandy soil (G0Sa1, G0Sa2, G0Sa3) and with silty soil (G0Si1, G0Si2, G0Si3). 114

Table 7.3 Mean mobilized OC from the OM-coated goethite (MC), mean goethite-derived OC (GDC) in the solution and mean $Retained_{MC}$ (eq. 12), and the proportion of $retained_{MC}$ relative to the total amount of mobilized OC from the respective goethite sample (± standard deviation) in the three depths of the columns with sandy and silty soils. $Retained_{MC}$ represents the fraction of OC mobilized from the OM-coated goethite but retained in the soil core below the goethite and thus not transported out of the column. 129

List of Supplementary Materials

Table S5.1 qPCR primers and conditions. 58

Table S5.2 Enzyme activities in SUB20 and SUB120 samples with different treatment types (T = translocated, NT = non-translocated, 0% = no cellulose addition, 1% = 1% cellulose addition, 5% = 5% cellulose addition) and sampling dates. Data are presented as mean ± standard deviation (n =3). 59

Table S5.3 Cellulose addition, translocation and sampling date effects on enzyme activities tested with three-way ANOVA. The table shows F-ratios and P-values in parentheses. A = cellulose addition, T = translocation, D = sampling date, A*T = interaction between cellulose addition and translocation, A*D = interaction between cellulose addition and sampling date, T*D = interaction between translocation and sampling date, A*T*D = interaction between cellulose addition, translocation and sampling date. 60

Table S5.4 Mean respiratory response of 5 % cellulose addition samples after 12 month. 61

Figure S5.1 Absolute amount of ^{13}C-cellulose-derived C incorporated into gram-positive bacteria (PLFA$_{\text{gram+}}$), gram-negative bacteria (PLFA$_{\text{gram-}}$) and fungi (PLFA$_{\text{fungi}}$) in SUB20 (a, b, c) and SUB120 (d, e, f) samples under different translocation and cellulose addition treatments at the sampling dates July 2013, October 2013 and June 2014. Error bars indicate standard deviation (n=3). Not determined treatments are indicated with nd. 62

Figure S5.2 Increased amounts of added cellulose proportionally increase the affected soil volume and the number of microorganisms with access to cellulose in a carbon limited environment. 63

Table S6.1 Soil parameters of the field site. 97

Table S6.2 a: Root addition, translocation and sampling date effects on water content (%), extractable total nitrogen (ETN), extractable organic carbon (EOC) and cutin and suberin derived monomers tested with LME model.
b: Root addition, translocation and sampling date effects on microbial biomass C (C$_{\text{mic}}$), PLFA$_{\text{gram+}}$, PLFA$_{\text{gram-}}$, PLFA$_{\text{fun}}$ and Ergosterol tested with LME model.. 98

Table S6.3 Translocation and sampling date effects on relative root-derived C incorporation (%) into different fractions tested with LME models. The table shows significant effects with F-ratios and P-values in parentheses. T = translocation, D = sampling date. 99

Table S6.4 Translocation and sampling date effects on absolute root-derived C incorporation into different fractions tested with LME models. The table shows significant effects with F-ratios and P-values in parentheses. S = soil, T = translocation, D = sampling date. 100

Figure S6.1 Mean daily (a) air temperature (°C) and (b) precipitation (mm) at the experimental site from June 1, 2014 to June 31, 2015. 101

Figure S6.2 Exemplary front view of one of twelve tree facing profile walls with four soil containers (treatments: $\text{TOP5}_{\text{roots}}$, $\text{TOP5}_{\text{control}}$, $\text{SUB110}_{\text{roots}}$ and $\text{SUB110}_{\text{control}}$) randomly incorporated into 5 cm, 45 cm and 110 cm soil depths each. Due to the randomized distribution of the different containers in the three depths of each of the twelve profile pits, this is an exemplary incorporation pattern to illustrate the incorporation design.. 102

Figure S6.3 Mean gravimetric water content (%) in TOP5 and SUB110 samples translocated to different soil depths at the sampling dates September 2014, December 2014, March 2015 and June 2015. Error bars indicate standard error (n=3). The figure shows significant effects with respective P-values. A = root addition, T = translocation, D = sampling date. 103

Figure S6.4 Amount of extractable total nitrogen (ETN) in TOP5 (a) and SUB110 (b) samples under different translocation and root addition treatments for the sampling dates September 2014, December 2014, March 2015 and June 2015. Error bars indicate standard error (n=3). The figure shows significant effects with respective P-values. A = root addition, T = translocation, D = sampling date.. 103

Figure S6.5 Relative proportion (%) of root-derived ^{13}C in extractable organic carbon (EO^{13}C %, a and c) and absolute amount of ^{13}C-root-derived C in EOC (µg root-derived C in EOC g^{-1} DM, b and d) in TOP5 and SUB110 samples under different translocation and root addition treatments for the sampling dates September 2014, December 2014, March 2015 and June 2015. Error bars indicate standard error (n=3). The figure shows significant effects with respective P-values. S = soil origin, A = root addition, T = translocation, D = sampling date.. 104

Figure S6.6 Amount of ergosterol in TOP5 (a) and SUB110 (b) samples under different translocation and root addition treatments for the sampling dates September 2014, December 2014, March 2015 and June 2015. Error bars indicate standard error (n=3). The figure shows significant effects with respective P-values. A = root addition, T = translocation, D = sampling date. 105

Figure S6.7 Amounts of cutin (µg g^{-1} OC, a and c) and suberin (µg g^{-1} OC, b and d) in TOP5 and SUB110 samples under different translocation and root addition treatments at the sampling dates September 2014 and June 2015. Error bars indicate standard error (n=3). The figure shows significant effects with respective P-values. A = root addition, T = translocation, D = sampling date. 106

Table S7.1 qPCR primers and conditions. 143

Table S7.2 Selected soil and goethite parameters of the samples from the experimental run with pure goethite used for the qPCR analyses. 144

Table S7.3 Mean DOC concentrations (mg L^{-1}) of the outflow solutions of all experimental variations at the three respective depths (cm). 144

Table S7.4 Cumulative mean DOC inflow (mg), and outflow (mg) as well as the gross balance of both (± standard deviation). Negative values represent adsorption processes from the solution, whereas positive values represent desorption processes into the solution. The balance in percent is calculated relative to the inflow solution. 145

Table S7.5 Mean values of total specific UV absorbance (SUVA) at 280 nm (L mg C^{-1} cm $^{-1}$) of DOM in the inflow and in the outflow as well as the balance of both (± standard deviation). Negative values represent decreasing SUVA in the outflow whereas positive values represent increasing SUVA in the outflow. The balance in percent is calculated relative to the inflow solution. 146

Table S7.6 Mean OC concentration and $\delta^{13}C$ ratio of the soil samples before and after the experiment and the respective change of both, per depth increment and used soil, on basis of bulk EA-IRMS measurements. 147

Table S7.7 Surface coverage and isotopic data based on NanoSIMS images of OM-coated goethite before (G0) and after the experiment (G0 4 cm, G0 30 cm, G0 100 cm). We report mean atom% ^{13}C values of regions of interest (ROIs) that represented regions with OM coating and the respective bulk IRMS measurements for the whole sample. The ROIs with an atom% ^{13}C of <1.40 were considered to be related to newly sorbed OC (low ^{13}C enrichment), the ROIs with an atom% ^{13}C of >1.40 and <2.40 were considered to consist of a mixture of old and new sorbed OC (intermediate ^{13}C enrichment), and ROIs with an atom% ^{13}C of >2.40 were assumed to consist of mainly old OC (high ^{13}C enrichment). The table shows the relative proportion of the surface covered by OC of each category and the number of ROIs (n) in each category. 148

1 Summary

Soils are the largest terrestrial reservoir of organic carbon (OC). Substantial proportions of the stored OC are found in stabilized form in deeper soil layers. Beside the quality and quantity of C input from plant biomass, C storage in soil is primarily controlled by the microbial decomposition capacity. Various physical, chemical and biological factors (e.g., substrate availability, temperature, water content, pH, texture) vary within soil profiles and directly or indirectly influence the abundance, composition and activity of microbial communities and thus the microbial C turnover. While soil microbiological research has so far focused mainly on processes in topsoil, the mechanisms of C storage and turnover in subsoil are largely unknown. The objective of the present thesis was therefore to investigate the specific influence of substrate availability and different environmental factors as well as their interactions on microbial communities and their regulatory function in subsoil C-cycling.

This objective was addressed in three studies. In the first and second study, one-year field experiments were established in which microbial communities from different soil depths were exposed to altered habitat conditions to identify crucial factors influencing the spatial and temporal development of microbial abundance and substrate utilization within soil profiles. This was achieved by reciprocal translocation of soils between subsoil horizons (first study) and topsoil and subsoil horizons (second study) in combination with addition of ^{13}C-labelled substrates and different sampling dates. In the third study, a flow cascade experiment with soil columns from topsoil and subsoil horizons and soil minerals (goethite) coated with ^{13}C-labelled organic matter (OM) was established. This laboratory experiment investigated the importance of exchange processes of OM with reactive soil minerals for the quality and quantity of dissolved

OM and the influence of these soil microhabitats on microbial abundance and community composition with increasing soil depth.

For investigating the microbiological objectives, both classic soil biological methods (microbial C and N, enzyme activity, ergosterol) and modern molecular methods (quantitative polymerase chain reaction (qPCR), phospholipid fatty acid analysis (PLFA)) were utilized. The use of ^{13}C-labelled substrates allowed to determine flows between different C pools using isotopic ratio mass spectrometry (IRMS).

In the first study, the reciprocal translocation of subsoils from different soil depths revealed that due to comparable micro-climatic conditions and soil textures within the subsoil profile, no changes in microbial biomass, community composition and activity occurred. Moreover, increasing microbial substrate utilization in relation to the quantity of added substrate indicated that deep soil layers exhibit high potential for microbial C turnover. However, this potential was constrained by low soil moisture in interplay with the coarse soil texture and the resulting micro-scale fragmentation of the subsoil environment. The bacterial substrate utilization was more affected by this spatial separation between microorganisms and potentially available substrate than that of fungi, which was further confirmed by the translocation experiment with topsoil and subsoil in the second study. While the absolute substrate utilization capacity of bacteria decreased from the more moist topsoil to the drier subsoil, fungi were able to increase their substrate utilization and thus to partially compensate the decrease in C input from other sources. Furthermore, the addition of root litter as a preferential C source of fungal decomposer communities led to a pronounced fungal growth in subsoil. The third study demonstrated the high importance of reactive soil minerals both in topsoil and in subsoil for microbial growth due to extensive exchange processes of OM and the associated high availability of labile C. In particular copiotrophic bacteria such as *Betaproteobacteria* benefited from the increased C availability under non-limiting water conditions leading to a pronounced increase in bacterial dominance in the microbial communities of these soil micro-habitats.

In conclusion, this thesis showed that subsoil exhibits great potential for both bacterial and fungal C turnover, albeit this potential is limited by various factors. This thesis, however, allowed to determine the specific effects of these factors on bacteria and fungi and their function in subsoil C-cycling and thus to identify those factors of critical importance. The micro-climate in subsoil, in particular soil moisture, was the primary factor limiting bacterial growth and activity, whereas fungi were more strongly restricted by substrate limitations. With regard to future dynamics of long-term stabilized C in subsoil, e.g., under changing temperature and precipitation regimes, the fungal function in C-cycling is of particular interest due to the higher drought stress resistance of many fungal taxa and should be further investigated.

2 Zusammenfassung

Böden sind der größte terrestrische Speicher von organischem Kohlenstoff (OC). Ein erheblicher Anteil des gespeicherten OC liegt hierbei in tieferen Bodenschichten in stabilisierter Form vor. Neben der Qualität und Quantität des Eintrages aus pflanzlicher Biomasse wird die C-Speicherung in Böden hauptsächlich durch die mikrobielle Abbauleistung gesteuert. Eine Vielzahl von physikalischen, chemischen und biologischen Faktoren (z.B. Substratverfügbarkeit, Temperatur, Wassergehalt, pH, Textur) variieren innerhalb von Bodenprofilen und beeinflussen direkt oder indirekt die Abundanz, Zusammensetzung und Aktivität mikrobieller Gemeinschaften und somit den mikrobiellen C-Umsatz. Während die bodenmikrobiologische Forschung bisher verstärkt auf Prozesse im Oberboden ausgerichtet war, sind die Mechanismen der Speicherung und des Umsatzes von C im Unterboden weitgehend unbekannt. Das Ziel der vorliegenden Arbeit war es daher, den spezifischen Einfluss von Substratverfügbarkeit und verschiedener Umweltfaktoren sowie ihrer Wechselwirkungen auf die mikrobielle Gemeinschaft und ihre regulierende Funktion im C-Kreislauf des Unterbodens zu untersuchen.

Dieses Ziel wurde durch drei Studien angegangen. In der ersten und zweiten Studie wurden jeweils einjährige Feldexperimente etabliert, in denen Mikroorganismengemeinschaften verschiedener Bodentiefen veränderten Habitatbedingungen ausgesetzt wurden, um entscheidende Einflussgrößen auf die räumliche und zeitliche Entwicklung ihrer Abundanz und Substratnutzung innerhalb von Bodenprofilen zu identifizieren. Dies wurde durch eine wechselseitige Translokation von Böden zwischen Unterbodenhorizonten (erste Studie) und Oberboden- und Unterbodenhorizonten (zweite Studie) in Kombination mit Zugabe von ^{13}C-markierten Substraten und mehreren Probennahmezeitpunkten möglich. In der dritten Studie wurde ein Fluss-Kaskaden-Experiment mit Bodensäulen aus Ober- und Unterbodenhorizonten und mit ^{13}C-markiertem organischen Material (OM) belegten Bodenmineralen (Goethit) etabliert. Mit diesem Laborexperiment wurde die Bedeutung von Austauschprozessen von OM mit reaktiven Bodenmineralen für die Qualität und Quantität von gelöstem OM sowie der Einfluss dieser Boden-Mikrohabitate auf die mikrobielle Abundanz und Gemeinschaftszusammensetzung mit zunehmender Bodentiefe untersucht.

Für die Bearbeitung der mikrobiologischen Fragestellungen wurden sowohl klassische bodenbiologische (Enzymaktivität, mikrobieller C und N, Ergosterol) als auch moderne molekularbiologische Methoden (quantitative Polymerase-Kettenreaktion (qPCR), Phospholipid-Fettsäuren-Analyse (PLFA)) genutzt. Der Einsatz ^{13}C-markierter Substrate ermöglichte die Bestimmung von Flüssen zwischen C-Pools mittels Isotopenverhältnis-Massenspektrometrie (IRMS).

Durch die wechselseitige Translokation von Unterböden verschiedener Ursprungstiefen in der ersten Studie zeigte sich, dass aufgrund vergleichbarer mikroklimatischer Bedingungen und Bodentexturen innerhalb des Unterbodenprofils keine Veränderungen der mikrobiellen Biomasse, Gemeinschaftszusammensetzung und Aktivität auftraten. Die in Abhängigkeit von der Zugabemenge gesteigerte mikrobielle Substratnutzung verdeutlichte darüber hinaus, dass in tieferen Bodenschichten ein hohes Potential zum mikrobiellen C-Umsatz besteht. Dieses wurde jedoch durch die geringe Bodenfeuchtigkeit im Zusammenspiel mit der groben Bodentextur und einer daraus resultierenden kleinräumigen Fragmentierung im Unterboden stark eingeschränkt. Die bakterielle Substratnutzung war durch diese räumliche Trennung von Mikroorganismen und potentiell verfügbarem Substrat stärker betroffen als die pilzliche, was sich im Translokationsexperiment mit Ober- und Unterböden der zweiten Studie bestätigte. Während die absolute Substratnutzungskapazität der Bakterien vom feuchteren Oberboden zum trockeneren

Unterboden abnahm, konnten Pilze diese steigern und somit die Abnahme des C-Eintrages aus anderen Quellen teilweise ausgleichen. Des Weiteren führte die Wurzelstreu-Zugabe als präferentielle C-Quelle pilzlicher Zersetzergemeinschaften zu einem deutlichen Pilzwachstum im Unterboden. Die dritte Studie verdeutlichte, dass reaktive Minerale sowohl im Oberboden als auch im Unterboden aufgrund ausgeprägter Austauschprozesse von OM und einer damit einhergehenden hohen Verfügbarkeit von labilem C von großer Bedeutung für mikrobielles Wachstum sind. Insbesondere profitierten kopiotrophe Bakterien wie *Betaproteobacteria* unter den nicht wasserlimitierten Bedingungen von der gesteigerten C-Verfügbarkeit, was zu einer deutlichen Steigerung der bakteriellen Dominanz in der mikrobiellen Gemeinschaft dieser Boden-Mikrohabitate führte.

Zusammenfassend wurde durch diese Arbeit deutlich, dass in Unterböden ein großes Potential sowohl zu bakteriellem als auch pilzlichem C-Umsatz vorhanden ist. Dieses Potential wird jedoch durch verschiedene Faktoren begrenzt. Es war durch diese Arbeit indes möglich, die spezifische Wirkung dieser Faktoren auf Bakterien und Pilze und ihre Funktion im C-Kreislauf des Unterbodens aufzuzeigen und somit jene von entscheidender Bedeutung zu identifizieren. So war das Mikroklima im Unterboden, insbesondere Bodenfeuchte, der primär limitierende Faktor bakteriellen Wachstums und Aktivität, wohingegen pilzliches Wachstum stärker durch Substratlimitierungen begrenzt wurde. In Hinblick auf die zukünftige Dynamik des bisher langfristig stabilisierten C im Unterboden, z.B. unter Einfluss veränderter Temperatur- und Niederschlagsregime, ist auf Grundlage der Erkenntnisse dieser Arbeit die pilzliche Funktion im C-Kreislauf aufgrund der höheren Trockenstressresistenz vieler pilzlicher Taxa von besonderem Interesse und sollte weitergehend erforscht werden.

3 General Introduction

3.1 Soil as carbon reservoir

Soil organic matter (SOM) contains more than three times as much carbon (C) as the atmosphere or the terrestrial vegetation (Schmidt et al., 2011). Globally, the soil organic carbon (SOC) pool is estimated to be approximately 1500 gigatonnes (Gt; 1 Gt = 1 billion tonnes) in the first meter of soil (Jobbagy and Jackson, 2000). Soil C storage capacities show enormous variations over different spatial (local to global) scales. Among different biomes, for example, forest soils are of major importance for the global C-cycle due to their high C stocks and the large area covered by forests (Lal, 2005). This applies – as SOC stocks generally increase as the mean annual temperature decreases – in particular for forest soils in the northern hemisphere and thus in Europe with estimations of the European forest soil C stocks of up to 79 Gt (Baritz et al., 2010; Schils et al., 2008; Stockmann et al., 2013).

SOC pools represent a dynamic equilibrium between gains and losses of C (Lal, 2004). C input into soil originates from above- and belowground litter, root exudates, dissolved organic carbon (DOC) and sediment deposition. The sum of all dead material in varying states of decomposition in the soil containing organic carbon (OC) is defined as soil organic matter (SOM). The primary loss of C from soil occurs via carbon dioxide (CO_2) efflux due to microbial (heterotrophic) and root (autotrophic) respiration, although DOC leaching, erosion and anaerobic microbial respiration (methane; CH_4) can also be of importance (Sollins et al., 1996; Davidson and Janssens, 2006). Fundamental controls of SOC fluxes are soil microorganisms as primary degraders of SOM as well as the net primary production (NPP) of plants and the type of organic matter (OM) inputs (Stockmann et al., 2013). All these constituents are interconnected in various manners and mutually influence each other:

Soil microorganisms degrade SOM to yield C for energy production (catabolic pathway) and growth (anabolic pathway) and thus play a crucial role in soil C-cycling with major implications for SOC turnover and sequestration (Frey et al., 2013). Moreover, soil microorganisms have a key role in nutrient cycling and contribute to soil fertility, and plant diversity and growth through a variety of direct (e.g., nitrogen (N) -fixing bacteria) and indirect (e.g., nutrient mineralization of free-living microbes) effects (van der Heijden et al., 2008).

Plant growth and diversity determine the quantity and quality of above- and belowground litter inputs into the soil and are major controls on SOM formation and decomposition. For example, high C:N as well as high lignin:N ratios of plant residues lead to reduced degradability greatly influencing C and nutrient dynamics in soil (e.g., Silver and Miya, 2001). Also rhizodeposits in form of ,e.g., exudates or C flow from plants to mycorrhizal and bacterial symbionts for nutrient acquisition substantially account for OC allocations from plant to soil respectively microbial OC pools. Consequently, plant inputs can be described as the controlling pump of the C-cycle (Paul, 2016; Jones et al., 2009).

3.2 Deep soil – source or sink for carbon?

An increasing number of studies in recent years assessing soil C stocks included not only C stored in the upper layers of soil, but also C stored in deeper soil layers. The global C stocks in the top three meters of soil, for example, were estimated to be 2344 Gt, or 56% more C than the 1500 Gt stored in the first meter of soil (Jobbagy and Jackson, 2000). Therefore, subsoils play an important role in the global C-cycle and the response of this enormous C reservoir to changing conditions due to e.g. global climate change or human impact is of particular relevance considering the function of soil as source or sink of C.

A stronger focus on subsoil C-cycling is also of great importance since the mechanisms of C storage and turnover in deeper soil differ clearly from those in topsoil. The main sources of deep soil OM are plant roots and root exudates, dissolved organic matter (DOM) and via bioturbation translocated OM (Rumpel and Kögel-Knabner, 2011). Compared to topsoil, subsoil exhibits substantially lower C densities as well as a different chemical composition of the OM (Rumpel et al., 2002). Important processes contributing to the altered chemical composition of OM in deeper soil are the temporal and selective immobilization (sorption, precipitation) as well as microbial mineralization and transformation of DOM percolating down the soil profile. As a consequence, with increasing soil depth OM pools consist to a greater extent of aged plant-derived compounds and microbial residues (Kaiser and Kalbitz, 2012; Liang and Balser, 2008). Contrary, important pathways for fresh OC inputs into deeper soil are preferential flow paths differing from the soil matrix by higher concentrations and younger age of the C (Bundt et al., 2001). However, large areas in subsoil remain unaffected by fresh OC inputs and consequently subsoil OC pools exhibit a more heterogeneous distribution and considerably higher radiocarbon ages (up to several thousand years before present; B.P.) than those in topsoil (largely modern age) (Rumpel and Kögel-Knabner, 2011). The increasing age of the OC indicates an enhanced stabilization and a prolonged residence time of OM with soil depth due to pronounced inhibition of microbial degradation processes (Rumpel et al., 2004). Different mechanisms contributing to enhanced stabilization and long-term storage of the OM with increasing soil depth have been discussed:

Chemical recalcitrance describes the reduced biodegradability of OM due to a highly stable inherent chemical structure of certain compounds (e.g., lignin) of the OM. For example, root litter is an important C source in deep soil but comprises high lignin concentrations and might consequently contribute to an increased stabilization of subsoil OM due to the selective preservation of this chemically recalcitrant OM compound. However, the actual contribution of recalcitrant OM compounds to stabilization processes in deeper soil is controversially discussed, since recalcitrance was found to be ,e.g., only of major relevance in active surface layers and at early decomposition stages (Rasse et al., 2005; Rumpel and Kögel-Knabner, 2011; von Lützow et al., 2006).

Physical protection implies the occlusion of OM within micropores or aggregates leading to spatial protection against microbial decomposition. The protection is caused by reduced access to OM for microorganisms and their enzymes (e.g., decreased rates of enzyme diffusion into the inner space of aggregates) and reduced oxygen concentrations inhibiting aerobic decomposition. In subsoil, the physical protection of occluded particulate organic matter (oPOM) and clay associated OM in micro-aggregates has been found to be of particular importance. (Lützow et al., 2006; Rumpel and Kögel-Knabner, 2011).

Physico-chemical protection is the stabilization of OM by interaction with reactive soil minerals (e.g., adsorption to clay minerals or iron (Fe) oxides). The adsorption affinity of OM to soil minerals depends on the chemical structure of the OM and on the surface area and properties of the soil minerals. The resulting binding strength at the organo-mineral surfaces increases the resistance of OM against microbial and enzymatic attack and might ensure an effective protection against microbial decomposition. The radiocarbon age of C was found to be related to the mineral size fraction, with highest amounts of C with old radiocarbon ages on mineral fractions < 20 µm. Moreover, the protection of OM against microbial decomposition is further enhanced by combined processes of adsorption and occlusion (Dungait et al., 2012; Kaiser and Guggenberger, 2000).

Energy limitation of microbial SOM turnover describes the absence of, respectively the restricted access to fresh OC as energy source for soil microorganisms inhibiting microbial decomposition processes and thus maintaining the stability of SOC. Inputs of fresh OC into subsoil as an essential energy source for (fast) microbial C turnover are largely limited to preferential flow paths and root channels, while large areas of the soil matrix in deeper soil are disconnected from frequent fresh OC inputs and show very low C turnover rates. Consequently, SOC pools in subsoil show heterogeneous and spatially distinct radiocarbon ages varying between modern and up to several thousand years depending on amount and composition of OC inputs (Fontaine et al., 2007; Chabbi et al., 2009).

Increasing releases of C from subsoil OC pools can be induced by intensified destabilization processes. Destabilization is the overall process leading to lower resistance of OM against degradation due to increasing microbial accessibility or decreasing recalcitrance (Sollins et al., 1996). This increasing vulnerability of stabilized OC in subsoil could be facilitated by different direct or indirect effects of global climate change (e.g., increased soil temperature) or other human-induced environmental changes (see chapter 3.4).

3.3 Microbial biomass, community composition and activity with soil depth

The microbial biomass, community composition and activity are subject to great changes with increasing soil depth (Blume et al., 2002). Microorganisms in subsoil are exposed to distinctly different *habitat conditions* than those in topsoil, since almost all driving factors are typically changing with increasing soil depth (Eilers et al., 2012). This includes quantitative and qualitative C availability, nutrient status, soil temperature and moisture, pH, and oxygen (O_2) concentration. The spatial variability of all of these individual factors and their influence on microbial characteristics have been investigated in several studies (e.g., Holden and Fierer, 2005; Hansel et al., 2008; Herold et al., 2014).

The *microbial biomass* largely depends on C availability indicated by strongly decreasing microbial abundances in response to lower C concentrations with increasing soil depth (Taylor et al., 2002; Fierer et al., 2003). Furthermore, the increasing heterogeneity of C with depth is reflected in a patchy distribution of the microbial biomass in deep soil with highest microbial abundances in hotspots of substrate availability such as preferential flow paths (Bundt et al., 2001; Nunan et al., 2003). Nevertheless, deeper soil contains substantial numbers of microorganisms due to the large volume of subsoil horizons and the potential for C turnover and storage is immense (Eilers et al., 2012).

The *microbial community composition* in subsoil environments shows a decreased microbial diversity and species richness compared to microbial communities in topsoil (Fierer et al., 2003; Agnelli et al., 2004). For example, the bacterial diversity in subsoil of a Californian grassland site was found to be 75% lower than in surface soil (LaMontagne et al., 2003). Differences in microbial communities within a few decimetres of soil depth can be as large as between microbial communities of soils from different biomes with distances of several thousand kilometres (Eilers et al., 2012). Previous studies have found a characteristic pattern of the microbial community structure with soil depth: While the relative proportion of Gram-positive bacteria increases in microbial communities with depth, the proportions of Gram-negative bacteria and fungi decrease (Blume et al., 2002; Fierer et al., 2003). These typical changes in the microbial community structure are largely attributed to differences in resource availability with soil depth and to microbial group-specific feeding strategies (Kramer and Gleixner, 2008), although also environmental factors such as pH, temperature or moisture as well as their potential interactions among each other and with resource availability have been identified as important determinants (Blagodatskaya and Anderson, 1998; Brockett et al., 2012; DeAngelis et al., 2015). Differentiation of individual microbial taxa/phyla according to their environmental or resource requirements allows a detailed characterization of microbial communities and their function within soil profiles. While copiotrophic microorganisms (*r*-strategists, fast growth rates) such as *Betaproteobacteria* and *Bacteroidetes* have high resource requirements and predominate in e.g. rhizosphere soils, oligotrophic microorganisms (*K*-strategists, slow growth rates) such as *Acidobacteria* and *Actinobacteria* are most abundant under low nutrient content and qualitatively and quantitatively poor C supply such as in bulk soil compartments (Fierer et al., 2007; Hartmann et al., 2009). In addition to this metabolism- or resource-based classification, the environmental requirements (e.g., pH or soil moisture conditions) of microbial taxa/phyla allow a further specification of the microbial community and function. For example, *Acidobacteria* are most abundant at low pH and moist soil conditions, whereas *Actinobacteria* exhibit opposite abundance patterns (Lauber et al., 2009; Barnard et al., 2013).

The *microbial activity* - indicated either as functional (respiration, mineralization) or enzymatic activity - shows pronounced decreases with increasing soil depth reflecting altered habitat conditions within soil profiles (Taylor et al., 2002). As with microbial biomass and community structure, resource availability is the most critical factor influencing the microbial activity with soil depth. Moreover, there is a strong relationship between microbial activity and biomass, so that the specific metabolic activities of microorganisms in subsoil and topsoil are similar when normalized to microbial biomass (Fang and Moncrieff, 2005; Stone et al., 2014).

Characteristic differences in microbial activity within soil profiles are pronounced enzymatic activities in degradation processes of recalcitrant OM as well as higher sensitivity to nutrient and temperature increases in subsoil than in near-surface horizons (Herold et al., 2014; Fierer et al., 2003b). Subsoils show an increased occurrence of oxidative enzymes (e.g., peroxidase) involved in recalcitrant OM degradation, while soil compartments with higher proportions of more easily degradable substrates show enhanced rates of hydrolytic enzyme activities (e.g., β-glucosidase) (Uksa et al., 2015). Moreover, enzyme activity is affected by soil moisture, consequently spatial and temporal variations in soil moisture can distinctly influence the expression of enzyme activity within soil profiles (Baldrian et al., 2010; Brockett et al., 2012). The production of specific enzymes is related to the microbial community composition, thus enzyme activity patterns reflects shifts in microbial communities and their functioning under changing habitat conditions with increasing soil depth (Waldrop et al., 2000).

3.4 Changing habitat conditions and microbial SOM decomposition

Various natural (e.g., climate, parent material) and anthropogenic (e.g., land use type, management intensity) factors and the complex interplay of these factors directly or indirectly influence the microbial decomposition activity as well as plant growth and diversity and thus the development of SOC stocks within soil profiles (Grüneberg et al., 2010). Consequently, the feedback of SOC pools to altered environmental conditions such as temperature or moisture is of major concern as C releases from soil due to increasing microbial SOM decomposition are expected to exceed the C input via enhanced primary production of plants in future climate change scenarios (Davidson and Janssens, 2006). In this regard, subsoil OC pools are of particular relevance, since stable C was found to be at least as vulnerable as more labile C fractions to microbial decomposition under changing environmental conditions (Guenet et al., 2012; Fierer et al., 2005).

Soil microorganisms as main driver of SOM decomposition respond highly sensitive to increases in soil temperature with accelerated activity, and changes in microbial biomass and community composition (e.g., shifts from colder- to warmer-adapted taxa) affecting SOM decomposition and thus the efflux of CO_2 from soil C pools to the atmosphere via heterotrophic microbial respiration (Bardgett et al., 2008; Frey et al., 2008; DeAngelis et al., 2015). However, long-term estimations of the soil-atmosphere C exchange are subject to great uncertainties, since, e.g., SOM decomposition and CO_2 emission were found to show rapid increases following soil warming, but decline again after a certain time (Melillo et al., 2017). This phenomena has been explained by thermal adaption of the microbial decomposer community to altered temperature regimes, depletion of readily available substrates over time and varying temperature sensitivity of microbial decomposition dependent on substrate C quality (Bradford, 2013; Conant et al., 2011; Fierer et al., 2005).

Also changes in soil moisture - often accompanied by altered soil temperature - can cause changes in microbial biomass, composition and function and thus in SOM decomposition rates. Microorganisms can respond either directly to changing soil moisture conditions, or indirectly via related changes in pH or altered C translocation within soil profiles (Evans et al., 2014). Furthermore, changes in duration and frequency of droughts can lead to moisture-related limitations of the microbial activity and thus to an inhibition of C turnover, thereby altering the development of soil C pools (Bardgett et al., 2008). In this context, also the drying and rewetting patterns and the “stress history” of soils have great influence on microbial C dynamics, with rapid rewetting of dry soils potentially causing an increased release of CO_2 due to a strongly enhanced microbial activity (Fierer and Schimel, 2002).

Altered plant productivity and diversity - either due to changes in land use or climatic conditions - have also great impact on the development of SOC pools. Shifts in plant community composition or increased photosynthesis rates due to increased atmospheric CO_2 concentrations can lead to an enhanced input as well as altered composition of plant-derived C and thus stimulate increases in microbial abundance and activity, and enhanced C mineralization (priming effects) (Bardgett et al., 2008). With regard to the stability of subsoil C pools, an increased input of labile C into deeper soil is of particular relevance, since the relative magnitude of priming effects increases with soil depth (Karhu et al., 2016). Consequently, increasing labile C inputs accelerate the microbial activity in particular in subsoil leading to an increased decomposition of long-term stabilized C (Bernal et al., 2016; Fontaine et al., 2007). However, predictions on the effects of changing habitat conditions on the response of SOC pools and microbial degradation capacities within soil profiles are largely unreliable due to complex interactions of various factors. For example, when considering soil C dynamics, the mutual influence of plant and microbial characteristics (e.g., biomass or diversity) on each other must be taken into account (van der Heijden et al., 2008).

3.5 Stable isotopes in the research of soil carbon dynamics

The application of stable C isotopes in investigations of soil C fluxes offers a wide range of new research perspectives using either natural abundance or labelling techniques. With regard to microbial C pools, for example, it is possible to track C flows at different taxonomic resolutions from the total microbial biomass down to specific microbial taxa (e.g., ^{13}C microbial biomass ($^{13}C_{mic}$), ^{13}C phospholipid fatty acid (^{13}C-PLFA) or ^{13}C deoxyribonucleic acid (^{13}C-DNA) analyses).

The most common C isotopes ^{12}C und ^{13}C have generally a natural abundance of approximately 98.982% and 1.108% of total C, respectively.

Natural abundance techniques use variations in the ratio of ^{12}C and ^{13}C (or ^{14}C) between different C pools to trace sources and fluxes of C in soil environments. (Staddon, 2004). A well-known example and frequently used application of the natural abundance approach is the vegetation change from C3 to C4 plants or vice versa in SOM turnover studies (e.g., Balesdent et al., 1988).

Labelling methodologies comprise the use of substrates either enriched or depleted in rarer C isotopes (usually ^{13}C or ^{14}C) allowing to trace the fate of C from the introduced substrate into different C pools. An advantage of the labelling approach in comparison to the natural abundance approach is the higher sensitivity towards, e.g., low microbial C incorporation/turnover rates or large background C pools. Moreover, labelling of specific C pools/substrates of different complexity (e.g., CO_2, cellulose or whole plants) is possible and a variety of different labelled substrates are commercially manufactured. Consequently, the isotopic tracer can be introduced to the soil C-cycle either by labelling of the vegetation or single plants with labelled CO_2 (e.g., via pulse labelling) or by addition of readily labelled substrates such as plant litter (Staddon, 2004).

Complex investigations of, e.g., soil microbial food webs (e.g., Lueders et al., 2006) or the identification of soil microorganisms involved in specific processes (e.g., Bull et al., 2000) require the use of compound-specific isotope analysis respectively stable isotope probing (SIP) analyzing specific biomarkers (e.g., ^{13}C-PLFA or ^{13}C-DNA) (Radajewski et al., 2000; Boschker and Middelburg, 2002; Dumont and Murrell, 2005). The SIP method was first introduced for PLFA analysis (^{13}C-PLFA) and is widely applied. The ^{13}C-PLFA analysis is an important culture-independent approach and used for investigations on the contribution of specific microbial groups (e.g., fungi) and metabolic pathways in C-cycling (Evershed et al., 2006). For example, using this technique, it was shown that the (arbuscular) mycorrhizal pathway is more important than direct root exudation for the transfer of recently assimilated C from plants to soil microorganisms (Kaiser et al., 2015) or that the microbial community structure has a specific temporal dynamic during decomposition processes (Moore-Kucera and Dick, 2008).

4 Objectives

The mechanisms of C storage and turnover in subsoil as well as the physical, chemical and biological factors influencing these mechanisms have largely not been deciphered (Rumpel and Kögel-Knabner, 2011). Consequently, the comprehensive investigation of subsoil C dynamics in beech forest ecosystems in the north-west of Germany is the overall research objective of the SUBSOM research group. The focus of the present thesis, which was compiled within the framework of the research group, is on microbial decomposer communities and their regulatory function in C-cycling under the specific habitat conditions of subsoil environments. Habitat conditions with decisive influence on microbial parameters include substrate availability (quantity and type) as well as different micro-climatic conditions (soil temperature and moisture) and other environmental conditions such as pH, soil texture and oxygen availability (Waldrop and Firestone, 2004; Fierer et al., 2003; Allison et al., 2013). All of these factors directly or indirectly influence each other and show distinct changes with increasing soil depth. The effects of these depth-dependent changes on microbial decomposer communities and their regulative function in C-cycling are key aspects in the understanding of subsoil C-cycling and consequently their identification is the primary aim of this thesis. The thesis is structured into three studies:

The first and second study were vertical and reciprocal soil translocation experiments with amendments of ^{13}C-labelled substrates (cellulose, root litter) to the soil samples. The translocation exposed microorganisms from specific soil depths to different habitat conditions within the soil profile, while the substrate amendments increased the substrate availability for microbial decomposer communities. The interplay of the various factors acting on soil microorganisms was taken into account by conducting the two translocation experiments under *in situ* conditions. The use of ^{13}C-labelled substrates allowed following the spatial and temporal development of C flow from the substrates into different soil C pools. Both field experiments were conducted with soil samples from an acid and sandy Dystric Cambisol at the main experimental site of the SUBSOM research group in the Grinderwald, an approximately 100-year old beech (*Fagus sylvatica* L.) forest ~ 40 km north-west of Hannover in Lower-Saxony, Germany.

The first reciprocal translocation experiment with subsoil samples derived from 20 cm (upper subsoil) and 120 cm (lower subsoil) soil depth and particulate ^{13}C-labelled cellulose as additional substrate was conducted from June 2013 to June 2014 with soil samplings after 1, 4 and 12 months. Cellulose was used as additional substrate as it is a frequent component of plant biomass with known degradation pathways. The study was aimed to investigate the response of microbial communities from contrasting subsoil horizons to altered habitat conditions and different substrate availabilities. It was hypothesized (i) that translocation of different subsoil samples changes local environmental conditions (DOC, nutrient inputs, oxygen availability as well as amplitudes of temperature and water availability) and consequently soil microorganisms and C turnover and (ii) that increases in substrate availability change microbial community composition and function in subsoils, with relatively greater effects as soil depth increases. A specific focus of this study was on the response of the bacterial communities as well as of enzymatic activities to the different treatments.

In the second reciprocal translocation experiment, soil samples derived from 5-10 cm (topsoil) and 110-115 cm (subsoil) soil depth were incorporated into 5, 45 and 110 cm soil depth to include a wide range of habitat conditions within the soil profile. The experiment started in June 2014 and had a total duration of 12 months with four soil samplings in three month intervals. The addition of ^{13}C-labelled root litter as important C source in top- and subsoil habitats allowed tracing the flow of C from a natural and complex substrate into different C pools. The research focus of this study was on the potentially inhibiting effects of subsoil habitat conditions on the succession of microbial communities and their decomposition capacity and on factors influencing the rapid decline of fungal microorganisms with increasing soil depth ($^{13}C_{mic}$; ^{13}C-PLFA, ergosterol). Consequently, the hypotheses were that habitat conditions in subsoil (i) slow down the succession of root litter-decomposing fungi and bacteria and (ii) reduce microbial root-C utilization rates.

The third study was a laboratory flow cascade experiment with three connected and undisturbed soil columns from different depths of Dystric and Eutric Cambisol soils and integrated thin goethite layers in each column. The quality and quantity of DOM as an important microbial C source throughout soil profiles differs substantially between surface and deeper soil layers. These changes during the passage through the soil profile might be driven by (selective) sorption processes and – as postulated in the “cascade model” (Kaiser and Kalbitz, 2012) - by additional stepwise exchange processes on reactive minerals such as goethite. The experiment was conducted to quantify the OC adsorption and desorption and net OC exchange at goethite surfaces using ^{13}C labelling of OM, as well as to investigate the associated microbial community patterns (^{13}C analysis in solid and solution phase, NanoSIMS, qPCR). It was hypothesized that (i) the input of plant-derived DOM to mineral topsoils leads to selective adsorption of plant-derived compounds to reactive surfaces and that (ii) fresh DOM input partially replaces older mineral-associated OM, which subsequently gets remobilized and further transported to deeper soil. The third hypothesis was that (iii) these mineral-organic associations act as biogeochemical hotspots of high resource availability leading to changes in microbial abundance and community composition.

5 Microbial community response to changes in substrate availability and habitat conditions in a reciprocal subsoil transfer experiment

Soil Biology & Biochemistry 105 (2017) 138-152

DOI: 10.1016/j.soilbio.2016.11.021

Received: 4 May 2016, Revised: 10 November 2016, Accepted: 21 November 2016,
Published online: 29 November 2016

Sebastian Preusser[a*], Sven Marhan[a], Christian Poll[a] and Ellen Kandeler[a]

[a]Institute of Soil Science and Land Evaluation, Soil Biology Department, University of Hohenheim, Emil-Wolff Str. 27, 70599 Stuttgart, Germany

[*]Corresponding author: Tel.: +49 711 459 24065

E-mail address: s.preusser@uni-hohenheim.de

Abstract

While habitat conditions influencing the abundance of microorganisms in topsoil are well known, these dynamics have been largely unexplored in deeper soil horizons. We investigated the effects of different substrate availabilities and environmental conditions on microbial community composition and carbon flow into specific groups of microorganisms in subsoils using a reciprocal soil transfer experiment within an acid and sandy Dystric Cambisol from a ~100-year old European beech (*Fagus sylvatica* L.) forest in Lower Saxony, Germany. Containers filled with subsoil from 10-20 cm (SUB20) and 110-120 cm (SUB120) soil depths and with additions of different amounts of ^{13}C labelled cellulose (1% and 5% of the respective organic carbon content of both soil layers) were exposed either in their home field environment or transferred reciprocally between SUB20 and SUB120 horizons for periods of one, four and twelve months. During the exposure of twelve months, ^{13}C accumulated up to 15 percent in total microbial biomass and up to 25 percent in fungal PLFAs. Similar microbial ^{13}C incorporation rates in SUB20 samples located at either 20 or 120 cm depth indicated comparable microclimatic conditions in both soil environments with no depth-dependent effects on the decomposer communities. While low nitrogen availability (when primary C-limitation was alleviated) and water content limited bacterial growth and activity at both depths, fungal abundance and activity were less affected due to their ability to efficiently exploit resources in surrounding soil by hyphal growth and higher drought resistance. Consequently, bacterial PLFAs (phospholipid fatty acids) incorporated less ^{13}C than fungi. The relatively high, from 1 % to 5 % cellulose addition linearly increased ^{13}C incorporation rates in SUB120 samples at 120 cm depth, clearly showed the potential of efficient carbon turnover in deeper soil layers. Spatial separation between subsoil microorganisms and their substrates may therefore be an important factor influencing carbon accumulation in subsoil.

Keywords: Carbon cycle, Stable isotope probing, Phospholipid fatty acids (PLFAs), Soil microorganisms, Micro-environment, Micro-climate

5.1 Introduction

At the global scale, soil organic carbon (SOC) represents the largest active terrestrial organic carbon (C) pool, and prediction of future SOC content is a major uncertainty in climate change scenarios (Lal, 2004; Kandeler et al., 2005). Despite the much lower C concentrations in subsoil than in topsoil horizons (Jobbagy and Jackson, 2000), more than 50 % of organic carbon is stored in subsoils below 30 cm soil depth (Batjes, 1996). This highlights the importance of subsoils for accurate estimates of global SOC pools and their role as sources or sinks of greenhouse gases (Harrison et al., 2011; Lal, 2004). However, there is a discrepancy between the importance of carbon pools in surface and subsurface soil horizons and the limited number of studies focusing on the key role of soil microorganisms in terrestrial C cycling (e.g. Brockett et al., 2012; Zumsteg et al., 2013).

Carbon dynamics in subsoil vary from those in topsoil; subsoils harbour relatively more stabilised soil organic matter (SOM) than topsoils, as shown by the greater radiocarbon age of SOM in subsoil horizons (Rumpel et al., 2002). A variety of mechanisms have been suggested to explain this phenomenon. For example, the enhanced stabilisation of SOM is thought to be caused by spatial inaccessibility and organo-mineral interactions, separating soil microorganisms from SOM and leading to a heterogeneous distribution of stabilized C compounds (Lützow et al., 2006; Chabbi et al., 2009; Salome et al., 2010; Dungait et al., 2012). Chemical recalcitrance, however, has been suggested as less important than stabilization of organic C by mineral interactions (Eusterhues et al., 2005).

The lack of fresh C input as an energy source for microorganisms has been discussed as another factor which inhibits C mineralization in subsoils (Fontaine et al., 2007). The main sources of potentially available subsoil OM are root exudates and dissolved organic carbon (DOC) (e.g. Jobbagy and Jackson, 2000; Kaiser and Guggenberger, 2000). However, C availability in subsoils is highly variable, since the downward movement of these fresh C inputs occurs along preferential flow paths which are stable for long time periods (Bundt et al., 2001). Large soil volumes are therefore disconnected from the supply of fresh organic matter and result in low C turnover rates. Consequently, microorganisms in subsoil are heterogeneously distributed, with preferential colonisation in pores which are connected to preferential flow paths (Bundt et al., 2001; Nunan et al., 2003). The total microbial biomass in “hotspots” is 2-3 times higher and microbial diversity is also greater as compared to bulk soil (Marschner et al., 2012). In contrast to these microbial hotspots, microbial biomass in bulk soil generally decreases with soil depth (Taylor et al., 2002; Hartmann et al., 2009). For example, only 35 % of the total microbial biomass in the first 2 meters of soil depth was found below a depth of 25 cm (Fierer et al. 2003a). The decrease in microbial biomass was also accompanied by a decrease in microbial diversity and changes in community composition with increasing soil depth (LaMontagne et al., 2003; Hansel et al., 2008; Will et al., 2010). Metabolic activities of soil microorganisms in top- and subsoil also typically reflect differences in environmental conditions, while processes in subsoils are more influenced by higher sensitivity to temperature increases and nutrient availability (Fierer et al., 2003b). A study in top- and subsoils of three different forest sites in Germany concluded that enzyme activities decreased with soil depth, corresponding to declines in total C and nitrogen (N) concentrations, while the degradation of recalcitrant C compounds relatively increased with depth (Herold et al., 2014). Similarly, oxidative enzymes dominated in the bulk soil compartments of subsoils, while hydrolase activities increased in microbial hotspots such as the rhizosphere (Uksa et al., 2015). However, microbial activity in subsoil was found to be similar to that in topsoil when normalized to microbial biomass (Blume et al., 2002).

The main objective of this study was to characterize the responses of microbial decomposer communities from different subsoil horizons to altered environmental conditions and substrate availabilities. We hypothesized that (i) translocation of different subsoil samples changes local environmental conditions (DOC, nutrient inputs, oxygen availability as well as amplitudes of temperature and water availability) and consequently soil microorganisms and C turnover. Furthermore, we hypothesized that (ii) increases in substrate availability change microbial community composition and function in subsoils, with relatively greater effects as soil depth increases. We conducted a reciprocal soil transfer experiment under field conditions with subsoils from 10-20 and 110-120 cm soil depths in a ~100-year old temperate beech forest site in Lower Saxony, Germany. By adding different amounts of particulate ^{13}C-labelled cellulose we changed the quantitative substrate availability of the soil samples.

5.2 Materials and methods

Site description

The study site belongs to the SUBSOM-Project (www.subsom.de) and is located in the Grinderwald (52° 34' 22" N 9° 18' 51" E), a ~100-years old temperate beech (*Fagus sylvatica* L.) forest 40 km northwest of Hannover in Lower-Saxony, Germany. The climate is temperate and humid with mean annual precipitation and temperature in the time period from 1981 to 2010 of 762 mm and 9.7 °C, respectively. The climate data were provided by the German Meteorological Service (DWD) monitoring station in Nienburg in the vicinity of the study area. The soil is an acid and sandy Dystric Cambisol (IUSS Working Group WRB, 2014) with soil pH ($CaCl_2$)

values ranging from 3.3 (topsoil) to 4.5 (subsoil) and mean sand, silt and clay contents of 77.3 %, 18.4 % and 4.4 %, respectively. The mean nitrogen (N) contents were 0.45 g kg^{-1} in topsoil (10 cm depth) and 0.02 g kg^{-1} in subsoil (110 cm). Parent materials for pedogenesis are fluvial and aeolian sandy deposits from the Saale glaciation (Angst et al., 2016). Table 5.1 lists the soil properties of a soil profile at the Grinderwald site.

Table 5.1: *Soil parameters of the field site.*

Soil horizon	Depth (cm)	pH ($CaCl_2$)	SOC (g kg^{-1})	Sand (%)	Silt (%)	Clay (%)
AE	0-2	3.3	27	70	26	4
Bsw	2-12	3.4	17	65	30	5
Bw	12-36	4.4	7	67	29	4
BwC	36-65	4.5	3	73	24	3
C	65-125	4.4	0.4	95	4	1
2C	125-150	4.1	0.1	81	11	8
2Cg	150-180	4.2	0.8	72	19	9
3C	180+	4.2	<0.1	95	4	1

Experimental setup

In total, 12 treatments were established: soil originating from 10-20 and 110-120 cm x 3 levels of substrate availability x return of soils back into 20 and 120 cm. Each treatment was sampled in triplicate after 1, 4 and 12 months. Three beech trees with distances of between 25 and 30 m from each other and diameter at breast heights (DBH) of 35 to 40 cm were selected. Around each of these trees, three profile pits with a distance of 2.5 m between the tree facing profile wall and the tree were excavated. The positions of the profile pits around the trees were randomly selected. All nine profile pits had a length of 1.60 m and a depth of > 1.20 m. Prior to excavation of the profile pits the litter layer was removed and stored separately. During excavation of the nine profile pits, upper subsoil from 10-20 cm (Bsw-Bw horizon; thereafter: SUB20) and lower subsoil from 110-120 cm (C horizon; thereafter: SUB120) soil depths were taken, mixed separately for the two depths and passed through a 2.0 mm sieve to remove roots and stones.

One hundred eight PVC containers (2.0 cm height, 10.5 cm inner diameter, 173.1 cm^3 volume) were filled with 242.3 g SUB20 and 277.0 g SUB120 soils, respectively. These amounts were calculated according to the soil bulk densities: 1.4 g cm^3 at 20 cm depth and 1.6 g cm^3 at 120 cm depth. The top and bottom sides were closed with micro mesh PA-material with a mesh size of 500 µm to allow vertical water flow and microbial exchange between container and surrounding soil. To manipulate quantitative substrate availability, ^{13}C enriched cellulose (1.2 atom % ^{13}C, IsoLife B.V., Netherlands) derived from maize stem (*Zea mays* L.) with a mean particle size of approximately 100 µm was added in three different concentrations to both SUB20 and SUB120 samples: no addition, 1%, and 5% of the total carbon content of the Bsw and C horizons, respectively. The amount added to the SUB20 samples was 41.2 mg ^{13}C-cellulose (1%) and 206.0 mg ^{13}C-cellulose (5%), while that to the SUB120 samples was 8.3 mg ^{13}C-cellulose (1%) and 41.5 mg ^{13}C-cellulose (5%). Cellulose and soil were thoroughly mixed to ensure homogeneous distribution of the cellulose. This resulted in six types of containers (2 soil depths x 3 cellulose additions).

The containers were incorporated into the tree-facing, undisturbed profile walls (Fig. 5.1). In each pit, one container of each type was incorporated into the profile wall at 20 cm and at 120 cm soil depths. The positions of the different containers within each soil depth at any one pit were randomly selected. The distance between neighboring containers was 12 cm and the positions of the containers in the upper layer were offset from the containers in the lower layer to minimize vertical interference. After incorporation, all profile pits were refilled with soil separately stored during excavation appropriately to the soil horizon sequence and litter was placed on the top corresponding to the initial litter amount and thickness.

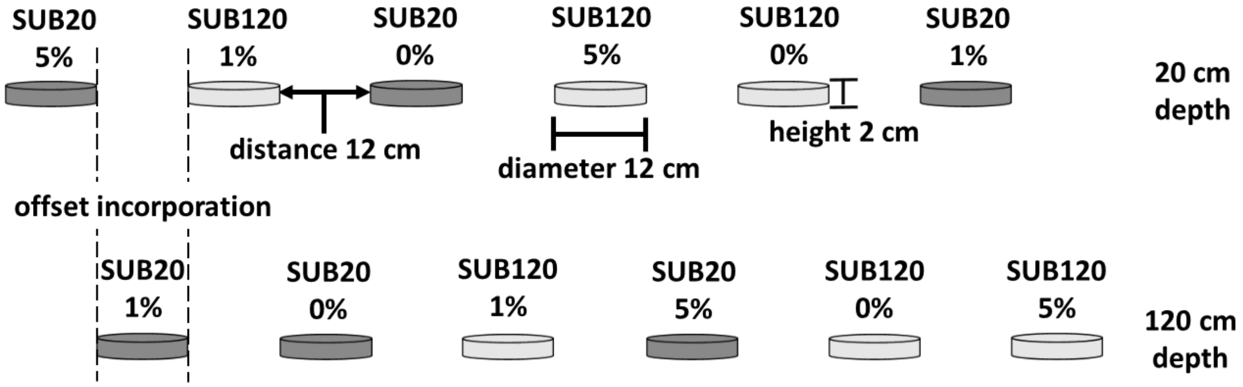
SUB20
5%
SUB120
1%
SUB20
0%
SUB120
5%
SUB120
0%
SUB20
1%
20 cm
depth
distance 12 cm
diameter 12 cm
height 2 cm
offset incorporation
SUB20
1%
SUB20
0%
SUB120
1%
SUB20
5%
SUB120
0%
SUB120
5%
120 cm
depth

Figure 5.1 Exemplary front view of one of nine tree facing profile walls with six soil containers (treatments: SUB20 + 0% cellulose, SUB20 + 1% cellulose, SUB20 + 5% cellulose, SUB120 + 0% cellulose, SUB120 + 1% cellulose and SUB120 + 5% cellulose) randomly incorporated into both soil depths (20 cm and 120 cm). Due to the randomized distribution of the different containers in the two depths of each of the nine profile pits this is an exemplary incorporation pattern to illustrate the incorporation design.

The experiment was established in June 2013 and one of the three profile pits surrounding each of the three trees was randomly selected and sampled after one (July 2013), four (October 2013) and twelve (June 2014) months. The samples were immediately cooled at 0°C for transport. After sieving (< 2 mm), the soil samples were stored at -23 °C until further analysis. Soil water content of each soil sample was determined gravimetrically after drying for 72 h at 60 °C and all presented data are related to soil dry weight.

Analyses

δ^{13}C of microbial biomass C, extractable organic C (EOC) and extractable N (ETN)

The chloroform fumigation extraction (CFE) method (Vance et al.,1987) was used to determine microbial biomass carbon (C_{mic}) according to Marhan et al. (2010). Microbial C was calculated using a k_{EC} factor of 0.45 (Joergensen and Mueller, 1996). Extractable organic carbon (EOC) and extractable total nitrogen (ETN) were calculated from the values of the non-fumigated samples.

The determination of δ^{13}C of microbial biomass C was done as described by Marhan et al. (2010).

The following equation was used for the calculation of δ^{13}C of microbial biomass:

$$\delta^{13}C_{mic} = \frac{C_{nf} x\ \delta_{nf} - C_f x\ \delta_f}{C_{nf} - C_f},$$

where C_{nf} and C_f are extracted organic C content (µg C g^{-1} soil) of the non-fumigated and fumigated samples and δ_{nf} and δ_f are the corresponding δ^{13}C values.

The calculation of cellulose-derived C (%) was done using the following equation:

$$\%\ C - cellulose = \frac{\delta_{sample} - \delta_{reference}}{\delta_{cellulose} - \delta_{soil}} x100,$$

where δ_{sample} is the δ^{13}C value of the respective sample, $\delta_{reference}$ is the δ^{13}C mean value of the respective non-^{13}C-addition sample, $\delta_{cellulose}$ is the average δ^{13}C value of the added cellulose (98.8 ‰), and δ_{soil} is the average δ^{13}C value of the upper (-27.93 ‰) or lower (-26.67 ‰) subsoil used for the transfer experiment.

Fungal biomass

Fungal biomass in soil was determined following the method of Djajakirana et al. (1996). For the extraction of ergosterol, one gram of SUB20 subsoil and four g of SUB120 subsoil were used and analysed as described by Müller et al. (2016).

δ^{13}C Phospholipid fatty acid analyses (PLFA)

For lipid extraction and fractionation according to the method of Frostegård et al. (1991), 16 g of field moist SUB20 subsoil and 24 g of field moist SUB120 subsoil were used and fatty acid methyl esters (FAMEs) were determined according to Kramer et al. (2013). The abundances of individual FAMEs were expressed in nmol per g soil. The fatty acids i15:0, a15:0, i16:0, 16:1ω7, i17:0, cy17:0, 18:1ω7 and cy19:0 were considered as bacterial PLFAs ($PLFA_{bac}$) Furthermore, i15:0, a15:0, i16:0 and i17:0 represented Gram-positive bacteria and cy17:0 and cy19:0 represented Gram-negative bacteria, following Kandeler et al. (2008), Frostegård and Baath (1996) and Zelles (1999). Fungal biomass was considered to be represented by the PLFA 18:2ω6 (Frostegård et al., 1993).

$\delta^{13}C_{PLFA}$ values were determined with the HP 6890 Gas Chromatograph (Agilent Inc., USA) coupled via a combustion III Interface (Thermo Finnigan, USA) to a Delta Plus XP mass spectrometer (Thermo Finnigan MAT, Germany) as described by Müller et al. (2016).

Calculation of cellulose-derived C (%) was done as described for microbial biomass C. Mean ^{13}C incorporation into the different microbial groups was calculated considering the relative proportion of the respective fatty acids to the total amount of the group-associated fatty acids. In addition, the total amount of ^{13}C-cellulose derived C incorporated into each microbial group (mg C g^{-1} added ^{13}C-cellulose) was calculated.

Bacterial abundance using quantitative PCR analyses

The FastDNA SPIN Kit for soil (BIO101, MP Biomedicals, USA) was used for extraction of the DNA from 0.3 g soil. The extracted DNA was quantified with a Nanodrop ND-2000 spectrophotometer (Thermo Scientific, USA) followed by dilution of the samples with ultra-pure water to a target concentration of 5 ng DNA µl^{-1}. The quantification of the abundances of *β-Proteobacteria*, *Actinobacteria*, *Acidobacteria*, *Firmicutes*, *Verrucomicrobia* and *Gemmatimonadetes* taxa via quantitative PCR (qPCR) (Fierer et al., 2005; Philippot et al., 2009; Bacchetti De Gregoris et al., 2011) was carried out with an ABI prism 7500 Fast System (Applied Biosystems, USA). Each qPCR run included two no template controls showing no or negligible values. The relative abundances of the specific taxa were calculated by dividing the absolute abundance of a specific taxon by the sum of the absolute abundances of all investigated taxa. Table S5.1 lists the primers, thermal cycling conditions and efficiencies.

Enzyme activity analyses

Potential activities of β-glucosidase (EC 3.2.1.21), β-xylosidase (EC 3.2.1.37), N-acetyl-β-glucosaminidase (EC 3.2.1.52) and cellulose 1-4-β-cellobiosidase (EC 3.2.1.91) were measured according to the method of Marx et al. (2001) described by Kramer et al. (2013) in detail using four g of soil per sample. Xylanase activity was analysed according to the method developed by

Schinner and von Mersi (1990) and modified by Ali et al. (2015). Potential activities of phenoloxidase and peroxidase were measured as described by Johnsen and Jacobsen (2008).

Microbial nutrient status

Microbial nutrient status was measured after 12 months in soils amended with 5% cellulose using a Respiration Measurement System (RMS, ETS, Darmstadt, Germany) with automated electrolytic microrespirometers (Scheu, 1992). Measurements were conducted in a water bath (Julabo CF41, Julabo GmbH, Germany) at 20°C. Microbial nutrient status was determined as the respiratory response of soil microorganisms to different carbon and nutrient amendments (C, C+N, C+P and C+N+P). C was added to each amendment type since previous measurements revealed a primary C limitation (C compared to H_2O), and the respiratory responses of N, P and N+P amendments alone were much lower as compared to amendments including C. The amendments were added as aqueous solutions with a quantity of 100 µl g^{-1} soil fresh weight, 6 mg glucose g^{-1} soil fresh weight for SUB20 samples, and 2 mg glucose g^{-1} soil fresh weight for SUB120 samples. Nitrogen (as $(NH_4)_2SO_4$) and phosphorus (as KH_2PO_4) were added respecting a C:N:P mass ratio of 10:2:1 (Anderson and Domsch, 1980). Fifteen g (SUB20) or 20 g (SUB120) soil were weighed into sample chambers, respectively, and measured for up to 40 h. After an initial phase (4 to 6 h) of maximal initial respiratory response (MIRR; Anderson and Domsch, 1978) microorganisms began to grow. This microbial growth, expressed by cumulative additional microbial respiration up to a maximum respiration rate (AMR), was used to determine the microbial nutrient status (Scheu, 1993). The relative changes (%) in AMR of the C+N, C+P and C+N+P treatments compared to C amendment alone were used as indicators of nutrient limitations to microbial growth after removing the primary C limitation.

Statistical analyses

Effects of cellulose addition (cellulose), translocation, sampling date (date) and interactions of these factors were analysed with linear mixed-effects (lme) models separately for SUB20 and SUB120 samples. Due to the experimental design, tree was set as random factor. Effects of cellulose addition, translocation and sampling date on the bacterial community structure were tested by MANOVA with tree as independent factor. Effects of nutrient addition (C, C+N, C+P, C+N+P), translocation, and their interactions on microbial respiration (microbial nutrient status) were analysed with lme models separately for SUB20 and SUB120. Significance was tested for $p < 0.05$ in all cases. Homogeneity of variance was tested for all parameters by Levene's test. All statistical analyses were carried out with R statistics version 3.2.1 (R Core Team, 2013) using the nlme package (Pinheiro et al., 2015).

5.3 Results

Water content, pH and extractable organic C (EOC) and extractable total N (ETN)

Gravimetric water content in the SUB20 soils was higher (9 - 13 %) than in the less organic SUB120 samples (4 – 7 %) and generally below 30 % of the water holding capacity (WHC; data not shown) of both layers. Soils incorporated into 20 cm soil depth showed a clear seasonal variation (SUB20: 12 % (July), 9 % (October), 11 % (June); SUB120: 7 %, 4 %, 6 %) with the lowest water content in October 2013. In contrast, soils incorporated into 120 cm soil depth had generally higher water content and showed less seasonal variation (SUB20: 12 % (July), 12 % (October), 13 % (June) ; SUB120: 7 %, 7 %, 7 %) (date x translocation; SUB20: $F_{2, 40} = 5.4$, $p < 0.01$; SUB120: $F_{2, 40} = 5.7$, $p < 0.01$).

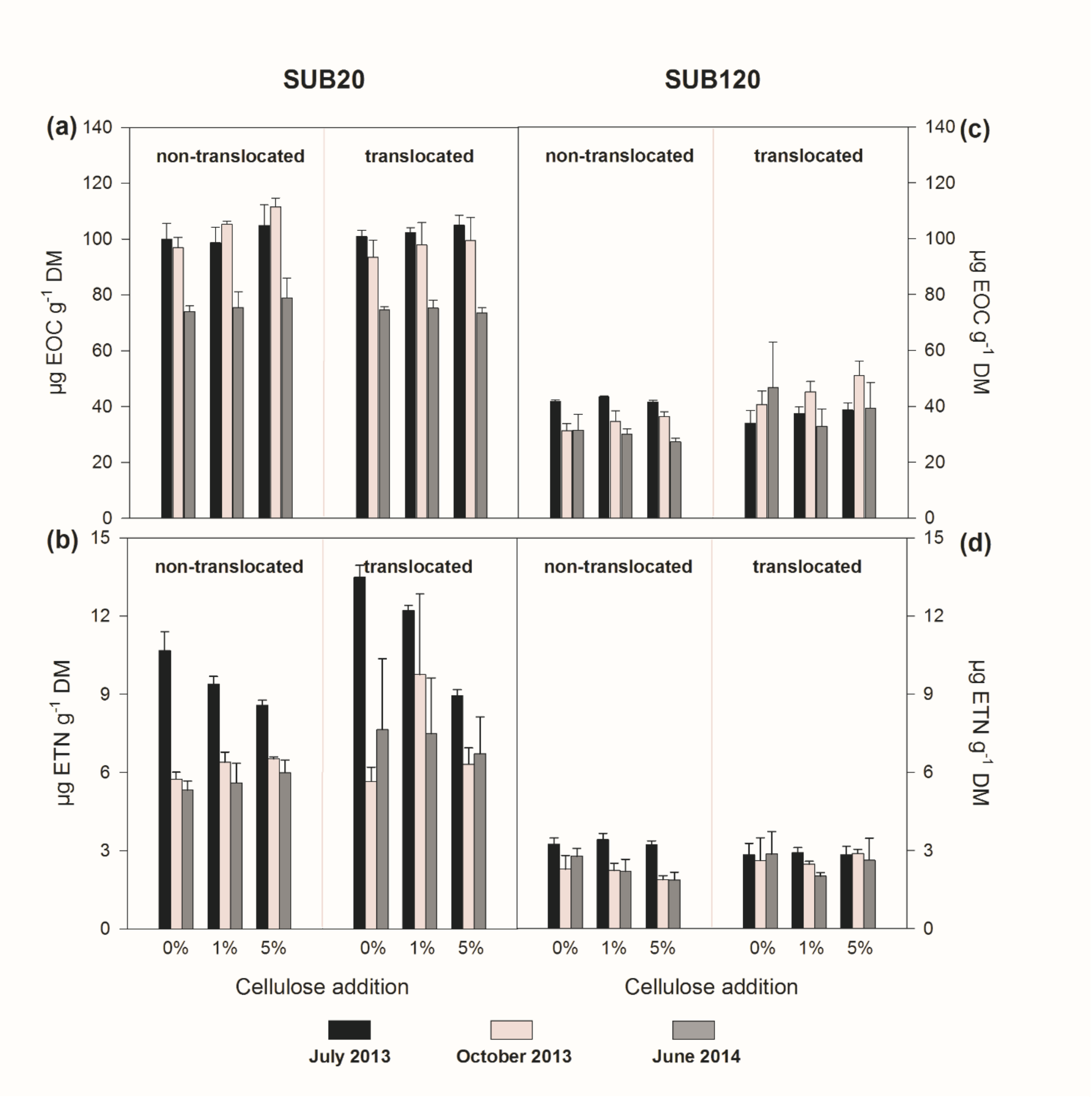

Figure 5.2 Amount of extractable organic carbon (EOC) (a and c) and extractable total nitrogen (ETN) (b and d) in SUB20 and SUB120 samples under different translocation and cellulose addition treatments at the sampling dates July 2013, October 2013 and June 2014. Error bars indicate standard deviation (n=3).

The pH values of SUB20 and SUB120 soils were not affected by translocation or cellulose addition and remained constant over the entire experimental period (data not shown).

EOC in SUB20 samples increased with increasing amounts of cellulose addition (cellulose; $F_{1, 40} = 8.5$, $p < 0.01$) and steeply decreased between the second and third sampling dates ($F_{2, 40} = 133.6$, $p < 0.001$) (Fig. 5.2 a). While EOC in translocated SUB120 samples showed no cellulose effects, EOC in non-translocated samples decreased over time; it increased from first to second and decreased from second to third sampling dates in translocated samples (date × translocation; $F_{2, 40} = 8.8$, $p < 0.001$) (Fig. 5.2 c).

ETN in SUB20 samples was generally higher if located at 120 cm depth (translocation; $F_{1, 40} = 13.1$, $p < 0.001$) (Fig. 5.2 b). Increasing amounts of added cellulose decreased ETN only at the first sampling date (date × cellulose; $F_{2, 40} = 4.0$, $p < 0.05$). In SUB120 samples, the ETN decreased from the first to second sampling dates in non-translocated samples only (date × translocation; $F_{2, 40} = 3.8$, $p < 0.05$) (Fig. 5.2 d).

Microbial biomass

Mean microbial biomass varied between 63.4 and 128.9 µg C_{mic} g^{-1} DM in the SUB20 treatments and 8.3 and 37.2 µg C_{mic} g^{-1} DM in the SUB120 treatments (Fig. 5.3 a and c). Whereas sampling time significantly influenced microbial biomass in both SUB20 and SUB120 samples (SUB20: $F_{2, 34} = 3.8$, $p < 0.05$; SUB120: $F_{2, 34} = 3.4$, $p < 0.05$), neither addition of cellulose nor reciprocal transfer of soils influenced C_{mic}.

Incorporation of ^{13}C into C_{mic} of SUB20 samples increased with increasing amounts of added cellulose (SUB20: $F_{1, 22} = 23.2$, $p < 0.001$) with the highest mean incorporation rate of 13 % at the third sampling date (Fig. 5.3 b). In SUB120 samples (Fig. 5.3 d) ^{13}C incorporation increased over time only in the 5% cellulose addition treatments (date × cellulose; $F_{2, 22} = 5.2$, $p < 0.05$) with up to 27 % cellulose derived C in C_{mic} at the last sampling date. Cellulose-C incorporation into microbial biomass was generally not affected by translocation.

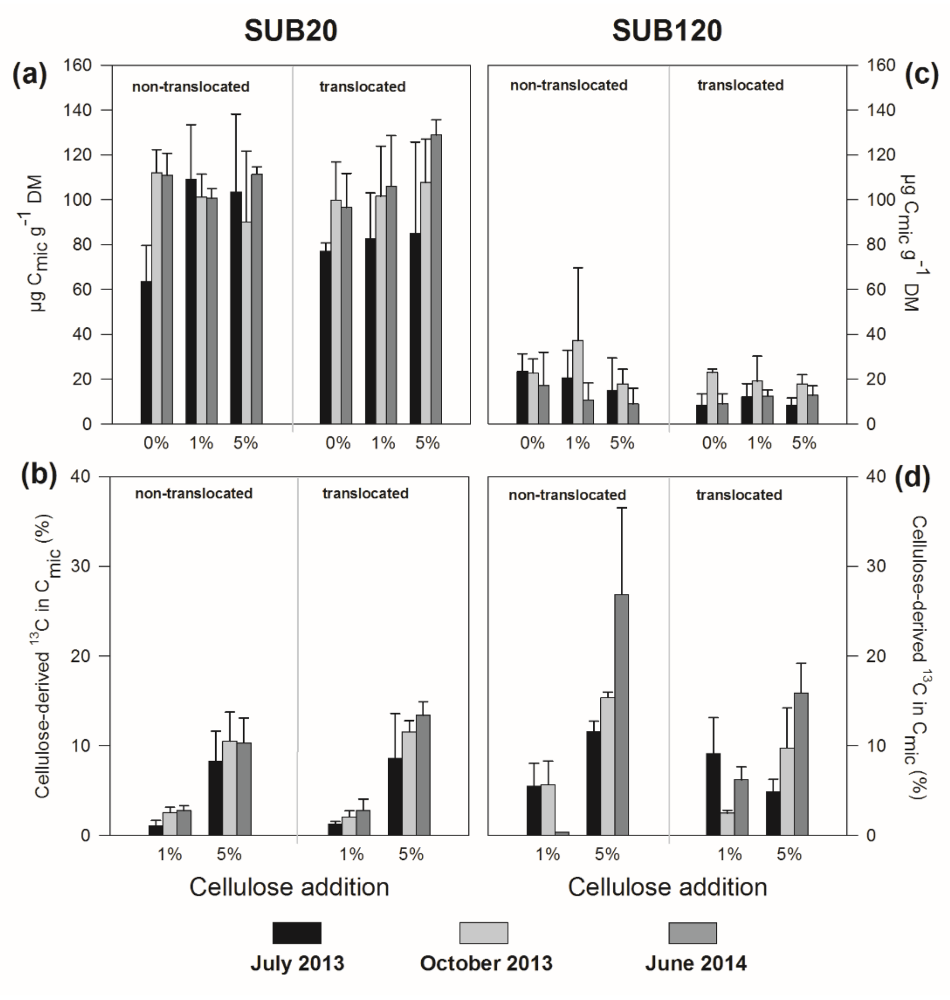

Figure 5.3 Microbial biomass C (a and c) and relative incorporation of ^{13}C-cellulose-derived C into C_{mic} (b and d) in SUB20 and SUB120 samples under different translocation and cellulose addition treatments at the sampling dates July 2013, October 2013 and June 2014. Error bars indicate standard deviation (n=3).

PLFAs

In general, $PLFA_{bacteria}$ and $PLFA_{gram+}$ showed similar patterns and results of $PLFA_{bacteria}$ are, therefore, not described here. The abundances of $PLFA_{gram+}$, $PLFA_{gram-}$ and $PLFA_{fungi}$ in SUB20 samples (Fig. 5.4 a – c) were neither affected by cellulose addition nor by translocation, but $PLFA_{fungi}$ abundance increased over time ($F_{2, 34} = 23.7$, $p < 0.001$). However, the fungal to bacterial ratio in SUB20 samples (Table 5.2) increased due to cellulose addition ($F_{1, 40} = 11.7$, $p < 0.01$), decreased due to translocation ($F_{1, 40} = 14.0$, $p < 0.001$) and generally increased over the experimental period ($F_{2, 40} = 36.9$, $p < 0.001$).

The abundance of PLFAs in SUB120 samples (Fig. 5.4 d – f) was not affected by cellulose addition, but translocation to the upper subsoil environment increased abundances of $PLFA_{gram+}$ ($F_{1, 34} = 14.1$, $p < 0.001$) and $PLFA_{gram-}$ ($F_{1, 34} = 4.9$, $P < 0.05$). Furthermore, the abundance of $PLFA_{fungi}$ in SUB120 samples increased over time in translocated samples (date × translocation; $F_{2, 33} = 4.8$, $p < 0.05$). The fungal to bacterial ratio (Table 5.2) increased due to translocation ($F_{1, 40} = 24.7$, $p < 0.001$) and varied between the sampling dates ($F_{2, 40} = 6.1$, $p < 0.01$). Microbial PLFAs were highly correlated with C_{mic} ($r = 0.78$; $p < 0.001$).

In general, fungal PLFAs showed higher relative cellulose-C incorporation than bacterial PLFAs (Fig. 5.5 a - f). In both SUB20 and SUB120 samples, the highest cellulose-C incorporation into $PLFA_{fungi}$ (25.3 % and 20.8 % relative incorporation, respectively) was found in the treatments with 5 % cellulose addition (SUB20: date × cellulose; $F_{2, 22} = 6.5$, $p < 0.01$; SUB120: $F_{1, 22} = 31.7$, $p < 0.001$; Fig. 5.5 a - f). For SUB120 samples, relative incorporation rates into $PLFA_{fungi}$ were higher in non-translocated than in translocated samples (translocation; $F_{1, 22} = 7.8$, $p < 0.05$).

In SUB20 samples $PLFA_{gram+}$ showed increasing relative incorporation over time depending on the amount of added cellulose (date × cellulose; $F_{2,\,22} = 6.3$, $p < 0.001$). Furthermore, cellulose-C incorporation into $PLFA_{gram-}$ increased with increasing cellulose amount ($F_{1,\,14} = 88.1$, $p < 0.001$) and over time ($F_{2,\,14} = 7.4$, $p < 0.05$). For SUB120 samples, cellulose-C incorporation (%) into $PLFA_{gram+}$ increased with time, which was pronounced in non-translocated samples (date × translocation; $PLFA_{gram+}$: $F_{2,\,22} = 6.6$, $p < 0.01$) and in samples with addition of 5 % cellulose (date × cellulose: $F_{2,\,22} = 5.7$, $p < 0.05$). Increasing amounts of added cellulose increased relative incorporation into $PLFA_{gram-}$ (cellulose; $F_{1,\,22} = 105.4$, $p < 0.001$). ^{13}C PLFAs were highly correlated with $^{13}C_{mic}$ ($r = 0.82$; $p < 0.001$).

Table 5.2: *Mean ratios of $PLFA_{fungi}$ / $PLFA_{bacteria}$*

		SUB20			SUB120		
Incorporation depth (cm)	**Cellulose addition**	**July 2013**	**October 2013**	**June 2014**	**July 2013**	**October 2013**	**June 2014**
20	0%	0.05	0.06	0.09	0.13	0.24	0.52
20	1%	0.05	0.07	0.08	0.12	0.34	0.39
20	5%	0.06	0.06	0.13	0.10	0.24	0.37
120	0%	0.04	0.05	0.08	0.08	0.08	0.08
120	1%	0.04	0.04	0.09	0.08	0.11	0.17
120	5%	0.05	0.05	0.11	0.09	0.12	0.14

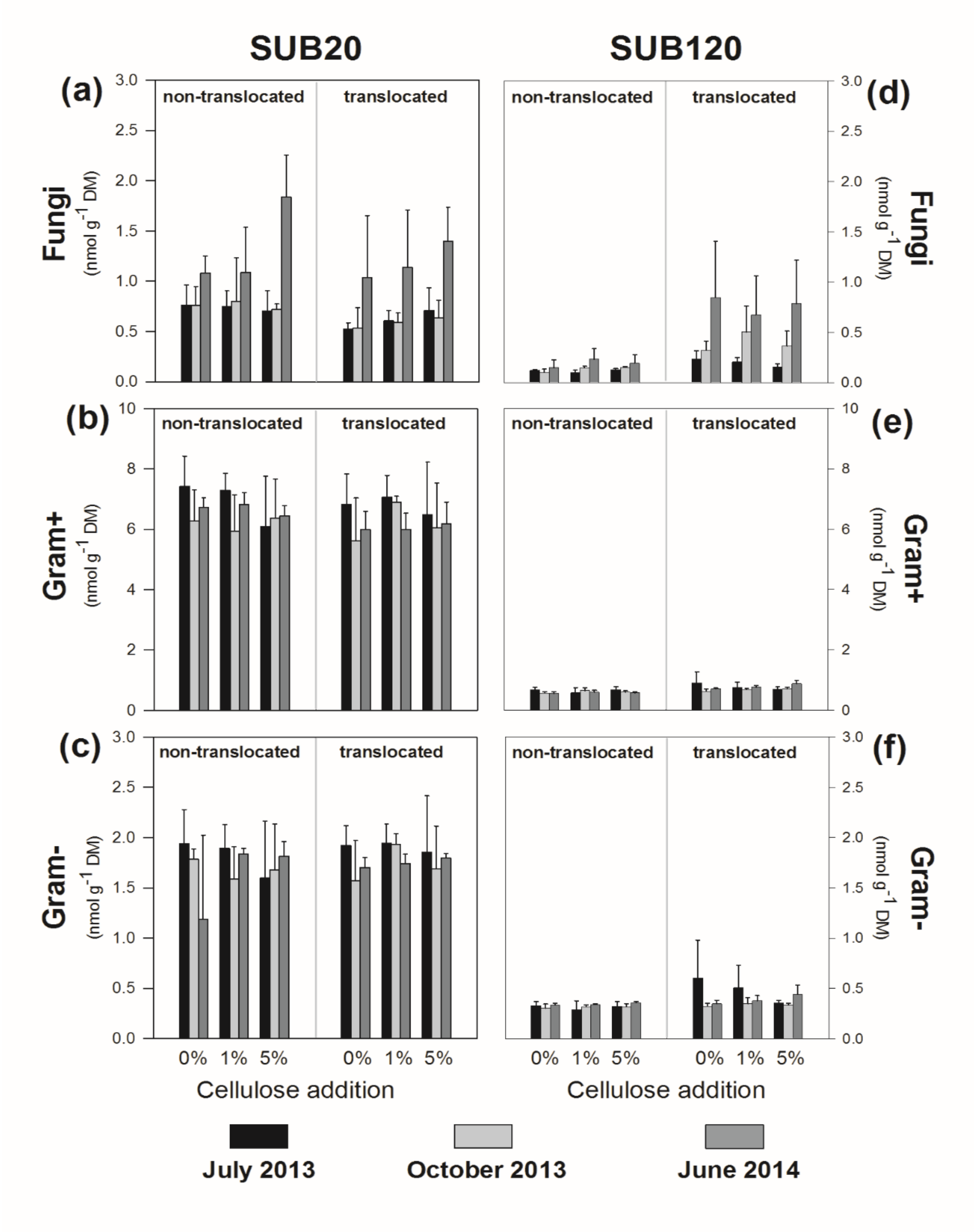

Figure 5.4 Abundance of gram-positive bacteria ($PLFA_{gram+}$), gram-negative bacteria ($PLFA_{gram-}$) and fungi ($PLFA_{fungi}$) in SUB20 (a, b, c) and SUB120 (d, e, f) samples under different translocation and cellulose addition treatments at the sampling dates July 2013, October 2013 and June 2014. Error bars indicate standard deviation (n=3).

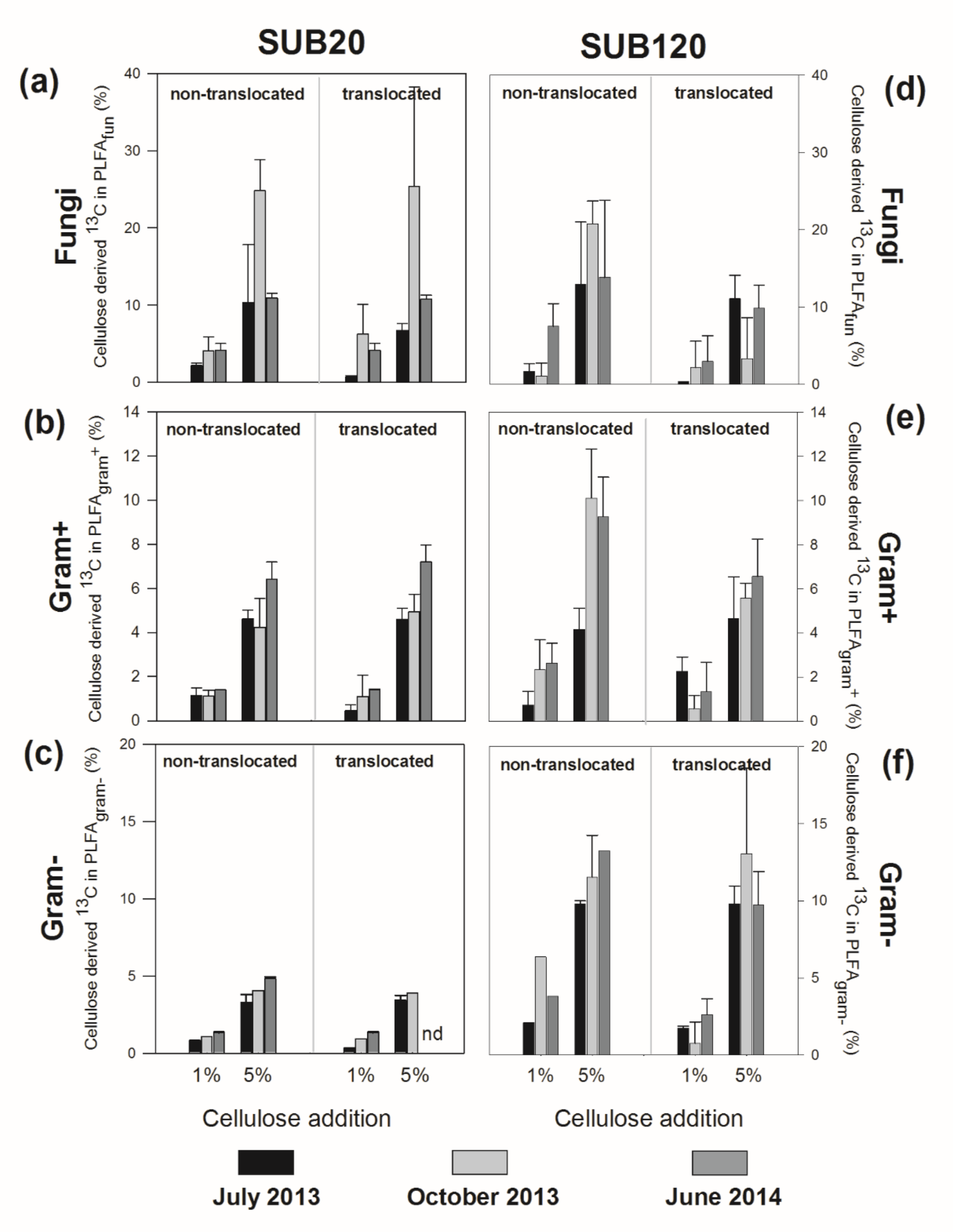

Figure 5.5 Relative incorporation of ^{13}C-cellulose-derived C into gram-positive bacteria (PLFA$_{gram+}$), gram-negative bacteria (PLFA$_{gram-}$) and fungi (PLFA$_{fungi}$) in SUB20 (a, b, c) and SUB120 (d, e, f) samples under different translocation and cellulose addition treatments at the sampling dates July 2013, October 2013 and June 2014. Error bars indicate standard deviation (n=3).

Absolute amounts of incorporated cellulose-C (mg ^{13}C-cellulose derived C g^{-1} cellulose) followed similar temporal patterns to those of relative incorporation. The treatment patterns, however, differed between absolute amount incorporation and relative incorporation, with absolute amount incorporation showing comparable proportions of added cellulose-C incorporated into the 1% and 5% cellulose addition treatments. The absolute amount of incorporated cellulose in PLFA$_{gram+}$ and PLFA$_{fungi}$ in SUB20 samples (Fig. S5.1 a - c) was not affected by cellulose addition or translocation, but increased during the experiment (PLFA$_{gram+}$: $F_{2, 22} = 4.7$, $p < 0.05$; PLFA$_{fungi}$: $F_{2, 22} = 13.7$, $p < 0.001$). The absolute amount incorporated into PLFA$_{gram-}$ was much lower than for the other groups and increased over the experimental period with slightly higher values in samples with 1% than with 5% cellulose addition (date × cellulose; $F_{1, 14} = 6.4$, $p < 0.05$).

In SUB120 samples (Fig. S5.1 d - f), the absolute amount of incorporated cellulose-C into PLFA$_{fungi}$ increased over time ($F_{2, 22} = 4.8$, $p < 0.05$) and was not influenced by added cellulose and translocation. Cellulose-C in PLFA$_{gram+}$ was higher in non-translocated samples and generally increased with time except for the translocated samples with addition of 1 % cellulose (date × translocation; $F_{2, 22} = 3.9$, $p < 0.05$). Incorporation of ^{13}C into PLFA$_{gram-}$ was higher in SUB120 than in SUB20.

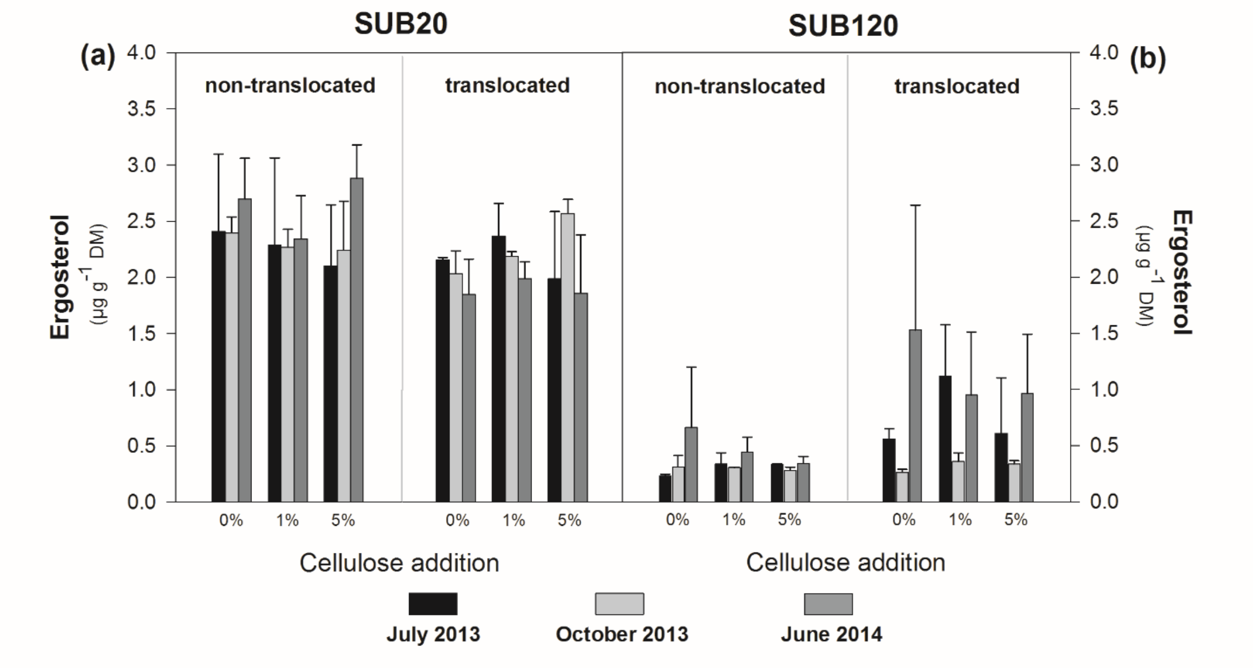

Figure 5.6 Amount of ergosterol in SUB20 (a) and SUB120 (b) samples under different translocation and cellulose addition treatments at the sampling dates July 2013, October 2013 and June 2014. Error bars indicate standard deviation (n=3).

Fungal biomass (ergosterol)

The mean ergosterol content varied between 1.85 and 2.88 µg g^{-1} DM in SUB20 and 0.23 and 1.53 µg g^{-1} DM in SUB120 samples (Fig. 5.6 a and b). Ergosterol content was not affected by cellulose additions, but translocation caused a significant decrease (-14 %) in SUB20 ($F_{1, 34} = 4.9$, $p < 0.05$) and an increase (+106 %) in SUB120 ($F_{1, 34} = 11.0$, $p < 0.01$) samples. Additionally, ergosterol content in SUB120 samples varied significantly between sampling dates ($F_{2, 34} = 3.4$, $p < 0.05$) with a decrease of -20 % from first to second sampling dates and an increase of +131% from second to third sampling dates.

Bacterial community structure

In SUB20 samples (Fig. 5.7 a - c), *Acidobacteria* were the dominant taxa in all treatments and at all sampling dates with mean relative abundance of up to 76 %. Relative abundance of *Acidobacteria* decreased in translocated samples (translocation; $F_{1, 38} = 4.3$, $p < 0.05$) while that of *Actinobacteria* increased (translocation; $F_{1, 39} = 9.4$, $p < 0.01$). Cellulose addition had no significant effect on the relative abundances of any investigated taxa in SUB20 samples. In SUB120 samples (Fig. 5.7 d - f), *Acidobacteria* and *Actinobacteria* were the dominant taxa with mean relative abundances of up to 52 and 46 %, respectively. The abundance of *Acidobacteria* increased over the experimental period (date; $F_{2, 38} = 7.1$, $p < 0.01$). Relative abundance of *Actinobacteria* decreased at the first and increased at the second and third sampling dates in translocated samples compared to non-translocated samples (date × translocation; $F_{2, 38} = 3.4$, $p < 0.05$). In contrast to SUB20 samples, *β-Proteobacteria* in SUB120 samples also exhibited high relative abundances of up to 25 %.

The MANOVA of bacterial community structure in SUB20 and SUB120 samples indicated no effects of cellulose addition. The community structure in SUB20 samples was also not influenced by translocation but changed over the experimental period ($F_{2, 66} = 2.9$, $p < 0.01$). However, the communities in SUB120 samples developed differently in non-translocated and translocated samples over time (date × translocation; $F_{2, 70} = 2.1$, $p < 0.05$).

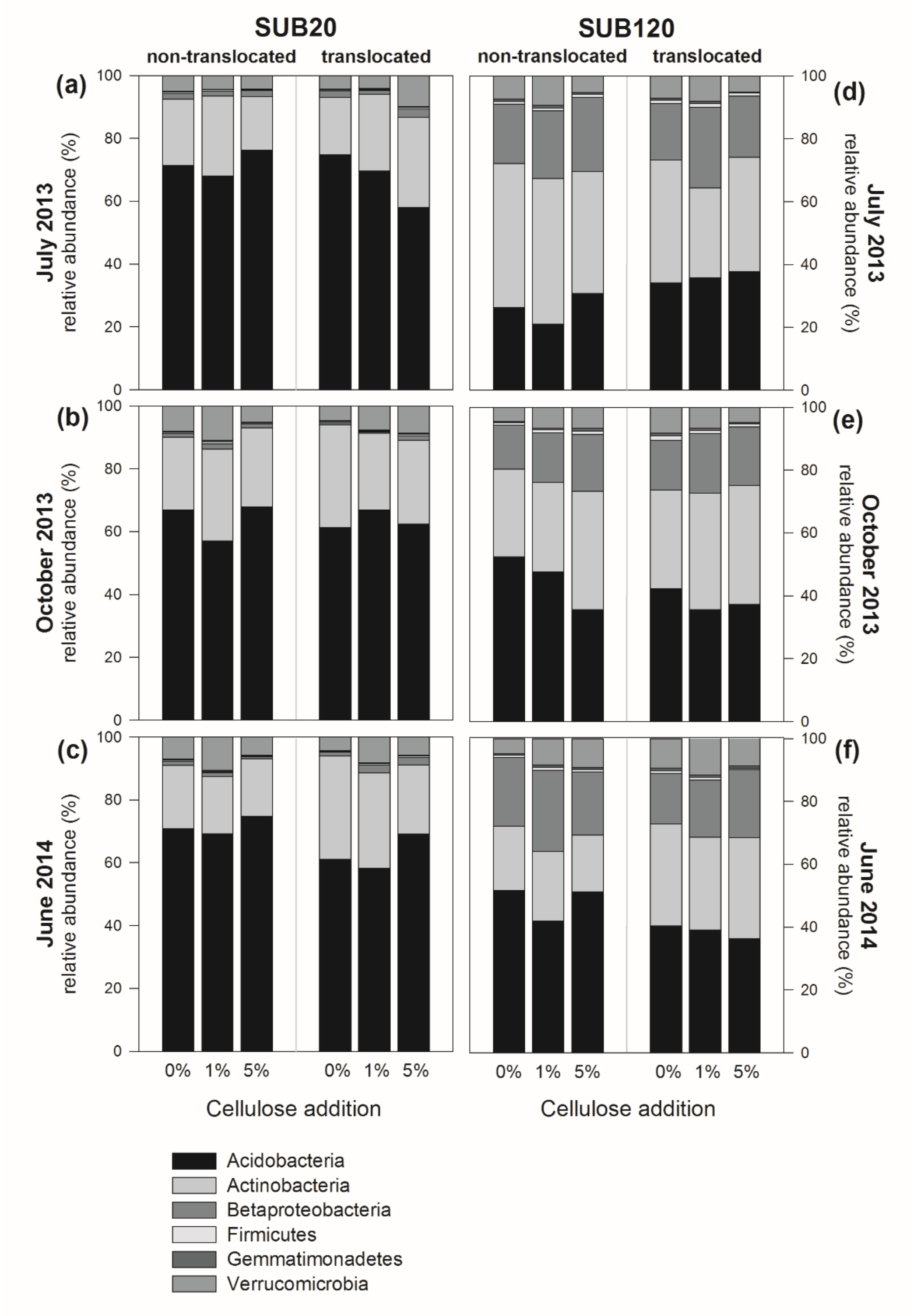

Figure 5.7 Bacterial community structures indicated by relative abundance (%) of the different bacterial taxa in SUB20 (a, b, c) and SUB120 (d, e, f) samples under different translocation and cellulose addition treatments at the sampling dates July 2013, October 2013 and June 2014.

Enzyme activities

Enzyme activities in SUB20 and SUB120 samples were mainly temporally variable over the sampling dates and were additionally affected by translocation (Tables S5.2 and S5.3). Cellulose addition increased the activities of 1-4-β-cellobiosidase (cellulose; $F_{2, 34} = 4.9$, $p < 0.05$) and xylanase (cellulose; $F_{2, 34} = 15.7$, $p < 0.001$) in SUB20 samples, while in SUB120 cellulose addition had no effect (Table S5.3). Translocation induced only minor changes with decreased 1-4-β-cellobiosidase activity (translocation; $F_{1, 34} = 6.1$, $p < 0.05$) and slightly increased phenoloxidase activity (translocation; $F_{1, 34} = 12.1$, $p < 0.01$). In contrast, enzyme activities in SUB20 samples showed no translocation effects.

Microbial nutrient status

Microbial respiratory responses indicated limitation of microbial growth by N when C-limitation was alleviated in both translocated and non-translocated SUB20 samples (Table S5.4). Mean respiration increased in samples with C+N amendments compared to samples with C amendments only (N; $F_{1, 16} = 164.9$, $p < 0.001$) and this was more pronounced in non-translocated samples, which increased 46 % (± 15) compared to translocated samples, which increased 30 % (± 8) (N × translocation; $F_{1, 6} = 5.4$, $p < 0.05$). Samples receiving C+P amendments showed similar respiratory responses to those receiving C amendments only. Furthermore, measurements revealed a subsequent P limitation when C and N limitations were excluded. This was seen in the samples amended with C+N+P, in which the mean respiratory increase was the highest with 154 % (± 37) and 106% (± 12) in non-translocated and translocated samples, respectively (N+P; $F_{1, 16} = 49.4$, $p < 0.001$).

Microbial nutrient status of the SUB120 samples showed a pattern similar to the SUB20 samples with C-limitation followed by N-limitation when C-limitation was alleviated (Table S5.4). Here, C+N amendments led to a mean respiratory increase of 75 % (± 37) in non-translocated and 57% (± 24) in translocated samples compared to samples with amended with C only (N; $F_{1,\ 16} = 31.8$, $p < 0.001$). Samples amended with C+P exhibited a lower but still significant increase in respiration of 16 % (± 9) and 28 % (± 15) for non-translocated and translocated samples, respectively (P; $F_{1,\ 16} = 20.5$, $p < 0.001$). The highest respiratory responses in both non-translocated and translocated SUB120 samples appeared in samples amended with C+N+P, with increases of 508 % (± 172) and 284 % (± 159) (N+P; $F_{1,\ 16} = 15.5$, $p < 0.01$).

5.4 Discussion

Effects of translocation on microbial abundance and function

The reciprocal transfer experiment made it possible to separate the importance of habitat conditions from substrate availability for microbially regulated C turnover in subsoils. Due to differences in habitat properties such as oxygen, substrate availability, or soil moisture, we expected a decrease in microbial biomass in SUB20 samples transferred to 120 cm depth and an increase in biomass in SUB120 samples transferred to 20 cm depth compared to the respective non-translocated samples. However, we did not find any changes in microbial biomass (Fig. 5.3 a and c) and, therefore, changes in habitat conditions were either not effective or not present.

We did not measure the oxygen concentrations in the two soil depths during the experiment but it may be that throughout the profile of the well aerated sandy textured soil, oxygen concentration conditions did not change in such a way as to limit microbial biomass. A study under similar site conditions by Chirinda et al. (2014) found non-limiting oxygen concentrations, not lower than 16 %, in subsoils with loamy and sandy textures, while a study of Salome et al. (2010) revealed that even oxygen levels of 5 % were sufficiently high to avoid limiting conditions. The water content at 120 cm depth was significantly higher and more stable over time than at 20 cm depth, but these differences in water content appear not to have directly influenced the microbial biomass. In general, however, the water content was below 30 % of the water holding capacity (WHC; data not shown) of both layers and, therefore, water content of both layers may have restricted microbial activity and abundance (Gordon et al., 2008), whereas oxygen concentration did not limit microbial growth in our study site.

Besides oxygen concentration and soil moisture, resource availability, especially carbon, has been identified as the most common microbial growth limiting factor in soils (Joergensen and Scheu, 1999; Ekblad & Nordgren, 2002; Demoling et al., 2007). In accordance with these studies, our respiration measurements under different C, N and P amendments revealed a primary C limitation followed by a subsequent N limitation for both SUB20 and SUB120 soil samples irrespective of translocation and sampling date. The N limiting conditions may have been induced by leaching of N during water pulses after heavy rainfall events (Austin et al., 2004; Gordon et al., 2008), as shown by increased concentrations of nitrogen in water that had percolated into deeper soil layers at the study site (Leinemann, personal communication). We expected improved substrate availability in translocated SUB120 samples due to increased C input by root exudation or DOC transport from organic horizons. However, EOC content as an indicator for substrate availability did not change and, thus may explain similar microbial activity and abundance in the two layers.

In general, microbial community structure changes significantly with increasing soil depth (Ekelund et al., 2003; Eilers et al., 2012). Consequently, we expected significant changes in microbial diversity and abundance of specific microbial groups due to translocation. Fungal abundance (ergosterol) decreased in translocated SUB20 and increased in translocated SUB120 samples (Fig. 5.6); therefore, fungal life in subsoils was restricted and transfer of deeper subsoil into upper subsoil stimulated fungal abundance. Nevertheless, we can only hypothesize as to which group of soil fungi profit from the transfer and develop into key drivers of organic matter decomposition in upper subsoils. This topic is especially interesting because recent studies have found that closely related microbial taxa can have similar capacities to utilize resources in natural systems (Talbot et al., 2013, 2015). Considering that transferred subsoils may also be colonised by saprotrophic as well as ectomycorrhizal fungi, future studies should clarify the phylogeny of soil fungi and sort single taxa according to their functional traits (either saprotrophic or ectomycorrhizal fungi). Recalcitrance of organic matter in subsoils may also be related to restricted growth of both saprotroph as well as ectomycorrhizal fungi. Consequently, the transfer of subsoil may increase not only the incorporation of C into fungal biomass, but also stimulate saprotrophic and ectomycorrhizal organic matter decomposition in the beech forest. The main factor may have been increased carbon availability (root exudates, DOC) in this environment (Fig. 5.2), with higher root density and closer spatial proximity to the litter/organic layer. Since EOC content was not affected in translocated SUB120 samples, fungi may have been able to translocate resources within their mycelia, enabling fungi to overcome local limitations in heterogeneously distributed resources at the µm to mm scale (Frey et al., 2000; Boberg et al., 2010, 2014). Additionally, fungi may have benefited from generally higher soil temperatures during summer in the upper subsoil environment (Castro et al., 2010).

While fungal abundance decreased slightly in translocated SUB20 samples, Gram$^+$ and Gram$^-$ bacteria (PLFA data; Fig. 5.4 b and c) remained at relatively constant levels. In line with this, bacterial community composition investigated with qPCR measurements showed only minor changes (Fig. 5.7). The relative increase in *Actinobacteria* in translocated SUB20 samples and the high abundance of these taxa in both SUB20 and SUB120 samples may be related to their adaptation to resource- or moisture-limited conditions and to the diverse metabolic capabilities within this phylum (Hartmann et al., 2009; Barnard et al., 2013). Also the highly abundant *Acidobacteria* are able to survive desiccation stress (Castro et al., 2010) and are generally the dominant phylum in slightly acidic and carbon rich soils (Rawat et al., 2012). Their metabolic versatility allows specific strains of this phylum to cope with low resource availability (Eichorst et al., 2011; Naether et al., 2012).

The main difference between the bacterial communities in SUB120 and those in SUB20 samples was the higher abundance of *β-Proteobacteria* in SUB120 samples. Several studies have described increased relative abundances of *β-Proteobacteria* in soils with pH > 4 (e.g. Lauber et al., 2009; Rousk et al., 2010). Since both translocated and non-translocated SUB120 samples had pH values of ~ 4 and thus higher pH values than SUB20 samples, this may explain the higher abundance of *β-Proteobacteria* in soils from the lower subsoil environment. However, none of the investigated bacterial phyla benefited from considerably higher carbon content in translocated SUB120 samples, highlighting the role of nutrient limitation, which only fungi were able to overcome.

Effects of cellulose addition on microbial abundance and function

To alleviate substrate limitation of soil microorganisms, we added cellulose. However, cellulose addition generally did not affect microbial biomass either in translocated or non-translocated SUB20 and SUB120 samples, respectively (Fig. 5.3 a and c). This may have been due to the relatively constant habitat conditions (e.g. oxygen and pH) within the soil profile.

Nevertheless, the micro-environment as well as the amount of added cellulose affected the relative ^{13}C incorporation from cellulose into soil microorganisms (Fig. 5.3 b and d). Specifically, reduced microbial ^{13}C incorporation in translocated SUB120 samples with 5 % cellulose addition indicated that, in accordance with the observed enhanced fungal growth in these samples, the added cellulose contributed a smaller proportion to the total substrate pool than in non-translocated samples. Although a substantial amount of cellulose-derived C was incorporated into the microbial biomass, the reduction of the primary growth limiting factor, carbon, did not result in a net increase in microbial biomass. This underscores the observation in our results that microorganisms were N limited in the presence of C (Table S5.4), and is in accordance with other studies investigating microbial growth limiting factors (Göransson et al., 2011; Kamble et al., 2013).

Since microbial communities generally change with increasing soil depth, we also expected changes in activity and function of individual microbial groups associated with carbon turnover. However, translocation affected relative ^{13}C incorporation into the different microbial groups only in SUB120 samples (Fig. 5.5), while ^{13}C-cellulose incorporation generally differed between microbial groups and between the 1 % and 5 % cellulose additions. The relatively higher ^{13}C incorporation into fungi compared to bacteria in both SUB20 and SUB120 samples emphasized the preferential use of cellulose by fungal decomposers. Despite the potentially high proportion of bacterial cellulose decomposers, e.g. *Actinobacteria*, *β-Proteobacteria* and *Bacteroidetes*, cellulose utilisation is more common in fungal decomposer communities (Edwards et al., 2008; Stursová et al., 2012; Větrovský et al., 2014). Additionally, fungi might have benefited from their higher tolerance to low pH values compared to bacterial decomposers (Rousk et al., 2010). For the discussion of experiments with the addition of substrates to soils with different microbial densities, it is critical to distinguish between the effects of either altered substrate to SOC ratios or changes in the substrate to volume ratios. For example, adding 5% cellulose to both non-translocated SUB20 and SUB120 samples resulted in higher relative ^{13}C incorporation rates with time into Gram^{+} bacteria in SUB120 samples than in SUB20 samples (Fig. 5.5), although the cellulose to SOC ratio was the same in both cases. We explain this by the observed increasing C limitation with depth, where C was found to be largely spatially inaccessible to microorganisms due to a pronounced heterogeneous distribution of C substrates in deeper soil layers (Niebuhr et al., unpublished results). The amount of added cellulose was similar for the 1% addition to SUB20 and the 5% addition to SUB120, resulting in the same cellulose to volume ratio; i.e. the same amount of cellulose could be used by soil microorganisms in a specific soil volume. However, the number of microorganisms in close vicinity to cellulose particles was lower and, at the same time, the cellulose to SOC ratio was higher in the 5% SUB120 samples, resulting in much higher incorporation rates (%) in these samples as compared to the 1% SUB20 samples. Increasing the amount of added substrate increased substrate accessibility for soil microorganisms (1 % < 5 % cellulose treatment) in both soil depths, respectively. This reduced energy-limited habitat conditions, and thus enhanced C-assimilation by soil microorganisms.

In contrast to SUB20 samples, relative ^{13}C incorporation into microbial groups in SUB120 samples was affected by translocation, resulting in decreased relative incorporation into Gram^{+} bacteria and fungi (Fig. 5.5). This underscores our hypothesis that generally increased carbon availability in the upper subsoil environment affects microbial habitat conditions and, therefore, microbial function. However, the degree of cellulose utilization in translocated SUB120 samples was as high as in non-translocated samples, as indicated by similar absolute amounts of incorporated ^{13}C g^{-1} cellulose (Fig. S5.1). This indicates a high energy demand and associated carbon turnover due to fungal growth and higher microbial activity, which was satisfied by additive utilization of cellulose and larger carbon pools (e.g. DOC) in this environment.

Among the bacterial communities in SUB20 samples, *Actinobacteria* may have been key decomposers of the cellulose due to their dominance in abundance and to the high proportion of cellulose derived C in Gram^{+} bacteria in SUB20 samples (Fig. S5.1). In contrast, the low amount of ^{13}C incorporated into Gram^{-} bacteria in SUB20 samples suggests that this group either used other carbon sources to a greater extent or remained in a dormant state (Fig. S5.1). For example, Pankratov et al. (2011) described Gram^{-} *Acidobacteria* as slow cellulose degraders, not competitive with other cellulose degrading phyla. This is in contrast to other studies, in which *Acidobacteria* were identified as important cellulose decomposers (Stursová et al., 2012), but this may be restricted to C-rich soils, which are clearly different from those at our experimental site. Relative incorporation into Gram^{-} bacteria in SUB120 samples was considerably higher than in the SUB20 samples (Fig. 5.5). *Acidobacteria*, as the most abundant phylum of Gram^{-} bacteria, were only to a limited extent involved in cellulose decomposition and, therefore, the higher incorporation rates into Gram^{-} bacteria in SUB120 samples were probably caused by high cellulose decomposition activities of *β-Proteobacteria*, which showed considerably higher abundances in SUB120 than in SUB20 samples (Fig. 5.7).

Spatial separation as an important factor for carbon accumulation in deeper soil layers

While the amount of added cellulose affected ^{13}C incorporation (%) into microbial PLFAs, ^{13}C utilization g^{-1} added cellulose was not affected by the amount of added cellulose (Fig. S5.1). We explain this by stressing the importance of the small-scale distribution of substrate and microorganisms and the consequences of their spatial separation. The cellulose was not added in suspension but as crystalline cellulose particles and, even though the cellulose particles were homogeneously distributed within the soil volume, each particle created, therefore, a hot spot of substrate availability affecting a specific soil volume. Based on the assumption that the amount of cellulose per newly created hot spot was similar for both the 1% and 5% addition treatments, we expected the number of newly created hot spots to increase with increasing amounts of added cellulose (Fig. S5.2). In addition to the number of hot spots, the cellulose degradation capacity of the local community within each hot spot is of great importance. We observed generally increasing ^{13}C incorporation (%) into microbial PLFAs during the exposure time of 12 months (Fig. 5.5). We hypothesize, therefore, that the capacity for complete cellulose degradation was too low to degrade the amount of cellulose available in each hot spot. Increasing the number of cellulose hot spots could, theoretically, result in an overlap of hot spots. In such a case, overall ^{13}C utilization g^{-1} added cellulose (Fig. S5.1) would have decreased based on the low capacity to degrade cellulose. Since we did not observe lower ^{13}C utilization g^{-1} added cellulose in the 5% treatments compared to 1% cellulose addition, we hypothesize that even in the treatment with 5% cellulose addition cellulose hot spots were spatially separated from each other. Consequently, increasing the amount of added cellulose proportionally, i.e. linearly, increased the affected soil volume and the number of microorganisms affected by cellulose addition (Fig. S5.2). Although SUB20 and SUB120 soils showed similar patterns, the results of the two soil samples are not directly comparable in terms of spatial separation. Both soils differed in habitat conditions, such as the availability of C substrates, which may have resulted in changes of microbial physiological traits such as longer microbial biomass turnover times with increasing soil depth (Spohn et al., 2016).

The explanation of our results is supported by the following: The soil has a sandy texture with low aggregation, which results in a rather high contribution of large soil pores to the overall soil pore volume. Large soil pores as well as low moisture content of the site may have further limited the spatial extent and size of cellulose hot spots, since the relocation of enzymes, substrate and metabolites in the soil suspension may have been inhibited by spatial fragmentation of water-filled pores. Although fungi are potentially able to bridge air-filled pores, we suggest that this ability is directly related to the availability of energy. Energy limitation as well as a high proportion of air-filled pores may, therefore, have constrained fungal exploitation in our study to a rather small scale. The capacity of soil microorganisms to degrade cellulose is directly related to the activity of extracellular enzymes. Adding cellulose could potentially result in an increase in cellulose degrading enzymes such as β-glucosidase. However, in our study enzyme activities were generally low and showed only minor responses to cellulose addition (Table S5.2 and S5.3). Enzyme production is a nutrient demanding process (Schimel and Weintraub, 2003) and we suggest, therefore, that the N limitation in our soils inhibited the additional enzyme production needed to increase cellulose degradation. In addition, low enzyme activities may be explained by energy conservation of a mainly dormant microbial community in an energy limited soil environment, where microorganisms avoid the energy-intensive enzyme production which may exceed a possible energy gain through newly exploited carbon resources (De Nobili et al., 2001; Spohn et al., 2016). A laboratory experiment with top- and subsoils derived from samplings along three vertical transects in a grid sampling pattern from the same experimental site also indicated that spatial separation is an important factor for low C-turnover in subsoils (Niebuhr et al., unpublished results). They detected, with multi-substrate enzymatic assay and substrate induced respiration experiments, the presence of labile SOC in subsoil, but largely spatially inaccessible for microorganisms, leading to highly variable microbial activities and C-turnover restricted mainly to “hotspots”. Finally, the incorporation rates for both SUB20 and SUB120 samples (Fig. 5.5) indicate that spatial separation of substrates and soil microorganisms could be an important factor influencing low C-turnover and, consequently, carbon accumulation in subsoil with increasing relevance with depth.

5.5 Conclusion

The reciprocal translocation of subsoils revealed no or only minor depth-dependent effects on microbial biomass, community structure and activity, indicating comparable environmental conditions (e.g. oxygen availability) in both subsoil environments. Therefore, our hypothesis regarding depth-dependent effects on soil microbial parameters due to translocation must be largely rejected. However, nutrient and water limitation inhibited microbial net growth in SUB120 samples translocated to the growth promoting (via carbon availability) upper subsoil environment, while the carbon stock in translocated SUB20 samples remained sufficiently high to keep the microbial biomass abundance constant. In general, fungi responded more strongly than bacteria to changes in environmental conditions and substrate availability. Fungal growth in the upper subsoil environment was accelerated by both high availability of carbon resources (e.g. DOC, rhizodeposits) and added cellulose. Since substrate effects were lower than hypothesized, factors like N and water limitation may have masked the response of bacterial decomposers in particular. Furthermore, spatial separation between substrates and decomposers may be an important factor contributing to carbon accumulation in subsoil, an effect which is accelerated under low moisture conditions. Future studies should investigate bacterial and fungal responses to changes in micro-environmental conditions and substrate availability under non-limiting water and nutrient conditions to improve the predictions of future SOC content and storage potential of subsoils. In addition, there is still a need to understand the dynamics and drivers of fungal communities in subsoils to better understand long-term carbon storage in forest ecosystems. Specifically, we need to know why fungal life in subsoils is restricted and why changing the micro-environment by transferring deeper subsoil into lower subsoil stimulates fungal abundance and activity of subsoils.

5.6 Acknowledgments

We would like to thank Stefanie Heinze and Bernd Marschner for the project coordination, Sabine Rudolph and Heike Haslwimmer for their great support in the laboratory, Wolfgang Armbruster at Institute of Food Chemistry at University of Hohenheim for IRMS measurements, Kathleen Regan for English corrections and the many helpers during the establishment of the experiment and soil samplings at the field site. We also thank the Associate Chief Editor Carmen Trasar Cepeda and two anonymous reviewers for their constructive comments. This study was carried out within the framework of the Research Unit “The Forgotten Part of Carbon Cycling: Organic Matter Storage and Turnover in Subsoils (SUBSOM)” funded by the Deutsche Forschungsgemeinschaft DFG (FOR1806, KA 1590/11-1).

5.7 Supplementary materials

Table S5.1: *qPCR primers and conditions.*

Gene	Primer*	Thermal profile**	No. of Cycles	Efficiency mean (%)	Reference
Acidobacteria	Acid31 Eub518	95°C – 10 m 95°C – 15 s, 55°C – 30 s, 72°C – 30 s, 76°C – 30 s	1 35	95%	(Philippot et al., 2009)
Actinobacteria	Act920F3 Act1200R	95°C – 10 m 95°C – 15 s, 61.5°C – 30 s, 72°C – 30 s, 76°C – 30 s	1 35	82%	(De Gregoris et al., 2011)
β-Proteobacteria	Eub338 Bet680	95°C – 10 m 95°C – 15 s, 55°C – 30 s, 72°C – 30 s, 80°C – 30 s	1 35	111%	(Philippot et al., 2009)
Firmicutes	Lgc353 Eub518	95°C – 10 m 95°C – 15 s, 60°C – 30 s, 72°C – 30 s, 79°C – 30 s	1 35	108%	(Fierer et al., 2005)
Verrucomicrobia	Verr 349 Eub 518	95°C – 10 m 95°C – 15 s, 60°C – 30 s, 72°C – 30 s, 77°C – 30 s	1 35	95%	(Philippot et al., 2009)
Gemmatimonadetes	Gem440 Eub518	95°C – 10 m 95°C – 15 s, 58°C – 30 s, 72°C – 30 s, 78°C – 30 s	1 35	109%	(Philippot et al., 2009)

*Primer concentration was 10 pmol μl^{-1}
**Additionally, a 60°C to 95°C step was added to each run to obtain the denaturation curve specific for each amplified sequence.

***Table S5.2:** Enzyme activities in SUB20 and SUB120 samples with different treatment types (T = translocated, NT = non-translocated, 0% = no cellulose addition, 1% = 1% cellulose addition, 5% = 5% cellulose addition) and sampling dates. Data are presented as mean ± standard deviation (n =3)*

			Treatment					
Soil	**Parameter**	**Sampling date**	**0% NT**	**1% NT**	**5% NT**	**0% T**	**1% T**	**5% T**
SUB20	β–glucosidase [nmol/ g DM x h]	July 2013	4.95 (±1.92)	4.83 (±2.47)	4.33 (±2.29)	3.95 (±3.27)	3.97 (±2.59)	5.61 (±3.12)
		October 2013	13.07 (±4.42)	10.64 (±6.37)	12.06 (±1.58)	9.27 (±2.27)	10.32 (±0.95)	18.69 (±2.91)
		June2014	10.67 (±5.66)	12.96 (±3.80)	11.90 (±7.37)	6.73 (±3.10)	5.38 (±4.92)	14.95 (±3.40)
SUB120	β–glucosidase [nmol/ g DM x h]	July 2013	0.97 (±0.86)	1.49 (±1.56)	0.81 (±0.58)	0.79 (±0.38)	1.02 (±0.58)	0.98 (±0.48)
		October 2013	3.67 (±1.29)	3.40 (±1.10)	4.17 (±1.01)	2.23 (±0.24)	4.22 (±2.64)	1.76 (±1.07)
		June2014	3.87 (±2.09)	3.06 (±1.29)	2.73 (±1.33)	4.97 (±1.94)	3.62 (±1.48)	2.21 (±0.35)
SUB20	β–xylosidase [nmol/ g DM x h]	July 2013	3.44 (±1.92)	3.37 (±2.34)	3.02 (±2.22)	2.66 (±2.02)	2.78 (±2.20)	3.87 (±2.30)
		October 2013	7.37 (±0.76)	5.24 (±2.95)	9.46 (±2.30)	7.42 (±2.23)	7.67 (±1.46)	11.04 (±1.79)
		June2014	7.68 (±1.67)	10.92 (±3.28)	7.92 (±4.92)	4.08 (±3.38)	6.45 (±4.91)	11.22 (±0.68)
SUB120	β–xylosidase [nmol/ g DM x h]	July 2013	0.34 (±0.33)	0.53 (±0.41)	0.43 (±0.27)	0.27 (±0.26)	0.59 (±0.25)	0.35 (±0.30)
		October 2013	1.37 (±0.79)	1.20 (±0.70)	1.63 (±0.95)	0.57 (±0.07)	0.57 (±0.07)	0.68 (±0.22)
		June2014	1.71 (±0.23)	1.16 (±0.83)	0.89 (±0.82)	1.78 (±0.45)	1.78 (±0.14)	1.21 (±0.42)
SUB20	N–acetyl–β–glucosaminidase [nmol/ g DM x h]	July 2013	8.93 (±3.21)	9.45 (±4.68)	6.76 (±2.34)	5.27 (±4.56)	5.52 (±4.38)	6.85 (±4.87)
		October 2013	24.90 (±7.44)	11.83 (±5.45)	21.33 (±3.72)	15.77 (±3.45)	20.58 (±11.77)	16.72 (±4.28)
		June2014	13.72 (±5.10)	19.42 (±7.35)	12.73 (±6.90)	16.39 (±17.57)	10.49 (±12.06)	14.42 (±9.94)
SUB120	N–acetyl–β–glucosaminidase [nmol/ g DM x h]	July 2013	1.10 (±1.09)	0.91 (±0.80)	1.05 (±0.94)	0.78 (±0.29)	1.46 (±0.90)	0.92 (±0.36)
		October 2013	2.31 (±0.32)	4.28 (±2.48)	6.10 (±5.52)	2.57 (±0.42)	3.38 (±0.26)	3.81 (±2.60)
		June2014	8.27 (±2.37)	4.38 (±2.78)	2.05 (±0.51)	3.63 (±2.44)	6.67 (±5.59)	2.52 (±1.48)
SUB20	Cellulose 1.4-β-cellobiosidase [nmol/ g DM x h]	July 2013	0.91 (±0.22)	0.92 (±0.36)	0.90 (±0.71)	0.38 (±0.35)	0.55 (±0.24)	0.10 (±0.26)
		October 2013	1.45 (±0.24)	1.47 (±0.87)	2.49 (±0.53)	1.03 (±0.43)	1.82 (±1.24)	3.74 (±1.55)
		June2014	1.46 (±0.59)	2.24 (±1.50)	2.32 (±0.97)	2.01 (±0.64)	1.31 (±0.83)	1.49 (±1.42)
SUB120	Cellulose 1.4-β-cellobiosidase [nmol/ g DM x h]	July 2013	0.35 (±0.00)	0.44 (±0.00)	0.33 (±0.00)	0.08 (±0.05)	0.23 (±0.00)	0.16 (±0.10)
		October 2013	1.46 (±0.57)	1.69 (±0.61)	1.33 (±0.49)	0.41 (±0.19)	0.40 (±0.26)	0.38 (±0.25)
		June2014	1.05 (±0.48)	1.37 (±0.95)	1.38 (±0.61)	1.20 (±0.28)	1.58 (±0.29)	1.19 (±0.35)
SUB20	Xylanase [µg GE/g DM x 24 h]	July 2013	360.92 (±101.07)	351.01 (±28.59)	391.75 (±90.75)	291.01 (±11.02)	247.77 (±54.16)	408.12 (±57.94)
		October 2013	254.72 (±67.30)	292.87 (±25.34)	375.28 (±20.83)	304.18 (±12.55)	378.31 (±86.53)	551.44 (±47.14)
		June2014	240.01 (±24.96)	285.92 (±49.49)	386.32 (±55.55)	273.42 (±81.50)	305.92 (±54.98)	349.38 (±45.40)
SUB120	Xylanase [µg GE/g DM x 24 h]	July 2013	43.11 (±24.78)	25.19 (±22.35)	65.11 (±11.26)	53.17 (±41.74)	43.43 (±12.13)	84.77 (±30.64)
		October 2013	69.69 (±21.68)	110.51 (±19.65)	96.88 (±14.86)	47.84 (±36.95)	70.69 (±22.82)	54.81 (±30.39)
		June2014	59.53 (±17.82)	87.17 (±44.46)	119.72 (±45.46)	65.87 (±4.40)	62.99 (±20.98)	73.222 (±13.83)
SUB20	Phenoloxidase [A 630nm/ g soil x h]	July 2013	0.21 (±0.16)	0.39 (±0.01)	0.33 (±0.05)	0.48 (±0.03)	0.35 (±0.17)	0.34 (±0.12)
		October 2013	0.11 (±0.05)	0.22 (±0.14)	0.30 (±0.23)	0.26 (±0.17)	0.34 (±0.21)	0.32 (±0.26)
		June2014	0.25 (±0.09)	0.29 (±0.10)	0.19 (±0.15)	0.27 (±0.15)	0.16 (±0.18)	0.20 (±0.16)
SUB120	Phenoloxidase [A 630nm/ g soil x h]	July 2013	0.24 (±0.14)	0.36 (±0.04)	0.32 (±0.02)	0.32 (±0.14)	0.29 (±0.10)	0.33 (±0.11)
		October 2013	0.10 (±0.10)	0.16 (±0.07)	0.12 (±0.07)	0.35 (±0.11)	0.41 (±0.09)	0.32 (±0.09)
		June2014	0.19 (±0.04)	0.18 (±0.04)	0.21 (±0.01)	0.20 (±0.13)	0.22 (±0.08)	0.18 (±0.10)
SUB20	Peroxidase [A 630nm/ g soil x h]	July 2013	2.23 (±1.02)	2.23 (±1.03)	2.37 (±1.30)	1.96 (±0.99)	2.29 (±0.84)	2.22 (±0.53)
		October 2013	2.28 (±0.78)	2.24 (±0.52)	2.38 (±0.42)	2.16 (±0.49)	2.04 (±0.54)	2.10 (±0.53)
		June2014	2.39 (±0.06)	2.27 (±0.06)	2.53 (±0.33)	2.30(±0.58)	2.47 (±0.58)	2.36 (±0.45)
SUB120	Peroxidase [A 630nm/ g soil x h]	July 2013	0.52 (±0.20)	0.72 (±0.29)	0.39 (±0.19)	0.67 (±0.34)	0.73 (±0.24)	0.54 (±0.23)
		October 2013	0.72 (±0.18)	0.56 (±0.05)	0.68 (±0.10)	0.47 (±0.16)	0.37 (±0.12)	0.64 (±0.12)
		June2014	0.81 (±0.47)	0.55 (±0.09)	0.43 (±0.15)	0.53 (±0.10)	0.53 (±0.06)	0.54 (±0.17)

Table S5.3: *Cellulose addition, translocation and sampling date effects on enzyme activities tested with three-way ANOVA. The table shows F-ratios and P-values in parentheses. A = cellulose addition, T = translocation, D = sampling date, A*T = interaction between cellulose addition and translocation, A*D = interaction between cellulose addition and sampling date, T*D = interaction between translocation and sampling date, A*T*D = interaction between cellulose addition, translocation and sampling date.*

Soil	**Parameter**	**A**	**T**	**D**	**A*T**	**T*D**	**A*D**	**A*T*D**
SUB20	β–glucosidase	1.50 (0.2368)	3.08 (0.0884)	**4.31** **(0.0215)**	0.03 (0.9707)	0.81 (0.4538)	0.53 (0.7119)	0.14 (0.9661)
SUB120	β–glucosidase	0.80 (0.4564)	0.02 (0.8846)	3.14 (0.0562)	0.44 (0.6459)	0.38 (0.6839)	0.83 (0.5125)	0.31 (0.8680)
SUB20	β–xylosidase	1.99 (0.1525)	1.72 (0.1982)	**14.15** **(<.0001)**	0.05 (0.9519)	**4.55** **(0.0178)**	2.10 (0.0912)	0.36 (0.8360)
SUB120	β–xylosidase	1.97 (0.1545)	1.66 (0.2060)	**3.64** **(0.0370)**	0.31 (0.7322)	**4.05** **(0.0264)**	1.20 (0.3270)	0.62 (0.6534)
SUB20	N–acetyl–β–glucosaminidase	0.10 (0.9053)	0.58 (0.4506)	**7.23** **(0.0024)**	0.09 (0.9135)	0.01 (0.9852)	0.14 (0.9665)	1.15 (0.3491)
SUB120	N–acetyl–β–glucosaminidase	0.77 (0.4696)	0.20 (0.6579)	**4.82** **(0.0143)**	0.27 (0.7615)	0.66 (0.5217)	2.10 (0.1019)	0.12 (0.9761)
SUB20	Cellulose 1.4-β-cellobiosidase	**4.88** **(0.0137)**	0.21 (0.6511)	**11.55** **(0.0001)**	0.24 (0.7876)	1.13 (0.3337)	1.68 (0.1765)	1.10 (0.3710)
SUB120	Cellulose 1.4-β-cellobiosidase	0.14 (0.8727)	**6.13** **(0.0184)**	**31.71** **(<.0001)**	0.14 (0.8669)	**6.32** **(0.0046)**	0.44 (0.7780)	0.15 (0.9595)
SUB20	Xylanase	**15.65** **(<.0001)**	0.99 (0.3276)	2.62 (0.0870)	0.74 (0.4821)	**5.69** **(0.0074)**	1.18 (0.3363)	1.07 (0.3858)
SUB120	Xylanase	1.97 (0.1545)	1.66 (0.2060)	**3.64** **(0.0370)**	0.31 (0.7322)	**4.05** **(0.0264)**	1.20 (0.3270)	0.62 (0.6534)
SUB20	Phenoloxidase	0.80 (0.4574)	2.01 (0.1653)	2.65 (0.0848)	2.54 (0.0933)	1.92 (0.1624)	0.72 (0.5844)	0.83 (0.5168)
SUB120	Phenoloxidase	0.67 (0.5159)	**12.05** **(0.0014)**	**5.05** **(0.0120)**	0.31 (0.7336)	**4.02** **(0.0270)**	0.28 (0.8914)	0.05 (0.9948)
SUB20	Peroxidase	0.07 (0.9281)	1.39 (0.2457)	0.49 (0.6172)	0.20 (0.8196)	0.21 (0.8139)	0.18 (0.9470)	0.09 (0.9843)
SUB120	Peroxidase	2.14 (0.1334)	0.47 (0.4989)	0.02 (0.9845)	0.08 (0.9229)	0.10 (0.9033)	1.99 (0.1187)	1.07 (0.3845)

Table S5.4: *Mean respiratory response of 5 % cellulose addition samples after 12 month*

		SUB20		SUB120	
Incorporation depth (cm)	**Amendment type**	**Respiratory response / O_2 consumption (µl O_2 g^{-1} dw h^{-1})**	**Change in % to C amendment**	**Respiratory response / O_2 consumption (µl O_2 g^{-1} dw h^{-1})**	**Change in % to C amendment**
20	C	122.9	-	23.6	-
20	C+N	179.9	+46	36.9	+57
20	C+P	123.0	+0	30.2	+28
20	C+N+P	312.0	+154	90.3	+284
120	C	124.4	-	21.4	-
120	C+N	161.7	+30	37.4	+75
120	C+P	122.8	-1	24.9	+16
120	C+N+P	256.1	+106	129.8	+508

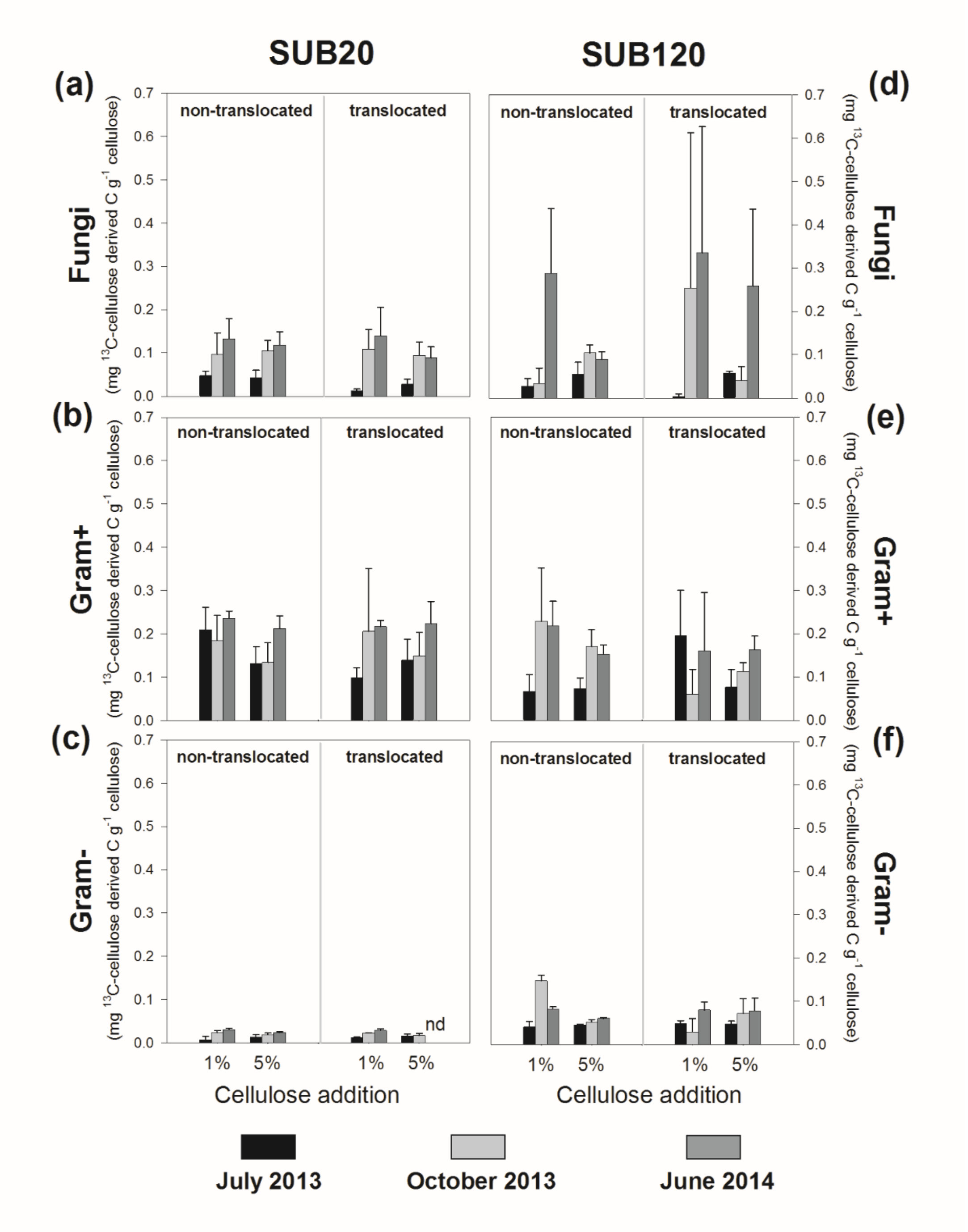

Figure S5.1 Absolute amount of ^{13}C-cellulose-derived C incorporated into gram-positive bacteria (PLFA$_{gram+}$), gram-negative bacteria (PLFA$_{gram-}$) and fungi (PLFA$_{fungi}$) in SUB20 (a, b, c) and SUB120 (d, e, f) samples under different translocation and cellulose addition treatments at the sampling dates July 2013, October 2013 and June 2014. Error bars indicate standard deviation (n=3). Not determined treatments are indicated with nd.

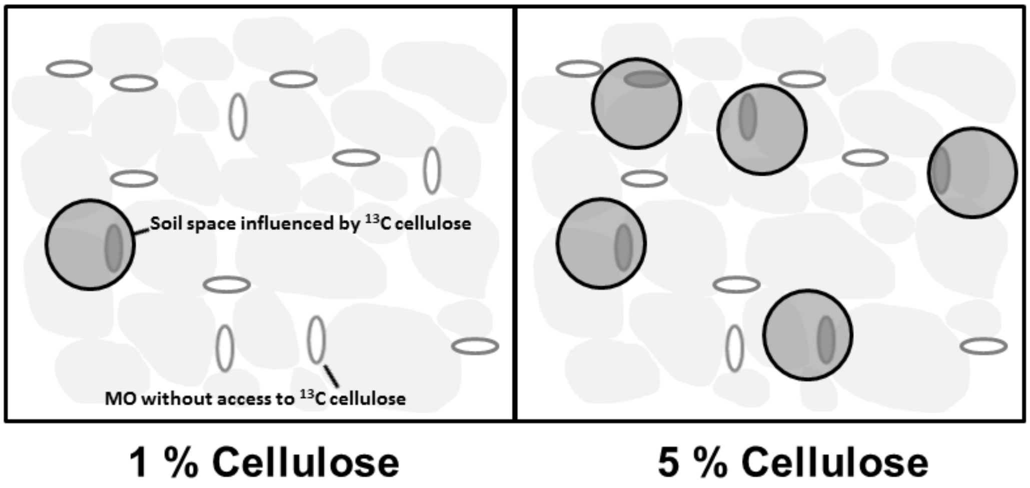
Soil space influenced by ^{13}C cellulose
MO without access to ^{13}C cellulose
1 % Cellulose
5 % Cellulose

Figure S5.2 Increased amounts of added cellulose proportionally increase the affected soil volume and the number of microorganisms with access to cellulose in a carbon limited environment.

6 Fungi and bacteria respond differently to changing habitat conditions within a soil profile

Soil Biology & Biochemistry 137 (2019) 107543

DOI: 10.1016/j.soilbio.2019.107543

Received: 14 November 2018, Revised: 18 July 2019, Accepted: 20 July 2019,

Published online: 22 July 2019

Sebastian Preusser[a]*, Christian Poll[a], Sven Marhan[a], Gerrit Angst[b,c], Carsten W. Mueller[b], Jörg Bachmann[d] and Ellen Kandeler[a]

[a]Institute of Soil Science and Land Evaluation, Soil Biology Department, University of Hohenheim, Emil-Wolff Str. 27, 70599 Stuttgart, Germany

[b]Lehrstuhl für Bodenkunde, TU München, Emil-Ramann-Str. 2, 85354 Freising, Germany

[c]Biology Centre of the Czech Academy of Sciences, Institute of Soil Biology & SoWa Research Infrastructure, Na Sádkách 7, CZ-37005, České Budějovice, Czech Republic

[d]Institute of Soil Science, Leibniz-Universität Hannover, Herrenhäuser Str. 2, 30419 Hannover, Germany

*Corresponding author: Tel.: +49 711 459 24065;

E-mail address: s.preusser@uni-hohenheim.de

Abstract

Contrasting environmental conditions in topsoil and subsoil determine both abundance and function of soil microbial communities, affecting carbon (C) dynamics throughout the entire soil profile. Although the response of soil microorganisms to single factors such as substrate availability or micro-climatic conditions has been frequently studied, fewer studies have focused on complex interactions between substrate availability and environmental conditions. To address this, we employed vertical soil translocations between topsoil and subsoil horizons of an acid and sandy Dystric Cambisol under European beech forest in Lower Saxony, Germany, to investigate the impact of changing habitat conditions on microbial decomposer communities. To follow microbial substrate utilization at different soil depths, we created hot spots of fresh organic matter (OM) by adding ^{13}C-labelled root litter. Soil samples were taken every three months over an experimental period of twelve months (June 2014 to June 2015).

Generally, microbial biomass was strongly controlled by C availability throughout the profile. The importance of root litter as a microbial C source increased from topsoil to subsoil, but changes in available C sources affected fungi and bacteria differently. Fungi preferentially used root litter-derived C throughout the entire soil profile, demonstrating that limited access to preferred substrates, rather than micro-climatic conditions, was the main driver of decreasing fungal abundance with soil depth. In contrast, bacteria intensified utilization of root-derived C only in the absence of alternative C sources in the subsoil and were more strongly affected by spatial separation from C sources. Low soil moisture in combination with the highly sandy subsoil environment limited bacterial access to their substrates and, consequently, bacterial growth. In conclusion, fungal C utilization relies mainly on the quantity of recent plant-derived substrates, whereas bacterial access to substrates is additionally controlled by environmental conditions. This study indicates that limited microbial access to their heterogeneously distributed substrates may be an important factor for C accumulation and stabilization in subsoils.

Keywords: Carbon cycle; Subsoil; Soil microorganisms; Stable isotopes; Habitat conditions; Detritusphere

6.1 Introduction

The abundance of soil microorganisms and their decomposition activity undergo significant changes with increasing soil depth. Microbial biomass generally decreases from topsoil to subsoil and is more heterogeneously distributed in subsoil than in topsoil (Ekelund et al., 2001; Taylor et al., 2002). With increasing soil depth, microbial community structure typically increases in its relative proportion of gram-positive bacteria, while the proportions of gram-negative bacteria and fungi decrease (Blume et al., 2002; Fierer et al., 2003). Deeper soil layers further exhibit decreased genetic and metabolic microbial diversity compared to surface soils (Eilers et al., 2012; Will et al., 2010; Goberna et al., 2005). Moreover, there are also pronounced differences in microbial activity between different microhabitats within soil profiles (e.g., rhizosphere vs. bulk soil), and decomposition rates of soil organic matter (SOM) generally decrease with increasing soil depth, while turnover times increase (Kuzyakov and Blagodatskaya, 2015; Gaudinski et al., 2000). In previous studies, these differences in abundances and activity of microbial decomposer communities between topsoil and subsoil have been attributed to a variety of factors such as altered and less easily available carbon (C) sources, increased physical inaccessibility (e.g. occlusion within soil aggregates) of nutrients and substrates, and harsher environmental conditions (e.g., water and oxygen content, temperature, pH, and soil texture) in deeper soil layers (Hansel et al., 2008; Drenovsky et al., 2004; Herold et al., 2014).

Compared to topsoil, subsoil exhibits substantially lower C density and organic matter (OM) with a different chemical composition (Rumpel et al., 2002). Important processes contributing to the altered chemical composition of OM in deeper soil are temporal and selective immobilization (sorption, precipitation), as well as continuous microbial mineralization and transformation of OM as it passes through the soil profile. As a consequence, with increasing soil depth, OM pools increasingly consist of aged plant-derived compounds and microbial residues (Kaiser and Kalbitz, 2012; Liang and Balser, 2008). A higher proportion of stabilized OM in deeper soil, as demonstrated by older radiocarbon ages of the soil organic carbon (SOC) in subsoil as compared to topsoil (Rumpel et al., 2002), indicates an increasing reduction in microbial decomposition processes (e.g., reduced substrate utilization rates) with soil depth. However, the determining factors accounting for these differences in C turnover and accumulation with soil depth are still under discussion. While some studies have attributed OM stabilization in subsoil to a greater abundance of chemically recalcitrant OM compounds (e.g. Krull et al., 2003; Rasse et al., 2005), other studies have suggested physico-chemical interactions (e.g., adsorption to mineral surfaces), or physical protection (e.g., occlusion of OM within soil aggregates) as the most important factors preventing microbial degradation (Eusterhues et al., 2005; Dungait et al., 2012; Moni et al., 2010; Salomé et al., 2010). Among these factors, spatial separation between OM and microbial degraders coupled with low input of fresh SOC as an energy source for microorganisms may also be important (Holden and Fierer, 2005; Fontaine et al., 2007).

Besides the importance of C characteristics, altered environmental conditions with soil depth also influence the development of microbial communities and C turnover. Changing temperature regimes have been found to alter microbial community composition as well as microbial carbon use efficiencies (CUE) and decay dynamics of stable OM compounds (Feng and Simpson, 2009; Frey et al., 2013). Another key environmental influence on microbial abundance and activity within soil profiles is soil moisture. For example, differences in soil moisture conditions have been found to shape microbial community composition and enzyme activity patterns; consequently, spatial and temporal variations in soil moisture within soil profiles can distinctly influence microbial decomposition processes (Baldrian et al., 2010; Brockett et al., 2012).

However, although the influences of either differences in substrate availability or changing environmental conditions on soil microorganisms and C turnover within soil profiles have been frequently investigated, previous studies have not been able to distinguish between the importance of biotic (e.g. substrate supply) and abiotic factors for reduced microbial C turnover in subsoils under *in situ* conditions (Kätterer et al., 2014; Sanaullah et al., 2016). A promising tool to decouple these two factors is the reciprocal translocation of soil samples combined with addition of substrates. Originally, this approach was developed to clarify the importance of different site-specific properties between ecosystems (e.g. meadow versus forest; Balser and Firestone, 2005; Boyle et al., 2006; Zumsteg et al., 2013). We have applied reciprocal translocation for the first time between different subsoil horizons (Preusser et al., 2017). In the current study, we extended this approach and reciprocally translocated topsoil and subsoil both with and without hotspots of substrate availability. Consequently, this approach allowed us to disentangle both the impact of depth-specific environmental conditions (via soil translocation) and the influence of substrate availability (via ^{13}C labelled root litter addition) as well as to investigate the influence of the complex interactions among these factors and microbial decomposer communities. One of the main objectives of the study was to investigate bacterial and fungal C assimilation under topsoil and subsoil environmental conditions. We followed the temporal and spatial patterns of C flow from root litter as a natural and complex substrate into microbial decomposers, as well as changes in microbial community structure through different stages of root litter decomposition, under a variety of depth-specific environmental conditions. The determination of the amount of incorporated root-C per gram of root addition allowed us to understand the microbial root-C utilization rates. We hypothesize that habitat conditions in subsoil (i) slow down the succession of root litter-decomposing fungi and bacteria and (ii) reduce microbial root-C utilization rates.

6.2 Materials and methods

Site description

The translocation experiment was conducted on the main experimental site of the SUBSOM-Project, a ~100-years old European beech (*Fagus sylvatica* L.) forest in Grinderwald (52° 34’ 22’’ N 9° 18’ 51’’ E; 100 m a.s.l.) 40 km northwest of Hannover in Lower-Saxony, Germany. Data from the closest German Meteorological Service (DWD) weather station in Nienburg indicate, for the period from 1981 to 2010, a temperate and humid climate with mean annual precipitation and temperature of 762 mm and 9.7 °C, respectively. Air temperature and precipitation for the actual period of the translocation experiment was provided by another weather station operated directly at the experimental site by the research group (Fig. S6.1). Additionally, three soil observatories on the site made it possible to measure soil temperature (°C) and volumetric water content (%) at 10, 30, 50, 90, 150 and 180 cm soil depths (Fig. 6.1) (Leinemann et al., 2016). The soil type of the experimental site is an acid and sandy Dystric Cambisol (IUSS Working Group WRB, 2014) with pH values of 3.3 in topsoil and 4.5 in subsoil. Mean sand, silt and clay content are 77.3 %, 18.4 % and 4.4 %, respectively. The predominant humus form is moder and the parent materials for pedogenesis are fluvial and aeolian deposits from the Saale glaciation (Angst et al., 2016a). Additional soil properties of the study site are listed in Table S6.1 (Preusser et al., 2017).

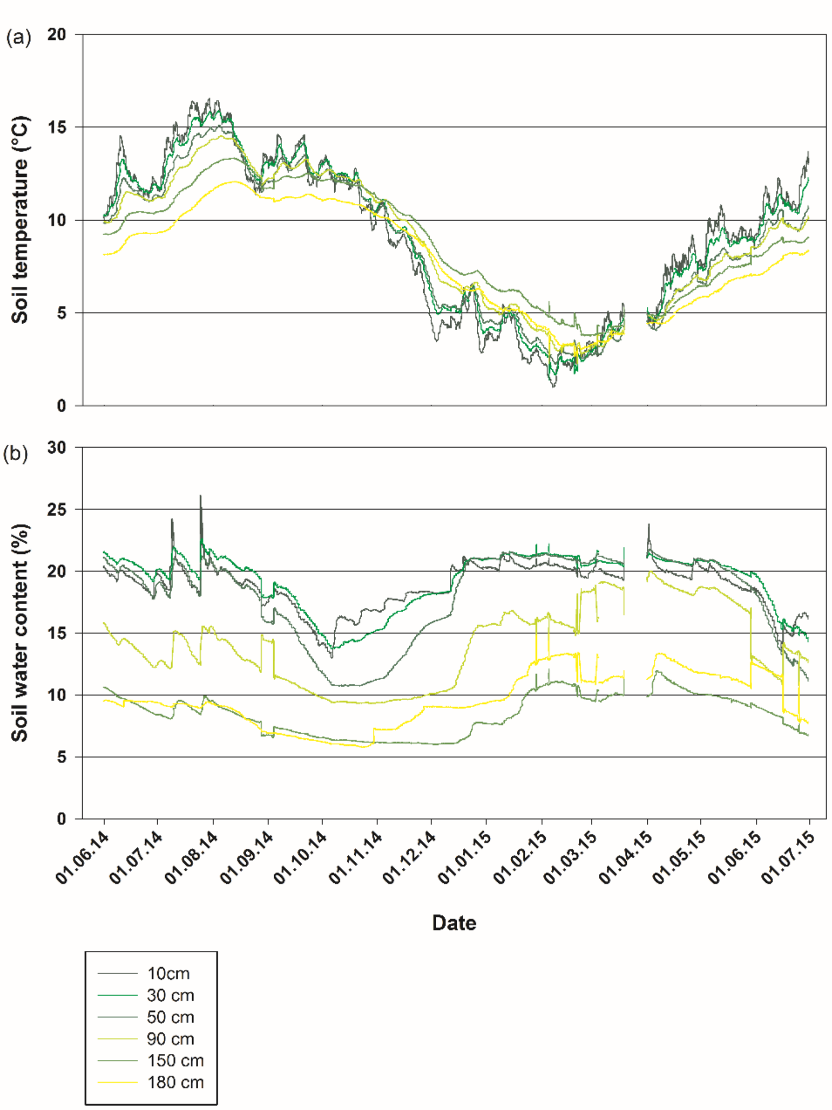

Figure 6.1 Mean daily (a) soil temperatures (°C) and (b) soil water content (%) from June 1, 2014 to June 31, 2015 at six different soil depths (10 cm, 30 cm, 50 cm, 90 cm, 150 cm and 180 cm) at the field site.

Experimental design

For the soil translocation experiment, twelve profile pits were randomly arranged around three mature beech trees of comparable age and growth (4 profile pits per tree), each located 2.5 m from the respective trees. During the excavation of each of the profile pits, the topsoil from 5 to 10 cm soil depth (Bsw horizon; 2.84 % C_{org}; hereafter referred to as TOP5) and the subsoil from

110 to 115 cm soil depth (C horizon; 0.11 % C_{org}; hereafter referred to as SUB110) were stored separately, then sieved (2 mm) and mixed with the soil from the respective soil depth of the other profile pits. Subsequently, 144 soil containers of height 2.0 cm, diameter 10.5 cm and volume 173.1 cm^3 were filled with either 242.3 g soil dry weight (bulk density 1.4 g cm^{-3}) of the TOP5 soil or 277.0 g soil dry weight (bulk density 1.6 g cm^{-3}) of the SUB110 soil. To mimic detritusphere hotspots of increased substrate availability, root litter was added to 36 of the 72 containers filled with TOP5 soil (1.73 g roots per container; corresponding to a root density of 10 g L^{-1}; 0.84 g root-C per container) and to 36 of the 72 containers filled with SUB110 soil (0.35 g roots per container; 2 g L^{-1}; 0.17 g root-C per container). The added root materials to TOP5 and SUB110 containers mimicked as closely as possible the naturally occurring root biomass in the respective soil depths. The air-dried ^{13}C-labelled European beech (*Fagus sylvatica* L.) roots (residual water content 6.2 %, 48.7 % C; 9.38 atom % ^{13}C; IsoLife B.V., Netherlands) were cut into 1 - 2 cm segments before addition and the root thickness fractions (∅ 0.5 - 2 mm) were homogeneously distributed within each container. Root addition increased C content in the containers filled with TOP5 and SUB110 soils by 12 % and 56 %, respectively. After filling, the containers were closed at the top and bottom with micro PA-material with mesh size of 500 µm to ensure unimpeded water flow in the upcoming experiment between the surrounding soil volume and the soil within the containers. To summarize, containers with four different filling types were prepared: topsoil with root addition ($TOP5_{roots}$), topsoil without root addition ($TOP5_{control}$), subsoil with root addition ($SUB110_{roots}$) and subsoil without root addition ($SUB110_{control}$).

Thereafter, soil containers were incorporated into the undisturbed tree-facing profile walls of the twelve profile pits according to the following pattern: In each soil profile one of each of the four container types ($TOP5_{roots}$, $TOP5_{control}$, $SUB110_{roots}$ and $SUB110_{control}$) was incorporated into 5 cm, 45 cm and 110 cm soil depths representing a gradient in abiotic and biotic habitat conditions (Fig. S6.2). The containers were, therefore, exposed to either non-altered environmental conditions (e.g. SUB110 incorporated into 110 cm soil depth) or to altered environmental conditions via vertical soil translocation (e.g. SUB110 incorporated into 5 cm or 45 cm soil depth). The positions of the four container types within each of the three soil depths were randomly selected. Additionally, the containers in each layer were horizontally offset from the containers in the other layers to minimize vertical interference. After incorporation, the profile pits were refilled with soil appropriate to the soil horizon sequence that had been separately stored during excavation, and the litter layer was restored to replicate the initial amount and thickness. The experiment began in June 2014 and samples were taken at three-month intervals (September 2014, December 2014, March 2015 and June 2015). At every sampling date, one of the four profile pits surrounding each of the three trees was randomly selected and a total of 36 containers (four filling types x three incorporation depths x three field repetitions) were removed and immediately stored at 0 °C for transport to the laboratory.

Analyses

All samples were sieved (<2 mm) after sampling to remove larger particles (including root residues) and the gravimetric water content of the samples was determined. The samples were stored at -23°C until further analysis.

δ^{13}C of microbial biomass C and extractable organic C (EOC) and N (ETN)

The chloroform fumigation extraction (CFE) method of Vance et al. (1987) was used to determine microbial biomass carbon (C_{mic}) as described by Marhan et al. (2010). Each sample was measured ten times to increase measurement accuracy. Microbial C was calculated using a k_{EC} factor of 0.45 (Joergensen, 1996). Extractable organic carbon (EOC) and extractable total nitrogen (ETN) were calculated using the values of the non-fumigated samples.

Microbial biomass δ^{13}C values were determined as described by Marhan et al. (2010). The following equation was used for the calculation of δ^{13}C of the microbial biomass:

$$\delta^{13}C_{mic} = \frac{\delta_{f}\, x\, C_{f} - \delta_{nf}\, x\, C_{nf}}{C_{f} - C_{nf}},$$

where C_f and C_{nf} are extracted organic C content (µg C g^{-1} soil) of the fumigated and non-fumigated samples and δ_f and δ_{nf} are the corresponding δ^{13}C values.

The calculation of root-derived C (%) was done using the following equation:

$$\%\, C - roots = \frac{\delta_{sample} - \delta_{reference}}{\delta_{roots} - \delta_{soil}}\, x100,$$

where δ_{sample} is the δ^{13}C value of the respective sample, $\delta_{reference}$ is the δ^{13}C mean value of the respective non-^{13}C-addition samples, δ_{roots} is the average δ^{13}C value of the added roots (8283 ‰), and δ_{soil} is the average δ^{13}C value of TOP5 (-27.8 ‰) or SUB110 (-25.5 ‰) soil used for the translocation experiment.

In addition, the absolute quantity of root-derived C incorporated into the microbial biomass (mg C g^{-1} added ^{13}C roots) was calculated.

δ^{13}C *phospholipid fatty acid analyses (PLFA)*

Twelve g field moist TOP5 soil and 24 g field moist SUB110 soil were used for lipid extraction and fractionation according to the method of Frostegård et al. (1991). The PLFAs were transformed into fatty acid methyl esters (FAMEs) using alkaline methanolysis (Kramer et al., 2013). The abundance of individual FAMEs was expressed in nmol per g soil. The fatty acids i15:0, a15:0, i16:0, 16:1ω7, i17:0, cy17:0, 18:1ω7 and cy19:0 were considered as bacterial PLFAs ($PLFA_{bac}$). Of these, i15:0, a15:0, i16:0 and i17:0 represented Gram-positive bacteria ($PLFA_{gram+}$) and cy17:0 and cy19:0 represented Gram-negative bacteria ($PLFA_{gram-}$) following Kandeler et al. (2008), Frostegård and Bååth (1996) and Zelles (1999). Fungal PLFA was considered as 18:2ω6,9 ($PLFA_{fun}$) (Frostegård et al., 1993).

The $\delta^{13}C_{PLFA}$ values were determined with an HP 6890 Gas Chromatograph (Agilent Inc., USA) coupled with a combustion III Interface (Thermo Finnigan, USA) to a Delta Plus XP mass spectrometer (Thermo Finnigan MAT, Germany) as described by Müller et al. (2016). Calculation of root-derived C (%) was done as described for microbial biomass C. Mean ^{13}C incorporation into the different microbial groups was calculated according to the relative proportions of the respective fatty acids to the total of the group-associated fatty acids. In addition, the absolute quantity of root-derived C incorporated into each microbial group (mg C g^{-1} added ^{13}C roots) was calculated.

Ergosterol

Ergosterol content as a proxy for fungal biomass was analysed using the method of Djajakirana et al. (1996). For extraction of ergosterol, one g TOP5 and four g SUB110 soil were analysed as described by Müller et al. (2016).

Cutin and suberin derived monomers

Soil samples from the first (September 2014) and last (June 2015) samplings were subjected to a sequential extraction procedure to release ester bound constituents of the lipid biopolymers cutin and suberin. Samples were processed following the protocol described by Angst et al. (2016a). Briefly, prior to saponification, solvent extractable lipids were extracted from 10 g soil by accelerated solvent extraction (dichloromethane (DCM)/methanol 9/1 v/v at 17 x 10^6 Pa and 75°C, Wiesenberg et al., 2004; Jansen et al., 2006). The solid extraction residues were subjected to alkaline hydrolysis in teflon lined bombs with 1 M methanolic potassium hydroxide solution (KOH) at 100°C for three hours. The extracts were dried under a stream of nitrogen and the dried extracts were re-dissolved in deionized water and DCM. The neutral fraction was extracted 3 times with DCM by liquid-liquid extraction. The residual water phase was adjusted to pH 1 and extracted 3 times with DCM to separate the acid fraction. The acid fraction was measured by GC/MS and quantified using an external standard (Angst et al., 2016b). Specific monomers indicative for cutin or suberin were chosen according to the results of a previous study at the same site (Angst et al., 2016c). The 8,9,10,ω-hydroxy hexadecanoic acids (subsumed under x,ω-C_{16}) were indicative for cutin and ω-hydroxy octadecenoic acid (ω-$C_{18:1}$), α,ω-octadecanedioic acid (C_{18}DA), and ω-hydroxy alkanoic acids $C_{20\text{-}24}$ with an even chain length (ω-C_{20}, ω-C_{22}, ω-C_{24}) were indicative for suberin.

Statistical analyses

Effects of root addition (A), translocation depth (T), sampling date (D) and interactions among these factors were analysed with linear mixed-effects (lme) models separately for TOP5 and SUB110 samples for all parameters except absolute incorporation rates. For the absolute incorporation rates, a direct statistical comparison of the TOP5 and SUB110 samples was possible due to the calculation of incorporation relative to one g added roots (mg C g^{-1} added ^{13}C roots). In this case, the additional factor soil origin (S) was included to compare samples from top- and subsoil origins. Due to the experimental design, tree was set as random factor. Significance was tested at $p < 0.05$ in all cases. Homogeneity of variance was tested for all parameters by Levene's test. All statistical analyses were carried out in the R statistical environment, version 3.2.1 (R Core Team, 2015) using the nlme package (Pinheiro et al., 2015) for lme models and the Hmisc package (Harrell et al., 2015) for correlations.

6.3 Results

Water content and extractable total N (ETN)

Gravimetric water content was generally higher in the less sandy TOP5 (10 - 20 %) than in the SUB110 samples (4 - 10 %) (Fig. S6.3 a). Water content of TOP5 and SUB110 showed high seasonal variation at the 5 cm soil depth, whereas soils translocated to greater depths experienced reduced seasonal variability, with lowest water content at 45 cm soil depth (Table S6.2 a).

Mean ETN content of TOP5 and SUB110 samples were between 9.5 and 25.2 µg g^{-1} DM and 1.3 and 7.2 µg g^{-1} DM, respectively (Fig. S6.4). The depth profiles of ETN were opposite one another for TOP5 and SUB110 samples, with highest content at the 110 cm depth for TOP5 samples and at 5 cm depth for SUB110 samples. Additionally, TOP5 samples with root addition had a generally higher ETN content (+ 28 %) than control soils (Table S6.2 a).

Extractable organic C (EOC)

Mean EOC content in TOP5 and SUB110 samples ranged from 130 - 198 µg g^{-1} DM and 15 - 82 µg g^{-1} DM, respectively (Fig. 6.2 a, c). Root addition led to an average increase in EOC content of 12 % in both TOP5 and SUB110 samples. Translocation of TOP5 samples to different soil depths did not change EOC content, whereas translocation of SUB110 samples to shallower soil depths led to an increase in EOC. In addition, greater seasonal fluctuation in EOC in SUB110 samples was observed at 5 cm than at 45 or 110 cm depths, with peaks in EOC at the second and third sampling dates (Table S6.2 a).

The mean relative proportion (%) of root-derived C in EOC ranged from 3.8 - 10.9 % in TOP5 and 1.5 - 10.0 % in SUB110 samples (Fig. S6.5 a, c). Root-derived C in the EOC fraction of

TOP5 samples was similar at all soil depths at the first sampling date and increased over the course of the experiment. The strength of this increase was positively correlated with soil depth. In contrast, the relative proportion of root-derived C in EOC in SUB110 samples was lowest at 5 cm depth throughout the experiment (Table S6.3).

The mean absolute value of ^{13}C in EOC per g added roots (mg C g^{-1} added ^{13}C roots) varied between 1.7 - 5.2 mg C g^{-1} added ^{13}C roots in TOP5 and 1.4 - 4.3 mg C g^{-1} added ^{13}C roots in SUB110 samples (Fig. S6.5 b, d). Absolute ^{13}C values in TOP5 were generally higher than in SUB110 samples and increased with soil depth, while those in SUB110 samples were highest at 45 cm soil depth. Peaks in incorporated ^{13}C in TOP5 samples were detected at the third or fourth sampling date and in SUB110 samples at the second sampling date (Table S6.4).

Microbial biomass

Mean microbial biomass of TOP5 and SUB110 treatments was between 98.2 - 200.4 µg C_{mic} g^{-1} DM and 1.4 - 42.2 µg C_{mic} g^{-1} DM, respectively (Fig. 6.2 b, d). Mean increases in microbial biomass in all samples with root addition were 17 % in TOP5 and 44 % in SUB110 samples, whereas increases in samples that had only been non-translocated were 15 % in TOP5 and 91 % in SUB110 samples (Table 6.1 a). Translocation to different soil depths led to highest mean microbial biomass at 45 cm depth for TOP5 and at 5 cm depth for SUB110 samples. In general, microbial biomass in TOP5 samples was highest at the first or second sampling and decreased over the duration of the experiment (Table S6.2 b).

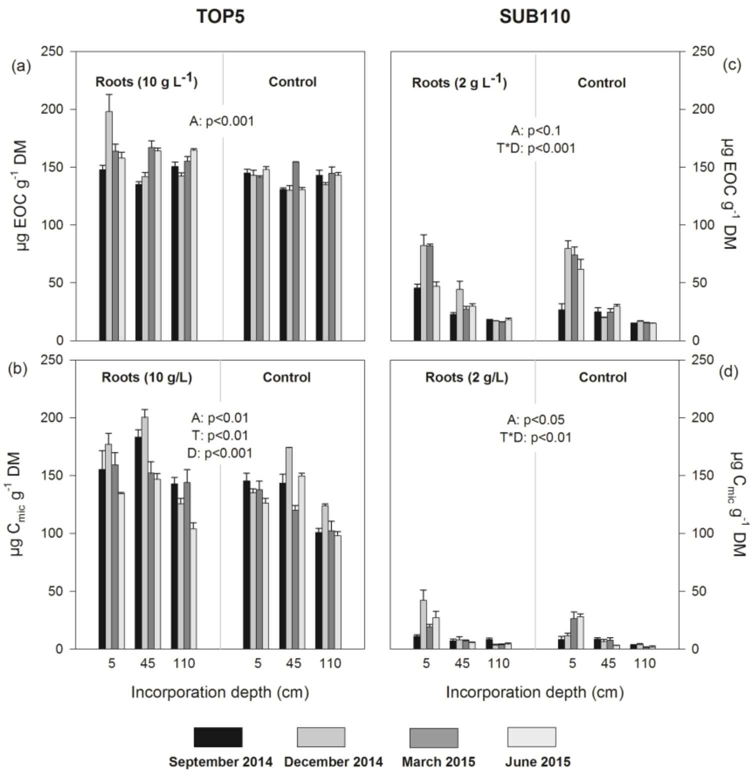

Figure 6.2 Amount of extractable organic carbon (EOC, a and c) and microbial biomass C (C_{mic}, b and d) in TOP5 and SUB110 samples under different translocation and root addition treatments for the sampling dates September 2014, December 2014, March 2015 and June 2015. Error bars indicate standard error (n=3). The figure shows significant effects with respective P-values. A = root addition, T = translocation, D = sampling date.

Mean ^{13}C incorporation (%) into C_{mic} of TOP5 and SUB110 samples ranged from 10.3 - 20.4 % and from 7.8 - 62.6 %, respectively (Fig. 6.3 a, c). Neither sampling date nor soil depth significantly influenced microbial ^{13}C incorporation into TOP5 soils. Microbial ^{13}C incorporation into SUB110 samples strongly increased at both 45 cm and 110 cm soil depths compared to the 5 cm layer. In addition, the peaks of microbial ^{13}C incorporation into SUB110 samples occurred later in the experiment with increasing soil depth (Table S6.3).

Table 6.1:
a: *Substrate addition effect: Mean increase (%) of microbial biomass C (C_{mic}), $PLFA_{gram+}$[*], $PLFA_{gram-}$[**], $PLFA_{fun}$[+] and Ergosterol in TOP5 and SUB110 samples with root addition compared to samples without root addition in different incorporation depths.*

b: *Translocation effect: Mean increase / decrease (%) of microbial biomass C (C_{mic}), $PLFA_{gram+}$[*], $PLFA_{gram-}$[**], $PLFA_{fun}$[+] and Ergosterol in TOP5 and SUB110 samples translocated to different incorporation depths based on the related non-translocated treatments with or without root addition, respectively.*

c: *Interaction effect of substrate addition and translocation: Mean increase / decrease (%) of microbial biomass C (C_{mic}), $PLFA_{gram+}$[*], $PLFA_{gram-}$[**], $PLFA_{fun}$[+] and Ergosterol in translocated TOP5 and SUB110 samples with root addition compared to the respective non-translocated samples without root addition.*

a

	Soil	Incorporation depth (cm)	C_{mic}	$PLFA_{gram+}$	$PLFA_{gram-}$	$PLFA_{fun}$	Ergosterol
SUBSTRATE EFFECT	**TOP5**	**5**	+15	+16	+15	+96	+39
		45	+16	+17	+19	+112	+20
		110	+21	+17	+16	+171	+44
	SUB110	**5**	+34	+50	+14	+45	+/-0
		45	+8	+124	+74	+188	+106
		110	+91	+111	+48	+427	+329

b

	Soil	Incorporation depth (cm)	Root addition	C_{mic}	$PLFA_{gram+}$	$PLFA_{gram-}$	$PLFA_{fun}$	Ergosterol
TRANSLOCATION EFFECT	**TOP5**	**45**	yes	+9	-1	+1	-6	-14
			no	+8	-1	-2	-13	-1
		110	yes	-18	-12	-5	-34	-26
			no	-22	-13	-6	-52	-29
	SUB110	**5**	yes	+395	+62	+46	+372	+154
			no	+605	+128	+90	+1134	+1177
		45	yes	+39	+56	+34	+187	+162
			no	+146	+47	+14	+425	+445

c

	Soil	Incorporation depth (cm)	C_{mic}	$PLFA_{gram+}$	$PLFA_{gram-}$	$PLFA_{fun}$	Ergosterol
INTERACTION EFFECT	**TOP5**	**45**	+25	+15	+17	+85	+20
		110	-5	+2	+9	+29	+3
	SUB110	**5**	+847	+242	+116	+1987	+989
		45	+166	+229	+98	+1412	+1024

[*] i15:0, a15:0, i16:0 and i17:0
[**] cy17:0 and cy19:0
[+] 18:2ω6

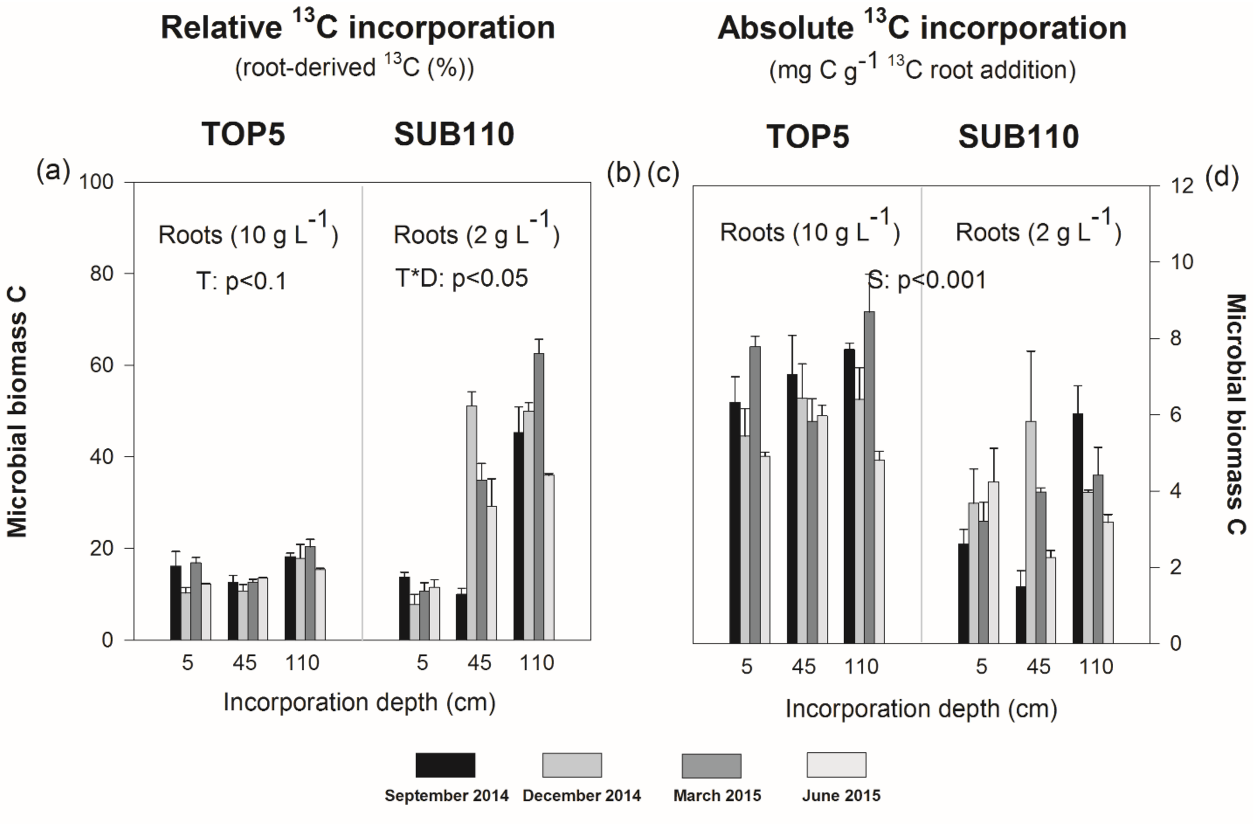

Figure 6.3 Relative incorporation (%) of ^{13}C-root-derived C into microbial biomass C ($^{13}C_{mic}$, a and c) and absolute amount of incorporated ^{13}C-root-derived C per g root addition (mg C g^{-1} added ^{13}C roots, b and d) in TOP5 and SUB110 samples under different translocation and root addition treatments at the sampling dates September 2014, December 2014, March 2015 and June 2015. Error bars indicate standard error (n=3). The figure shows significant effects with respective P-values. S = soil origin, A = root addition, T = translocation, D = sampling date.

The absolute values of ^{13}C per g added roots (mg C g^{-1} added ^{13}C roots) incorporated into the C_{mic} of TOP5 and SUB110 samples were not influenced by incorporation depth, sampling date or their interaction, but were generally higher in TOP5 than in SUB110 samples (Fig. 6.3 b, d; Table S6.4).

PLFAs

Root addition increased the abundances of $PLFA_{gram+}$, $PLFA_{gram-}$ and $PLFA_{fun}$ in TOP5 and SUB110 samples, and was more pronounced for fungi than bacteria (Fig. 6.4; Table S6.2 b). In addition, translocation of TOP5 samples decreased the abundances of $PLFA_{gram+}$ and $PLFA_{fun}$ with increasing soil depth. A similar pattern was found for the SUB110 samples, where translocation of the subsoil into upper soil layers led to increases in abundances of bacterial and fungal PLFAs (Table 6.1 b, Table S6.2 b). Root addition increased ($F = 20.16$, $p < 0.001$) and incorporation depth decreased ($F = 3.46$, $p < 0.05$) the fungal to bacterial PLFA ratio in TOP5 samples, while for SUB110 samples the ratio decreased only with increasing soil depth ($F = 14.30$, $p < 0.001$) (Table 6.2).

Table 6.2: *Fungi to bacteria ratios (18:2ω6 to bacterial PLFA) of TOP5 and SUB110 samples with and without root addition.*

Treatment	Depth (cm)	Mean fungi to bacteria ratio
TOP5 roots	5	0,12
	45	0,12
	110	0,10
TOP5 control	5	0,07
	45	0,07
	110	0,04
SUB110 roots	5	0,78
	45	0,65
	110	0,37
SUB110 control	5	0,81
	45	0,52
	110	0,13

Relative ^{13}C incorporation into bacterial PLFAs mirrored the pattern of $^{13}C_{mic}$ data (Figure 6.5 a, b, d and e; Fig. 6.3 a, c). $PLFA_{gram+}$, $PLFA_{gram-}$ and $PLFA_{fun}$ increased with soil depth at moderate rates in the TOP5 (for $PLFA_{gram-}$ only a tendency) and strongly in the SUB110 samples (Fig. 6.5 a - f). In TOP5 samples, fungi incorporated more root-derived C into their specific PLFA than bacteria, with incorporation rates of up to 80 % (Fig. 6.5 a - c). The variability of ^{13}C incorporation over time was higher for SUB110 samples than for TOP5 samples (Fig. 6.5 a - f). Maximum ^{13}C incorporation into PLFAs occurred after six months in SUB110 samples with incorporation rates of up to 100 % for fungi (Table S6.3).

While the absolute ^{13}C incorporation (mg C g^{-1} added ^{13}C roots) into the fungal PLFA was similar at all three incorporation depths, bacterial PLFAs exhibited, in most cases, increases in ^{13}C incorporation with soil depth. However, more ^{13}C was found in the fungal PLFA in SUB110 than in TOP5 samples, while bacterial PLFAs showed a contrasting pattern; higher quantities in TOP5 than in SUB110 samples with lower temporal variability in TOP5 than in SUB110 samples for $PLFA_{gram-}$ (Fig. 6.5 g - l; Table S6.4).

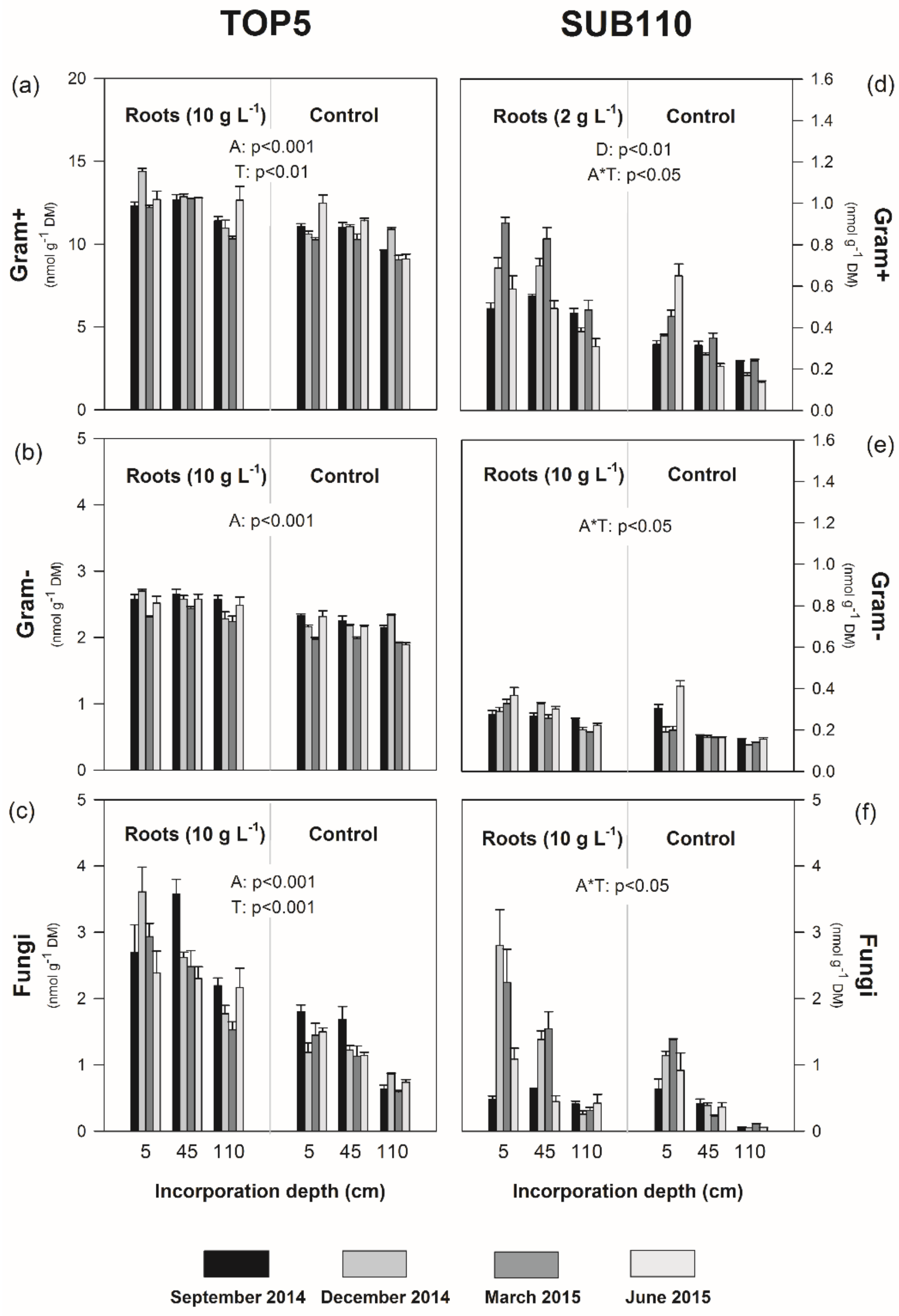

Figure 6.4 Abundance of gram-positive bacteria (PLFA$_{\text{gram+}}$), gram-negative bacteria (PLFA$_{\text{gram-}}$) and fungi (PLFA$_{\text{fungi}}$) in TOP5 (a, b, c) and SUB110 (d, e, f) samples under different translocation and root addition treatments for the sampling dates September 2014, December 2014, March 2015 and June 2015. Error bars indicate standard error (n=3). The figure shows significant effects with respective P-values. A = root addition, T = translocation, D = sampling date.

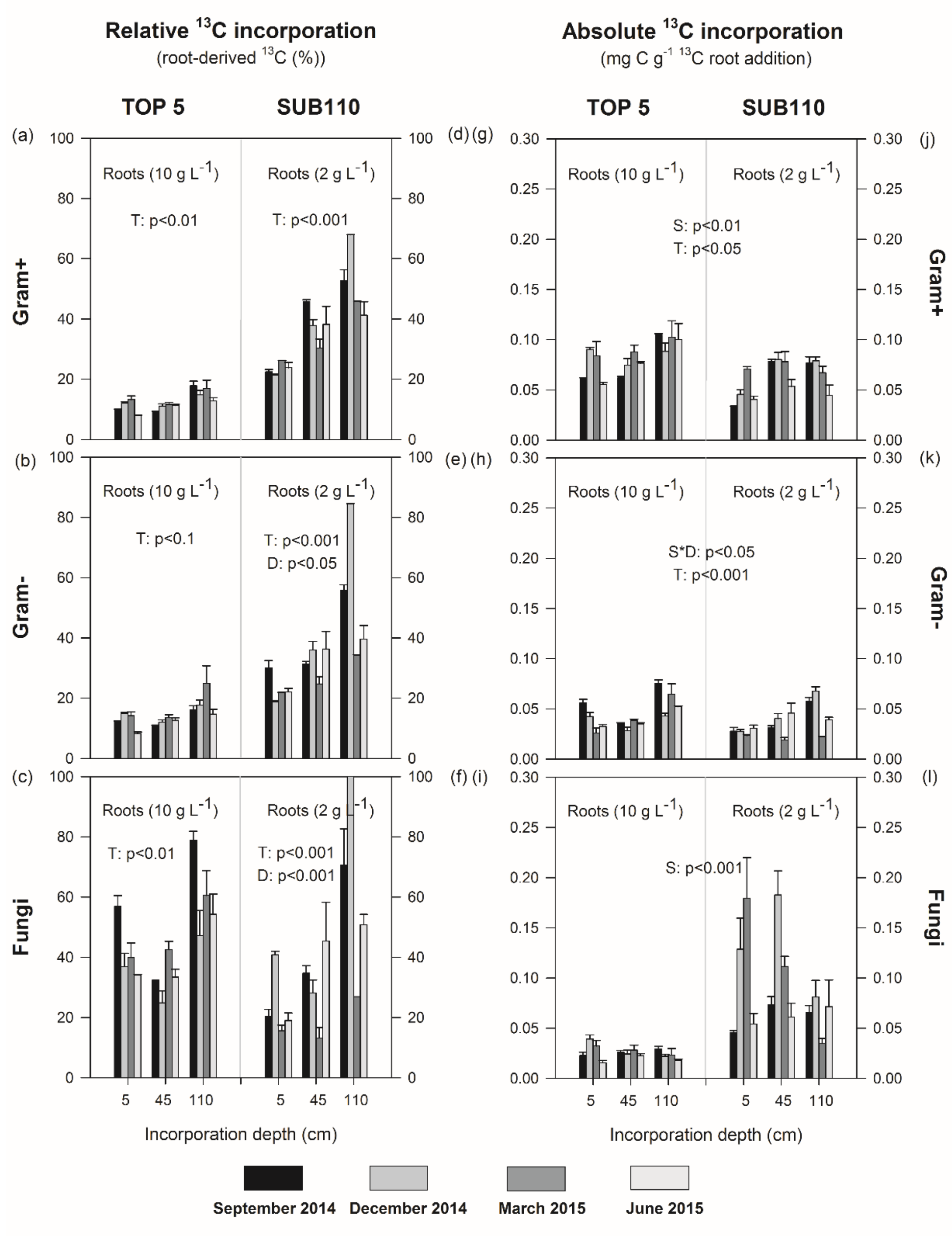

Figure 6.5 Relative (%) (a - f) and absolute (mg C g^{-1} ^{13}C root addition) (g -l) incorporation of ^{13}C-root-derived C into gram-positive bacteria (PLFA$_{\text{gram+}}$), gram-negative bacteria (PLFA$_{\text{gram-}}$) and fungi (PLFA$_{\text{fungi}}$) in TOP5 and SUB110 samples under different translocation and root addition treatments for the sampling dates September 2014, December 2014, March 2015 and June 2015. Error bars indicate standard error (n=3). The figure shows significant effects with respective P-values. S = soil origin, A = root addition, T = translocation, D = sampling date.

Ergosterol

Ergosterol content in TOP5 and SUB110 samples increased with root addition and decreased with depth (Fig. S6.6; Table 6.1 a, b). While TOP5 samples exhibited only minor temporal variability, ergosterol content in SUB110 samples showed clear seasonal fluctuations with occasional steep increases (up to +400 %) and decreases (up to -60 %) between the sampling dates (Table S6.2 b). The ergosterol content of the TOP5 and SUB110 samples was highly correlated with PLFA$_{fun}$ content (TOP5: $r = 0.64$, $p < 0.001$; SUB110: $r = 0.78$, $p < 0.001$).

Interactive effects of translocation and root addition on the abundances of bacteria and fungi

Calculating the mean increase or decrease (%) in microbial properties in translocated samples with root addition and comparing them to the respective non-translocated samples without root addition enabled us to quantify the magnitude of the interactive effects. While translocation of TOP5 soil without root addition decreased microbial properties in deeper soil layers (Table 6.1 b), root addition to translocated TOP5 samples counteracted the less favourable environmental conditions in subsoils (Table 6.1 c). The beneficial effect of root addition to translocated TOP5 soils could be seen in C$_{mic}$, bacterial and fungal PLFAs, and ergosterol content.

While translocation of subsoils (SUB110) alone led to an increase of 14 – 128 % for bacteria and 425 – 1134 % for fungi (Table 6.1 b), these responses were further pronounced with root addition (98 – 242 % for bacteria and 1412 – 1987 % for fungi; Table 6.1 c). Hence, we found an additive positive effect of root addition and translocation on subsoil microorganisms that were placed in the upper soil micro-environment.

Cutin and suberin derived monomers

The mean cutin and suberin content (µg g^{-1} OC) of SUB110 samples as well as the mean suberin content of TOP5 samples had significantly decreased by the last sampling date (June 2015) compared to the first (September 2014) (Fig. S6.7 b - d). Additionally, suberin content of TOP5 samples from the last sampling date were lowest at 45 cm soil depth. The mean cutin content of TOP5 samples did not show any significant effect of root addition, incorporation depth, or sampling date (Fig S6.7 a; Table S6.2 a).

6.4 Discussion

The reciprocal soil translocation combined with the addition of ^{13}C-labelled root litter allowed us to disentangle the impacts of depth-specific environmental conditions and substrate availability on microbial biomass, community structure, and substrate utilization capacity in both topsoil and subsoil of a temperate beech forest site.

Microbial responses to different environmental conditions within soil profiles

The increase in microbial biomass in subsoil samples without root addition translocated to the topsoil environment indicated that either higher and more diverse C inputs (e.g., higher root exudation and input of plant residues) in topsoil than in subsoil or more favourable abiotic conditions (e.g., soil moisture) determine gradients in microbial biomass within soil profiles. The reverse translocation of topsoil samples into the subsoil environment induced only a moderate decrease in microbial biomass, although the EOC content remained largely constant over the experimental period. This indicates that changes in microbial biomass in the investigated soil profile were primarily attributable to qualitative and quantitative changes in microbial C supply.

In our study, soil translocation shaped microbial community structure by changing both bacterial and fungal responses to shifts in available C sources, which is in accordance with previous studies (Fierer et al., 2003; Goberna et al., 2005). Recent plant-derived C is primarily available in the topsoil environment and, in particular, a major C source for certain fungal taxa (Rumpel et al., 2004; Hanson et al., 2008; Jumpponen et al., 2010). The pronounced response of fungal abundance to translocation was likely due to this dependence of certain fungal strains on recent plant C and, consequently, to changes in available C sources with soil depth. In contrast, bacteria (especially Gram$^+$ bacteria) utilize, to a greater degree, processed and chemically complex SOM-derived C (Kramer and Gleixner, 2006) and thus responded less strongly to the translocation of topsoil samples than fungi, resulting in increased dominance of bacteria in microbial communities in the subsoil environment.

Soil temperature and moisture are known to directly influence microbial activity, community structure, and function (Waldrop and Firestone, 2006; Treseder et al., 2016; Drenovsky et al., 2004; Brockett et al., 2012). In this experiment, however, differences in temperature within the soil profile were small (as compared to much greater seasonal temperature variability) and the temperature regimes in both top- and subsoil environments were well within the physiological limits of soil microbial communities of temperate climate zones. Consequently, we conclude that the rather small vertical temperature variation had little or no effect on microbial community structure within the translocated topsoil and subsoil samples.

In contrast, translocation of topsoil to dryer conditions in subsoil and vice versa may have enhanced or reduced environmental stress on the microbial decomposer community. For example, low soil moisture can disrupt the interconnections among soil pore spaces and thereby the associated substrate translocation via soil solution. This in turn leads to increased spatial separation between decomposer and substrate and thus reduces microbial C turnover and growth (Preusser et al., 2017). Accordingly, higher water content in topsoil than in subsoil may have facilitated increases in total microbial biomass in translocated subsoil samples in our experiment. However, fungi are known to be less moisture dependent than bacteria (Drenovsky et al., 2004). Consequently, the much stronger response of fungi compared to bacteria in subsoil samples translocated to the topsoil environment indicated that C availability rather than changes in micro-climatic conditions may have been the dominant factor influencing microbial biomass and community structure. Moreover, the influences of pH and oxygen content were negligible in our experiment, since neither substantial changes in pH nor oxygen limitations between soil depths and over time had been found in a previous experiment under similar conditions at the same experimental site (Preusser et al., 2017).

Microbial responses to substrate addition in topsoil and subsoil

Compared to topsoil, C in subsoil is scarce, more heterogeneously distributed, and largely protected (e.g., adsorption of OM to mineral surfaces) from rapid microbial decomposition (Rumpel and Kögel-Knabner, 2011; Chabbi et al., 2009). Therefore, microorganisms may be increasingly substrate limited with increasing soil depth. In our study, the addition of root litter underscored the role that access to degradable substrates plays in the development of microbial abundance in subsoils, with greater increases in microbial biomass in subsoil than in topsoil in non-translocated topsoil and subsoil samples with root addition. Moreover, microbial growth in subsoil samples resulted almost entirely from utilization of root litter derived-C. Consequently, although subsoils exhibit enormous potential for microbial growth and C turnover, this potential is largely restricted by C accessibility, as hotspots of substrate availability are scarce and large areas of subsoil are largely disconnected from frequent OC inputs (Rumpel et al., 2004).

At the group-specific level, differences in their capacities to explore heterogeneously distributed C sources likely drove the observed changes in bacterial and fungal substrate utilization within the soil profile. The moderate response of bacterial abundance to root addition in both topsoil and subsoil samples indicated either low bacterial dependence on root litter or the presence of other limiting factors. Near-surface environments contain C from various sources (e.g. DOC, leaf litter) with a low proportion of root litter-C in the total OC pool (Rumpel et al., 2002; Fröberg et al., 2007). In contrast, continuous and selective C utilization and retention during the transport of C through the soil profile led to a generally low quantity and diversity of available C in deeper soil layers (Rumpel et al., 2004). The observed bacterial root-C utilization in the present study reflected this shift in C availability with increasing soil depth: in the topsoil environment bacterial communities showed only moderate root-C incorporation rates, while bacteria in subsoil were adapted to the low C availability and extensively utilized root litter derived-C as it became available. However, despite this pronounced bacterial utilization of root-C, bacterial abundance increased only slightly, indicating that other factors had a role in limiting bacterial growth in subsoil.

The absolute root-C incorporation into microbial biomass in the non-translocated topsoil samples was found to be higher than in non-translocated subsoil samples. This contrasts with previous studies which found no depth-dependence of microbial C assimilation (Sanaullah et al., 2011; Solly et al.; 2015), but may be explained by distinct changes in habitat conditions with increasing soil depth. As also stated in a study by Gill and Burke (2002), the detected low water content and coarse soil texture in subsoil may have specifically impeded and spatially restricted bacterial access to the added root litter to a greater degree than in topsoil, reducing bacterial decomposition capacity due to spatial separation between substrate and decomposers.

In contrast to bacteria, the considerable increase in fungal abundance demonstrated the importance of root-litter as a preferred C source for fungal decomposers throughout the entire soil profile. Moreover, the fungal response to root addition was greater in subsoil as compared to topsoil samples, indicating that substrate limitation is a key factor accounting for low fungal abundance in deeper soils. However, the data obtained in this experiment do not allow further differentiation of the fungal community with respect to which fungal guild, e.g., saprotrophic vs. ectomycorrhizal fungi, responded to substrate addition. Even though saprotrophic fungi are key decomposers of OM, ectomycorrhizal fungi may also play an important role in degradation processes, as they were found to use OM for nutrient acquisition in previous studies (e.g., Shah et al., 2016).

The strong increase in fungal abundance as a response to root addition throughout the entire soil profile was paralleled by high relative root-C incorporation rates. This indicated the dominance of preferential root litter decomposers within the fungal communities in both topsoil and subsoil environments. This strong fungal dependence on recent plant residues within entire soil profiles was also found in a study following C flow from maize litter into microbial decomposers (Müller et al., 2016). Considering that the contribution of recent plant-derived C to subsoil OC pools is low (Kramer and Gleixner, 2008; Angst et al., 2018), the fungal root-C utilization pattern with soil depth in our study provides further evidence of the limitation of plant-derived C as a key factor accounting for low fungal abundance in subsoil.

Differences in biomass responses and root-C incorporation rates between bacteria and fungi were also reflected in absolute root-C incorporation. This suggests that the substrate assimilation capacity of fungi was less affected by the low water content than was that of bacteria. Fungal decomposers have been found to be less moisture sensitive than bacteria and are able to bridge air-filled pores via hyphal growth (Drenovsky et al., 2004; Preusser et al., 2017). This may explain why fungi, in contrast to bacteria, showed higher absolute root-C incorporation rates in subsoil than in topsoil samples despite the generally lower water content. Therefore, fungi were either not or only slightly constrained in their utilization of the added root litter in the subsoil environment, while bacterial utilization was clearly restricted. Consequently, our hypothesis regarding the impact of habitat conditions on microbial substrate utilization was confirmed for bacteria but not for fungi, indicating the importance of fungi in C-cycling under unfavourable conditions such as low soil moisture.

Interaction effects of substrate addition and soil translocation on microbial decomposers

Biotic and abiotic gradients within the soil profile had only minor influences on the development of root-degrading microorganisms in topsoil samples. The abundances as well as the relative and absolute root-C assimilation rates of bacteria in topsoil samples were not affected by incorporation depth, indicating both a constant contribution of various C sources to the SOC pool and unchanged SOC availability at the microbial scale (i.e., within the soil containers). In contrast, the fungal community was more sensitive than the bacterial community to both root litter addition and to altered environmental conditions with soil depth, showing a steep increase in relative root-C utilization from top- to subsoil. In the subsoil environment, fungal growth was almost entirely dependent on root-C; the concurrently decreasing fungal abundance with soil depth suggested that fungi relying on other C sources were disconnected from their substrates. In addition, the substantial shift in fungal C resources indicated pronounced alterations in the depth-specific fungal communities due to soil translocation, as also seen in a study investigating fungal communities within soil profiles of a cropland (Moll et al., 2015). However, the root litter degrading fungal community in topsoil samples remained constant, as reflected by unchanged absolute root-C incorporation within the entire soil profile. A change in microbial abundance or community structure, therefore, is not necessarily related to changes in a community-specific function such as root decomposition as also shown in a study by Waldrop and Firestone (2004).

In contrast to topsoil samples, root-C utilization patterns of both bacteria and fungi changed in subsoil samples. While the absolute bacterial root-C incorporation reflected constant bacterial root decomposition over the entire profile, we assume that bacterial sub-populations depending on other C sources benefited, for example, from increased DOC input into subsoil samples that had been translocated to the topsoil environment. This process diluted the ^{13}C signal in the bacterial community while increasing bacterial abundance. Hyphal growth of fungi supported increased growth of fungal sub-populations using either root-C or other C sources as indicated by the reduced relative ^{13}C incorporation and concurrently increased absolute ^{13}C incorporation. Consequently, growth of fungal root degraders may have been triggered by other available substrates or by improved accessibility to limiting nutrients such as nitrogen.

The relative fungal root-C utilization exceeded that of bacteria throughout the first twelve months of root decomposition. In previous studies, fungi were identified as the primary initial degraders of root litter, with the bacterial contribution increasing in later stages of decomposition (Sanaullah et al., 2016). However, we found no shift in microbial community structure or in the extent of group-specific root-C utilization throughout the major phase of root decay, in which fungi consistently exhibited both the greatest increase in abundance and the highest relative root-C incorporation. Moreover, changes in microbial community structure with ongoing root decay and increasing soil depth were not observed either in topsoil or in subsoil samples over the course of the experiment. This implies that although environmental conditions differed within the soil profile, they did not affect the development of the root degrading microbial community. Our hypothesis in this regard could therefore not be confirmed.

6.5 Conclusion

The reciprocal soil translocation of topsoil and subsoil revealed microbial access to degradable substrate as the key determinant of microbial C assimilation and growth. Microbial access is regulated by the quantity and quality of substrate inputs as well as by the spatial distribution of substrates within soil profiles. Interactions between low water content and soil structure can interrupt C transport via soil solution and result in spatial separation between microorganisms and their substrates. This applies, in particular, to soils with a coarse soil structure, such as the sandy Dystric Cambisol in this experiment, and to soils exposed to periodic droughts. At the group specific level, spatial separation between decomposer and their substrates restricts substrate utilization of bacteria to a higher extend than that of fungi. Since bacteria dominate microbial communities in subsoils, the inhibition of bacterial decomposition under low soil moisture strongly affects C dynamics and may thus contribute to stabilization of C in deeper soil layers.

6.6 Acknowledgments

We would like to thank Stefanie Heinze, Nils Borchard and Bernd Marschner for the project coordination, Sabine Rudolph and Heike Haslwimmer for their assistance in the laboratory, Wolfgang Armbruster at Institute of Food Chemistry at University of Hohenheim for IRMS measurements, Kathleen Regan for English corrections, and Mathias Bischoff and Andreas Lieb for their help during the soil samplings. This project was part of the Research Unit “The Forgotten Part of Carbon Cycling: Organic Matter Storage and Turnover in Subsoils (SUBSOM)” and funded by the Deutsche Forschungsgemeinschaft DFG (FOR1806, KA 1590/11-1, KA 1590/11-2, MA 4436/3-2, PO 1578/4-2).

6.7 Supplementary materials

Table S6.1: *Soil parameters of the field site.*

Soil horizon	Depth (cm)	pH ($CaCl_2$)	SOC (g kg^{-1})	Sand (%)	Silt (%)	Clay (%)
AE	0-2	3.3	27	70	26	4
Bsw	2-12	3.4	17	65	30	5
Bw	12-36	4.4	7	67	29	4
BwC	36-65	4.5	3	73	24	3
C	65-125	4.4	0.4	95	4	1
2C	125-150	4.1	0.1	81	11	8
2Cg	150-180	4.2	0.8	72	19	9
3C	180+	4.2	<0.1	95	4	1

Table S6.2:
a: *Root addition, translocation and sampling date effects on water content (%), extractable total nitrogen (ETN), extractable organic carbon (EOC) and cutin and suberin derived monomers tested with LME model.*

b: *Root addition, translocation and sampling date effects on microbial biomass C (C_{mic}), $PLFA_{gram+}$, $PLFA_{gram-}$, $PLFA_{fun}$ and Ergosterol tested with LME model.*

The table shows significant effects with F-ratios and P-values in parentheses. A = root addition, T = translocation, D = sampling date.

	Soil	Parameter	A	T	D	A*T	T*D	A*D	A*T*D
a	TOP5	Water content (%)					$F_{6,46} = 11.12$ $p < 0.001$		
	SUB110	Water content (%)					$F_{6,46} = 13.02$ $p < 0.001$		
	TOP5	ETN	$F_{1,46} = 4.10$ $p < 0.05$	$F_{2,46} = 10.64$ $p < 0.001$					
	SUB110	ETN		$F_{2,46} = 4.86$ $p < 0.05$					
	TOP5	EOC	$F_{1,46} = 12.81$ $p < 0.001$						
	SUB110	EOC	$F_{1,46} = 3.18$ $p < 0.1$				$F_{6,46} = 5.29$ $p < 0.001$		
	TOP5	Cutin							
	SUB110	Cutin			$F_{1,21} = 18.07$ $p < 0.001$				
	TOP5	Suberin					$F_{2,20} = 3.51$ $p < 0.05$		
	SUB110	Suberin			$F_{1,9} = 9.98$ $p < 0.05$				
b	TOP5	C_{mic}	$F_{1,46} = 10.77$ $p < 0.01$	$F_{2,46} = 9.14$ $p < 0.01$	$F_{3,46} = 113.21$ $p < 0.001$				
	SUB110	C_{mic}	$F_{1,46} = 5.62$ $p < 0.05$				$F_{6,46} = 4.66$ $p < 0.01$		
	TOP5	$PLFA_{gram+}$	$F_{1,46} = 21.82$ $p < 0.001$	$F_{2,46} = 6.63$ $p < 0.01$					
	SUB110	$PLFA_{gram+}$			$F_{3,46} = 5.86$, $p < 0.01$	$F_{2,46} = 4.40$ $p < 0.05$			
	TOP5	$PLFA_{gram-}$	$F_{1,46} = 18.95$ $p < 0.001$						
	SUB110	$PLFA_{gram-}$				$F_{2,46} = 4.28$ $p < 0.05$			
	TOP5	$PLFA_{fun}$	$F_{1,46} = 68.19$ $p < 0.001$	$F_{2,46} = 9.90$ $p < 0.001$					
	SUB110	$PLFA_{fun}$				$F_{2,46} = 4.56$ $p < 0.05$			
	TOP5	Fungi to bacteria ratio	$F_{1,46}=20.16$ $p < 0.001$	$F_{2,46}= 3.46$ $p < 0.05$					
	SUB110	Fungi to bacteria ratio		$F_{2,46}=14.30$ $p < 0.001$					
	TOP5	Ergosterol	$F_{1,46} = 31.03$ $p < 0.001$	$F_{2,46} = 12.60$ $p < 0.001$					
	SUB110	Ergosterol			$F_{3,46} = 5.09$ $p < 0.01$	$F_{2,46} = 10.57$ $p < 0.001$			

Table S6.3: *Translocation and sampling date effects on* ***relative root-derived C incorporation (%) into different fractions*** *tested with LME models. The table shows significant effects with F-ratios and P-values in parentheses. T = translocation, D = sampling date.*

	Soil	**Parameter**	**T**	**D**	**T*D**
Extractable organic C	TOP5	EO^{13}C (%)			**$F_{6, 22} = 3.52$ $p < 0.05$**
	SUB110	EO^{13}C (%)	**$F_{2, 22} = 16.51$ $p < 0.001$**		
Microbial biomass C	TOP5	^{13}C$_{\text{mic}}$ (%)	$F_{2, 22} = 2.95$ $p < 0.1$		
	SUB110	^{13}C$_{\text{mic}}$ (%)			**$F_{6, 21} = 2.73$ $p < 0.05$**
Phospholipid fatty acid (PLFA)	TOP5	^{13}C PLFA$_{\text{gram+}}$ (%)	**$F_{2,22} = 6.36$ $p < 0.01$**		
	SUB110	^{13}C PLFA$_{\text{gram+}}$ (%)	**$F_{2,22} = 24.41$ $p < 0.001$**		
	TOP5	^{13}C PLFA$_{\text{gram-}}$ (%)	$F_{2, 22} = 2.85$ $p < 0.1$		
	SUB110	^{13}C PLFA$_{\text{gram-}}$ (%)	**$F_{2,22} = 22.90$ $p < 0.001$**	**$F_{3,22} = 3.74$ $p < 0.05$**	
	TOP5	^{13}C PLFA$_{\text{fun}}$ (%)	**$F_{2,22} = 7.31$ $p < 0.01$**		
	SUB110	^{13}C PLFA$_{\text{fun}}$ (%)	**$F_{2,22} = 10.79$ $p < 0.001$**	**$F_{3,22} = 6.20$ $p < 0.001$**	

Table S6.4: *Translocation and sampling date effects on* ***absolute root-derived C incorporation into different fractions*** *tested with LME models. The table shows significant effects with F-ratios and P-values in parentheses. S = soil, T = translocation, D = sampling date.*

	Parameter	**S**	**T**	**D**	**S*T**	**S*D**	**T*D**	**S*T*D**
Extractable organic C	EO^{13}C (abs.)			**$F_{3,46} =$ 7.09 $p < 0.001$**	**$F_{2,46} =$ 4.34 $p < 0.05$**			
Microbial biomass C	$^{13}C_{mic}$ (abs.)	**$F_{1,45} =$ 19.29 $p < 0.001$**						
Phospholipid fatty acid (PLFA)	^{13}C PLFA$_{gram+}$ (abs.)	**$F_{1,46} =$ 9.45 $p < 0.01$**	**$F_{2,46} =$ 4.15 $p < 0.05$**					
	^{13}C PLFA$_{gram-}$ (abs.)		**$F_{2,46} =$ 14.27 $p < 0.001$**			**$F_{3,46} =$ 3.94 $p < 0.05$**		
	^{13}C PLFA$_{fun}$ (abs.)	**$F_{1,46} =$ 28.12 $p < 0.001$**						

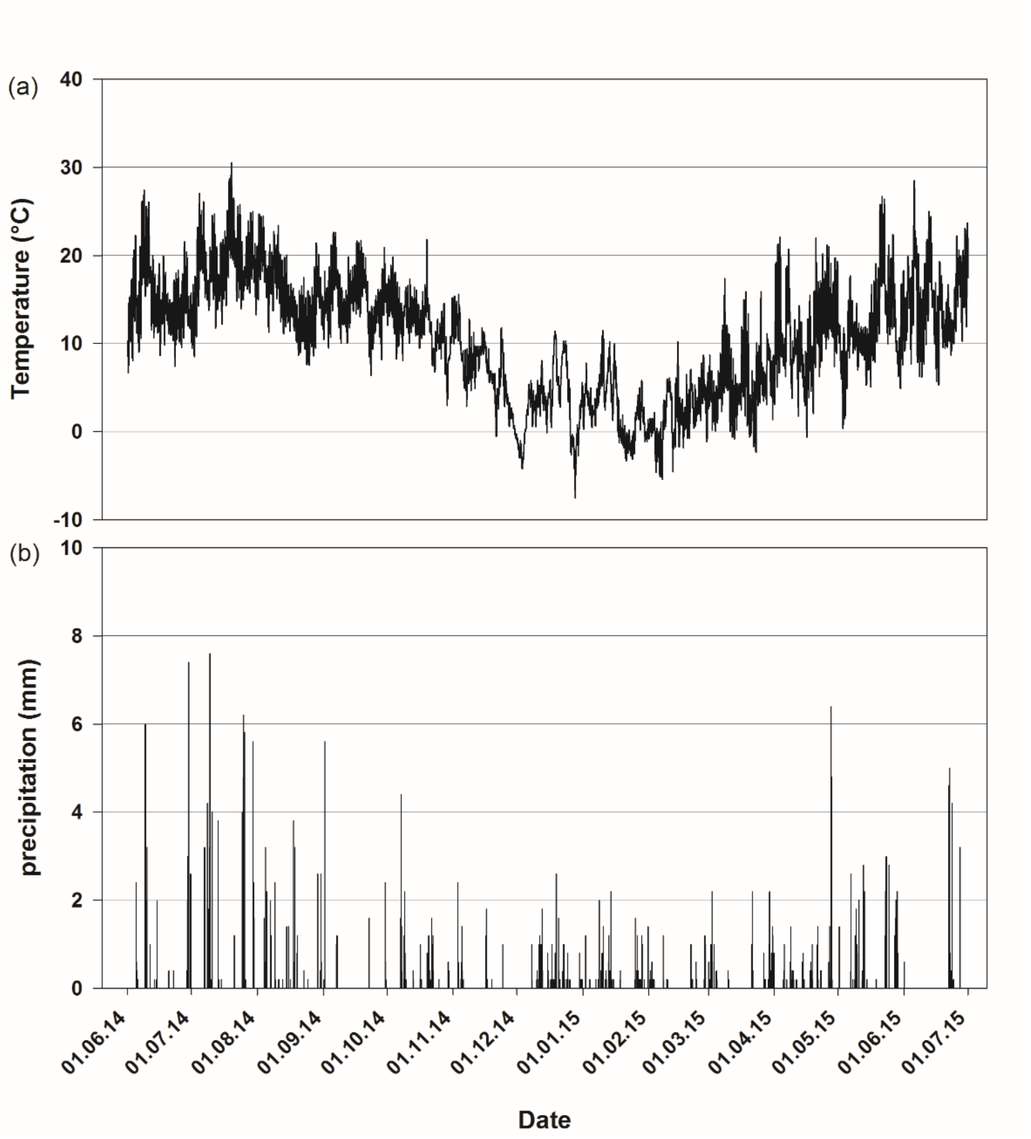

Figure S6.1 Mean daily (a) air temperature (°C) and (b) precipitation (mm) at the experimental site from June 1, 2014 to June 31, 2015.

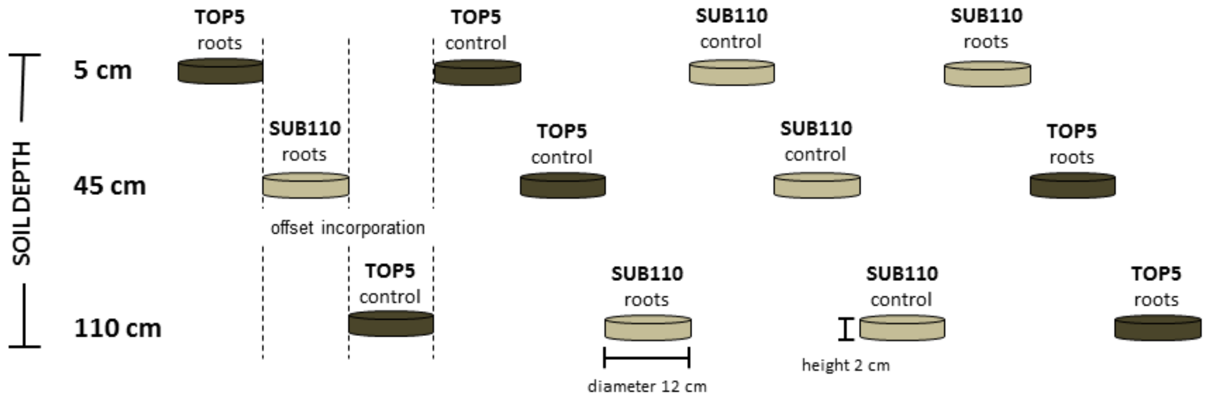
TOP5
roots
TOP5
control
SUB110
control
SUB110
roots
5 cm
SUB110
roots
TOP5
control
SUB110
control
TOP5
roots
45 cm
SOIL DEPTH
offset incorporation
TOP5
control
SUB110
roots
SUB110
control
TOP5
roots
110 cm
height 2 cm
diameter 12 cm

Figure S6.2 Exemplary front view of one of twelve tree facing profile walls with four soil containers (treatments: TOP5roots, TOP5control, SUB110roots and SUB110control) randomly incorporated into 5 cm, 45 cm and 110 cm soil depths each. Due to the randomized distribution of the different containers in the three depths of each of the twelve profile pits, this is an exemplary incorporation pattern to illustrate the incorporation design.

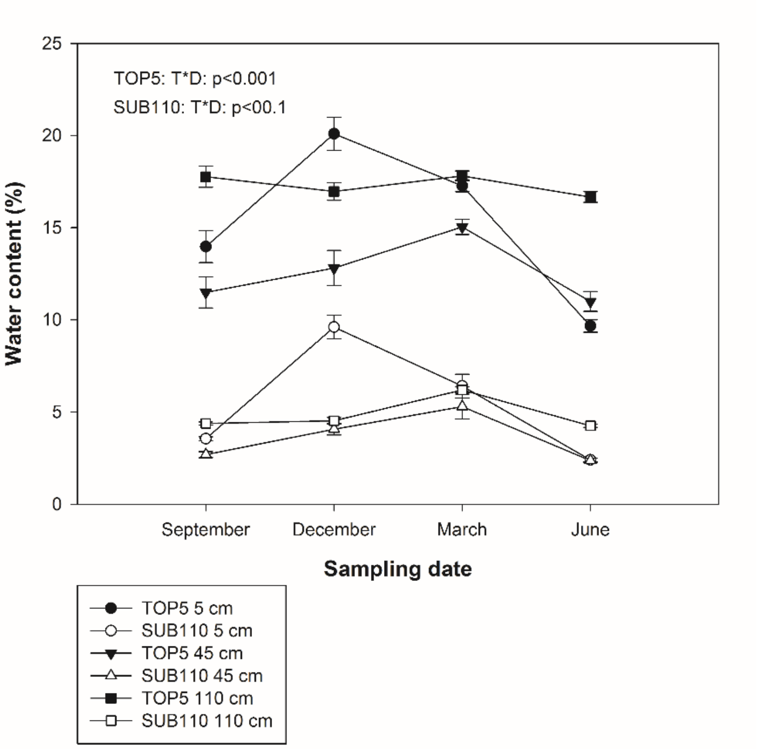

Figure S6.3 Mean gravimetric water content (%) in TOP5 and SUB110 samples translocated to different soil depths at the sampling dates September 2014, December 2014, March 2015 and June 2015. Error bars indicate standard error (n=3). The figure shows significant effects with respective P-values. A = root addition, T = translocation, D = sampling date.

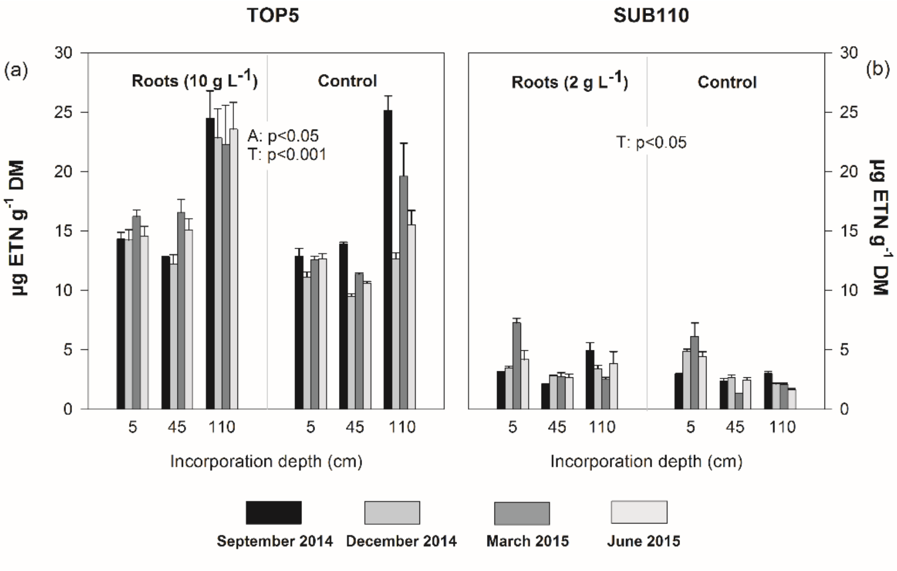

Figure S6.4 Amount of extractable total nitrogen (ETN) in TOP5 (a) and SUB110 (b) samples under different translocation and root addition treatments at the sampling dates September 2014, December 2014, March 2015 and June 2015. Error bars indicate standard error (n=3). The figure shows significant effects with respective P-values. A = root addition, T = translocation, D = sampling date.

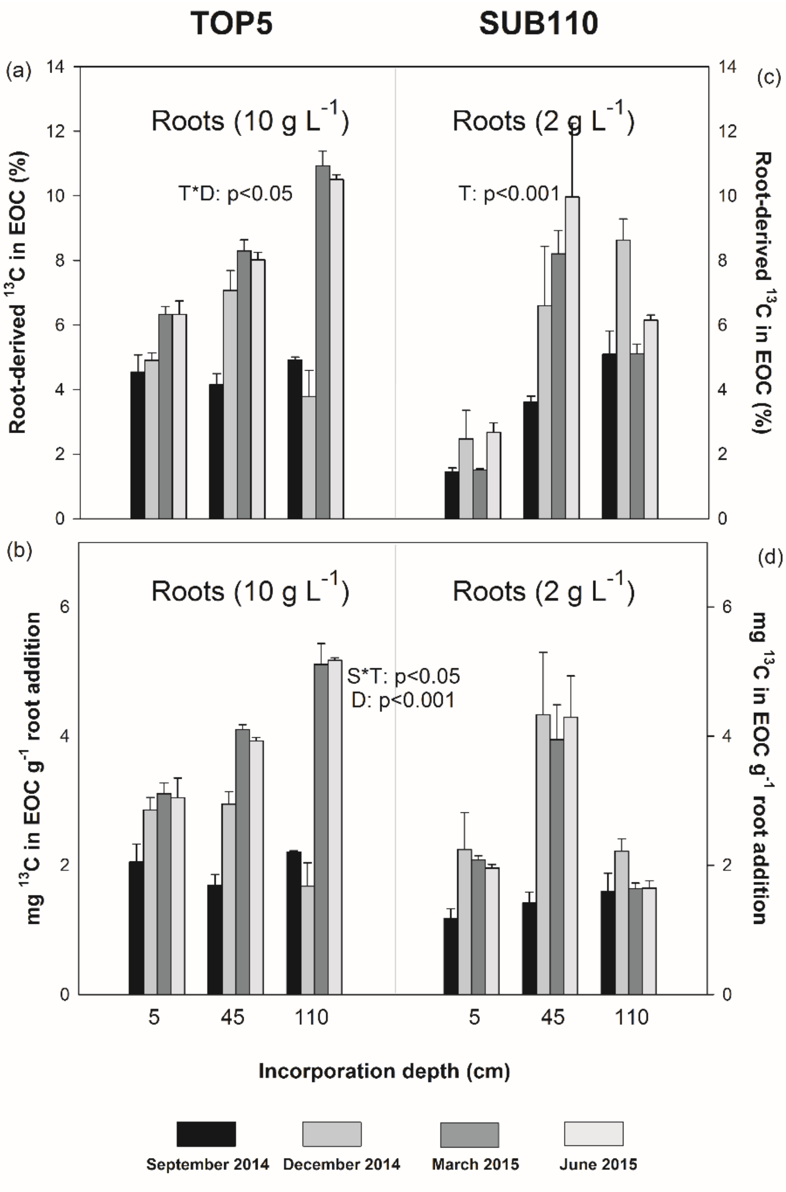

Figure S6.5 Relative proportion (%) of root-derived ^{13}C in extractable organic carbon (EO^{13}C %, a and c) and absolute amount of ^{13}C-root-derived C in EOC (µg root-derived C in EOC g^{-1} DM, b and d) in TOP5 and SUB110 samples under different translocation and root addition treatments at the sampling dates September 2014, December 2014, March 2015 and June 2015. Error bars indicate standard error (n=3). The figure shows significant effects with respective P-values. S = soil origin, A = root addition, T = translocation, D = sampling date.

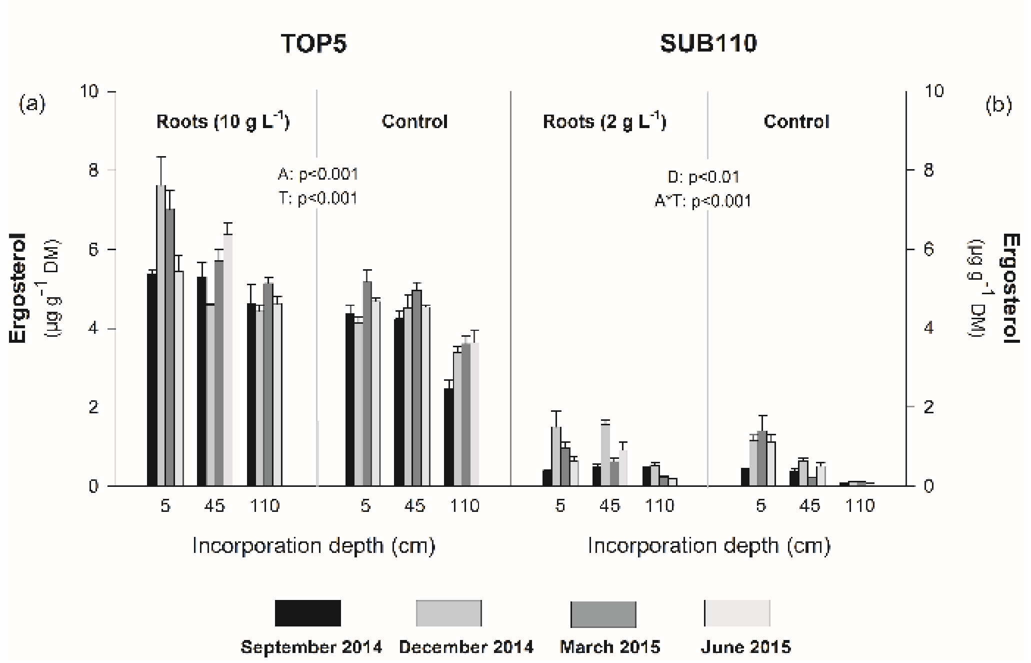

Figure S6.6 Amount of ergosterol in TOP5 (a) and SUB110 (b) samples under different translocation and root addition treatments at the sampling dates September 2014, December 2014, March 2015 and June 2015. Error bars indicate standard error (n=3). The figure shows significant effects with respective P-values. A = root addition, T = translocation, D = sampling date.

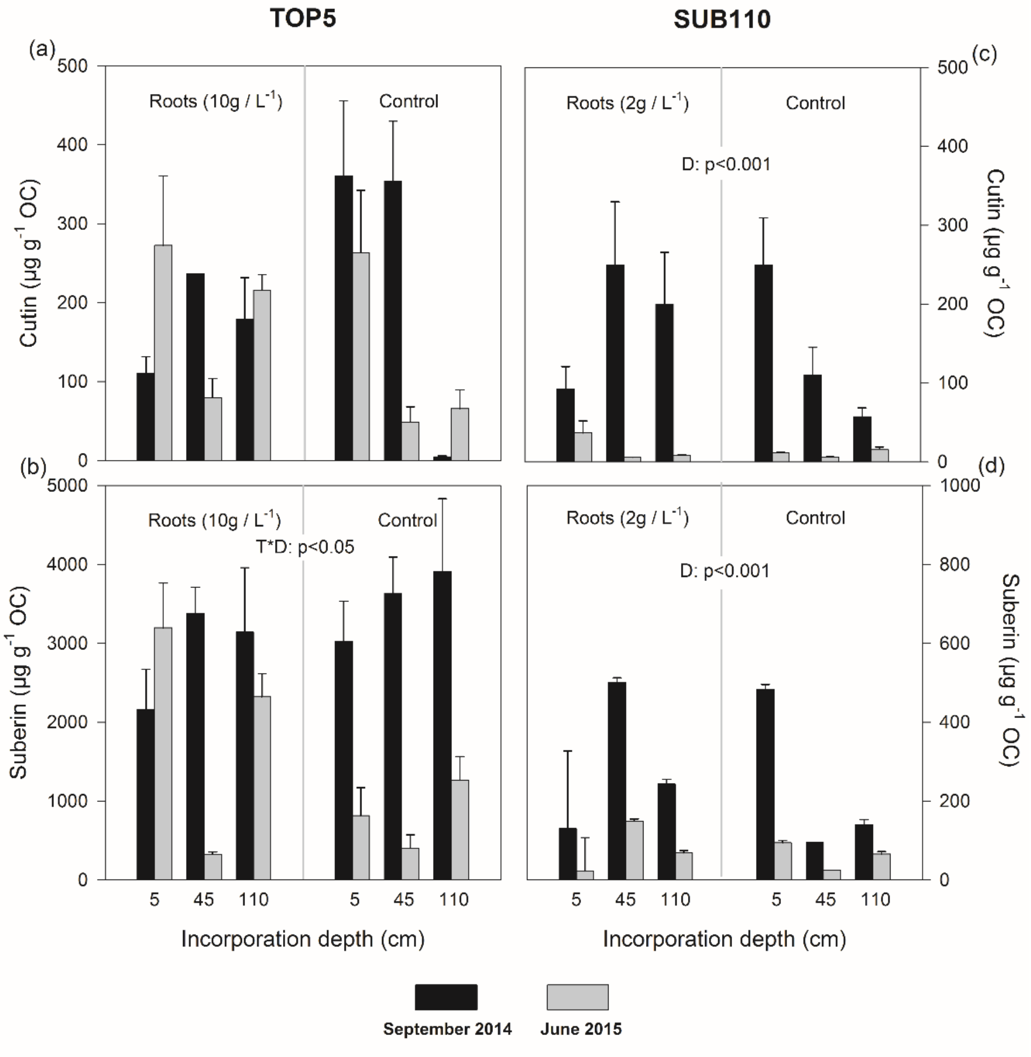

Figure S6.7 Amounts of cutin (µg g^{-1} OC, a and c) and suberin (µg g^{-1} OC, b and d) in TOP5 and SUB110 samples under different translocation and root addition treatments at the sampling dates September 2014 and June 2015. Error bars indicate standard error (n=3). The figure shows significant effects with respective P-values. A = root addition, T = translocation, D = sampling date.

7 Multiple exchange processes on mineral surfaces control the transport of dissolved organic matter through soil profiles

Soil Biology & Biochemistry 118 (2018) 79–90

DOI: 10.1016/j.soilbio.2017.12.006

Received: 20 September 2017, Revised: 6 December 2017, Accepted: 9 December 2017,
Published online: 22 December 2017

Timo Leinemann[a*], Sebastian Preusser[b], Robert Mikutta[c], Karsten Kalbitz[d], Chiara Cerli[e],

Carmen Höschen[f], Carsten W. Mueller[f], Ellen Kandeler[b] and Georg Guggenberger[a]

[a]Institute of Soil Science, Leibniz Universität Hannover, Herrenhäuser Straße 2,
30451 Hannover, Germany
[b]Institute of Soil Science and Land Evaluation, Soil Biology Department,
University of Hohenheim, Emil-Wolff Str. 27, 70599 Stuttgart, Germany
[c]Soil Science and Soil Protection, Martin Luther University Halle-Wittenberg,
Von-Seckendorff-Platz 3, 06120 Halle (Saale), Germany
[d]Institute of Soil Science and Site Ecology, Technische Universität Dresden, Pienner Strasse 19,
01737 Tharandt, Germany
[e]Institute for Biodiversity and Ecosystem Dynamics, Earth Surface Sciences Research Group,
Universiteit van Amsterdam, Sciencepark 904, 1098 XH Amsterdam, Netherlands.
[f]Chair of Soil Science, Department Ecology and Ecosystem Management, Center of Life and
Food Sciences Weihenstephan, Technische Universität München, Emil-Ramann-Straße 2,
85354 Freising, Germany

[*]Corresponding author

E-mail address: leinemann@ifbk.uni-hannover.de

Abstract

Organic topsoil layers are important sources of dissolved organic matter (DOM) transported to deeper soil layers. During passage through the mineral soil, both organic matter (OM) quality and quantity change markedly. Whether these alterations are due to sorption processes alone or to additional stepwise exchange processes of OM on mineral surfaces (“cascade model”) is not fully understood. To test the “cascade model”, we conducted a laboratory flow cascade experiment with undisturbed soil columns from three depths of two different soil profiles (Dystric and Eutric Cambisol) using carbon (C) isotope labelling. Each of the connected topsoil and subsoil columns contained a goethite (α-FeOOH) layer either with or without sorbed ^{13}C-labelled OM to assess the importance of OM immobilization / mobilization reactions with reactive soil minerals. By using a multiple method approach including ^{13}C analysis in the solid and solution phases, nanometer scale secondary ion mass spectrometry (NanoSIMS), and quantitative polymerase chain reaction (*q*PCR), we quantified organic carbon (OC) adsorption and desorption and net OC exchange at goethite surfaces as well as the associated microbial community patterns at every depth step of the column experiment. The gross OC exchange between OM-coated goethite and the soil solution was in the range of 15-32%. This indicates that a considerable proportion of the mineral associated OM was mobilized and replaced by percolating DOM. We showed that specific groups of bacteria play an important role in processing organic carbon compounds in the mineral micro-environment. Whereas bulk soils were dominated by oligotrophic bacteria such as *Acidobacteria*, the goethite layers were specifically enriched with copiotrophic bacteria such as *Betaproteobacteria*. This group of microorganisms made use of labile carbon derived either from direct DOM transport or from OM exchange processes at goethite surfaces. Specific microorganisms appear to contribute to the cascade process of OM transport within soils. Our study confirms the validity of the postulated “cascade model”, featuring the stepwise transport of OM within the soil profile.

Keywords: Cascade model; DOM; reactive minerals; ^{13}C; NanoSIMS; microbial community composition

7.1 Introduction

Dissolved organic matter (DOM) mobilized in topsoil and transported to subsoil horizons is an important source of carbon (C) throughout the soil profile. In most soils the concentration of dissolved organic carbon (DOC) declines strongly with soil depth, with up to 90% net loss in the first meter of the soil profile (Michalzik et al., 2001). This is likely due to its adsorption to reactive minerals such as iron (Fe) oxides (Kaiser and Guggenberger, 2000) and clay minerals (Saidy et al. 2013), or to co-precipitation with aluminium (Al) and Fe (Scheel et al., 2008; Mikutta et al., 2014). According to Kalbitz and Kaiser (2008), as much as 19-50% of the organic matter (OM) in the subsoil of a sandy Podzol can be derived from DOM.

Positive correlations between the content of pedogenic Al and Fe with the content of soil organic carbon (OC) (Kaiser and Guggenberger, 2000) and of OC resistant to chemical degradation (Mikutta et al., 2006) suggest that the association of OM with Fe and Al oxides is an important stabilisation mechanism for OM. Especially in acidic soil environments, such as in Dystric Cambisol subsoils, Fe oxides with high specific surface area (SSA) provide reactive surfaces that are important for the binding of OM (Eusterhues et al., 2005). Gu et al. (1994) and Kaiser et al. (1997) concluded that the adsorption of DOM to Fe oxides is dominated by ligand exchange involving carboxyl and hydroxyl functional groups, promoting oxidized aromatic moieties (i.e., lignin-degradation compounds) over carbohydrates in the sorption process (Chorover and Amistadi, 2001; Kaiser, 2003). Thus not only does the concentration of DOC decrease with soil depth but the composition of DOM also changes. A relative enrichment in carbohydrates and sugars along with the selective removal of carboxylated aromatic moieties from soil solution has been observed in batch experiments (Kaiser et al., 1997), saturated soil column experiments (Guo and Chorover, 2003), and in field experiments (Kaiser et al., 2004; McCarthy et al., 1996). Binding of DOM to Fe oxides such as goethite is not only selective for specific compounds, but can also lead to a strong reduction in SSA due to clogging of micropores by selective sorption at the mouths of pores (Kaiser and Guggenberger, 2007). At higher OM loadings, multiple layers of OM are possibly formed on the mineral surfaces, suggesting stronger binding and stabilization of OM that is in direct contact with the mineral surface (Kaiser and Guggenberger, 2003) and enhanced exposure of the outermost OM layer to desorption and exchange processes.

A major source of DOM in temperate forest soils is leaching from the forest floor, leading to highest DOC concentrations directly below the soil organic layer (Michalzik et al., 2001). Most of this DOM is either retained or consumed in the upper centimeters of the mineral soil (Fröberg et al., 2007), whereas DOM at greater soil depths is not directly derived from the organic layer (Hagedorn et al., 2004). Based on such observations, Kaiser and Kalbitz (2012) proposed a stepwise cascade of adsorption to reactive minerals, microbial transformation, and re-release into the soil solution during the transport of DOM down the soil profile. This cascade assumes that previously bound, more degraded OM moieties get remobilized by the input of fresh highly surface-reactive plant-derived DOM and are transported further down the soil profile where they replace and consequently remobilize even older OM. This conceptual view, therefore, could link the chemical fractionation of DOM during passage down the soil column with the increasing ^{14}C age of DOM and OM as soil depth increases (Sanderman et al., 2008), but experimental data is lacking.

The microbial community adapts to the quantity of bioavailable OM; thus microbial community composition indicates co-evolution with concurrently changing OM properties as soil depth increases (Heckman et al., 2013). In deeper soil, the magnitude of OM processing differs considerably between different soil compartments. Microbial densities are mostly low and heterogeneously distributed depending on OM availability and chemical composition (Preusser et al., 2017; Angst et al., 2016). In contrast to the generally slow process rates in subsoil, reactive minerals such as goethite are known as hotspots of biogeochemical interactions (Eusterhues et al., 2005) and may therefore be of major importance for OM processing in deeper soil layers. Nevertheless, several physicochemical characteristics of water-extractable OM (apparent molar mass, pH, and electrical conductivity) may modify responses of the bacterial and fungal communities in the presence of Fe and Al oxide phases (Heckman et al., 2013).

The objective of this study, therefore, was to test the “cascade model” of Kaiser and Kalbitz (2012) by elucidating whether changes in amounts and composition of DOM within soil profiles are due to sorption processes alone or to additional stepwise exchange of OM on mineral surfaces, processes which may be driven in part by microbial activity. We hypothesize that (i) the input of plant-derived DOM to mineral topsoils leads to selective adsorption of plant-derived compounds to reactive surfaces; (ii) fresh DOM input partially replaces older mineral-associated OM, which subsequently gets remobilized and further transported to deeper soil; and (iii) these mineral-organic associations act as biogeochemical hotspots of high resource availability leading to changes in microbial abundance and community composition. These hypotheses were tested by a column experiment using three connected undisturbed soil horizons from two soils (Dystric and

Eutric Cambisol), each horizon containing a thin interspersed layer of goethite coated with ^{13}C-labelled OM. Incorporation of the labelled OC made it possible to quantify net OC retention and DOM-induced exchange of goethite-associated OM. For selected samples, nanoscale secondary ion mass spectrometry (NanoSIMS) was used to study the microscale (im)mobilization of OM at the goethite surfaces. Concomitant shifts in microbial community composition in the bulk soil and the goethite layers were analyzed by domain- and taxa-specific quantitative polymerase chain reaction (*q*PCR) assays.

7.2 Materials and methods

Soil sampling

Undisturbed soil cores of 100 cm^3 (ø 5.7 cm, h 4.0 cm) were taken from two sites in Lower Saxony, Germany; a sandy Dystric Cambisol (IUSS Working Group WRB, 2014) developed from Pleistocene fluvial and aeolian sandy deposits at the Grinderwald (52° 34’22.12" N, 9° 18’ 49.76" E), and a silty Eutric Cambisol (IUSS Working Group WRB, 2014) developed from basalt near Dransfeld (51° 28' 35.60" N, 09° 45' 32.46" E). Both sites were covered with evenly aged (~100 years) European beech (*Fagus sylvatica* L.) forest. Soil cores were taken from three depths: 4 cm, 30 cm and 100 cm at the sandy site, and 4 cm, 12 cm and 26 cm at the silty site, because core sampling in deeper soil layers at the silty site was impossible due to high stone content near the solid bedrock (Table7.1).

Table 7.1: *Basic physical and chemical soil properties of the three sampling depths in each of the two soils before the experiment.*

Texture	Horizon	Depth (cm)	pH ($CaCl_2$)	C (mg g^{-1})	N (mg g^{-1})	C/N	$\delta^{13}C$ (‰)	Fe_d (mg g^{-1})	Sand (%)	Silt (%)	Clay (%)
Sand	AE	4	3.23	56.31	0.80	27.46	-28.32	2.97	54	41	5
Sand	Bw	30	4.27	5.99	0.32	18.80	-26.62	2.46	56	39	5
Sand	Cw	100	4.28	0.20	0.06	3.63	-26.41	1.38	76	23	1
Silt	A	4	3.85	48.79	3.75	13.02	-26.54	20.85	0	89	11
Silt	Bw	12	3.88	44.80	3.57	12.53	-26.28	21.49	0	87	13
Silt	Bw	26	4.27	30.25	2.77	10.94	-25.96	22.4	1	89	11

Preparation of goethite coated with ^{13}C-labelled organic matter

Goethite was produced by increasing the pH of a 0.5 M $FeCl_3$ solution to 12 with 5 M NaOH and subsequent aging of the precipitate to goethite at 55°C for 48 hours (Schwertmann and Cornell, 2000). The suspension was dialyzed against double deionized water until the conductivity was <10 µS cm^{-1} and subsequently frozen in liquid nitrogen, freeze-dried, and sieved <200 µm. For the organic matter coating, ^{13}C-labeled DOM was prepared by extraction of a mixture of 10 g labelled beech leaves (12.3 atom% ^{13}C) (IsoLife BV, Wageningen, Netherlands) and 240 g of naturally grown beech leaves in 2500 mL double deionized water (1:10, w/v), to limit the need for expensive ^{13}C-labelled plant litter. The litter material was ground to a maximum size of approximately 3 cm with a stick blender, mixed with the water, and then extracted after being held at room temperature for 16 h. The litter material was removed by a coarse sieve and the remaining solution was pre-filtered by pressure filtration through glass fibre filters (GF 92, Whatman, Chicago, USA) and finally pressure filtered through 0.45-µm cellulose nitrate filters (Sartorius, Göttingen, Germany). The bulk solution had a concentration of 1519.5 ± 15.3 mg C L^{-1} and 119.6 ± 1.6 mg N L^{-1}. The solution was diluted to 500 mg C L^{-1} with double deionized water for further handling. Ten g of goethite were shaken in 1000 ml of this DOM solution for 24 hours in the dark on an overhead shaker and subsequently centrifuged for 20 min at 2000 *g*. The supernatant was decanted and the residual goethite was washed two times for 10 minutes with ultrapure water und each time centrifuged for 10 minutes at 2000 *g* and decanted. The residual OM-coated goethite was freeze dried and stored in the dark until use. The OM-coated goethite had an OC concentration of 19.4 mg g^{-1} and 0.19 mg m^{-2}. SSA decreased considerably as a result of the OM loading (Table 7.2), even though the sorption capacity of the mineral was not reached as compared to investigations by Kaiser and Guggenberger (2007). The OM coating on the goethite had a δ^{13}C ratio of 1298.9‰ VBDP.

Table 7.2: *Specific surface area (SSA), carbon (C) and nitrogen (N) content, C/N ratio, change of carbon concentration over the course of the experiment (ΔC), δ^{13}C, proportion of C sorbed to the goethite derived from before the experiment (GDC), proportion of solution-derived C associated with goethite after the experiment (SDC), and previously bound OC that was either removed or replaced over the course of the experiment (MC). Results of the uncoated goethite before the experiment are shown (Gp), and the samples from the respective three depth compartments with sandy soil (GpSa1, GpSa2 GpSa3) and silty soil (GpSi1, GpSi2, GpSi3), the OM-coated goethite before the experiment (G0), and the respective three depth compartments with sandy soil (G0Sa1, G0Sa2, G0Sa3) and with silty soil (G0Si1, G0Si2, G0Si3).*

Sample	SSA (m^2 g^{-1})	C (mg m^{-2})	C (mg g^{-1})	N (mg m^{-2})	N (mg g^{-1})	C/N	ΔC (%)	δ ^{13}C (‰)	GDC (%)	SDC (%)	MC (%)
Gp	102.80	0.02	2.36	0.00	0.50	4.68	-	-20.58	-	-	-
G0	79.50	0.19	19.44	0.02	1.72	11.32	-	1298.92	100	0	-
G0Sa1	82.29	0.30	31.04	0.03	2.13	14.58	37.31 ± 2.31	631.43 ± 29.05	48.96 ± 3.44	51.04 ± 3.44	21.93 ± 3.89
G0Sa2	85.97	0.23	23.93	0.02	1.70	13.94	14.72 ± 21.15	893.84 ± 226.05	68.57 ± 17.20	31.43 ± 17.20	19.62 ± 2.27
G0Sa3	86.49	0.18	18.28	0.02	1.57	11.61	-6.77 ± 7.66	1146.55 ± 74.09	87.89 ± 6.13	12.11 ± 6.13	17.65 ± 2.25
G0Si1	84.91	0.24	24.51	0.02	1.43	13.05	20.71 ± 0.86	699.46 ± 19.83	54.35 ± 0.78	45.65 ± 0.78	31.46 ± 0.24
G0Si2	80.91	0.19	19.09	0.02	1.44	11.6	-1.82 ± 0.46	1029.33 ± 37.50	78.94 ± 1.64	21.06 ± 1.64	22.47 ± 1.96
G0Si3	84.80	0.18	18.04	0.02	1.42	12.62	-7.77 ± 1.55	1046.11 ± 36.31	80.37 ± 2.70	19.63 ± 2.70	25.44 ± 1.57

Column experiment

Two soil cores of one depth were assembled into one soil column, with 2.8 g of goethite embedded in a 200-µm polyester mesh (Franz Eckerd GmbH, Waldkirch, Germany) placed tightly in between the cores (Fig. 7.1). For both soil types two variations of the experiment were performed, one using pure goethite (PG) and one using OM-coated goethite (CG). This resulted in four treatments: pure goethite between sandy soil cores (Sa_{PG}), OM-coated goethite between sandy soil cores (Sa_{CG}), pure goethite between silty soil cores (Si_{PG}), and OM-coated goethite between silty soil cores (Si_{CG}). Each column was equipped with an inlet and outlet and sealed with a solvent free sealing compound (water stop, MEM Bauchemie GmbH, Leer, Germany). Dissolved OM used in the column experiment was extracted from air dried, ground beech leaves sampled in autumn 2014 from the Grinderwald forest floor in double deionized water at room temperature for 16 h (1:10, w/v) and subsequently filtered through 0.45-µm cellulose nitrate filters (Sartorius AG, Göttingen, Germany). The resulting concentration of 1246.7 ± 25.7 mg C L^{-1} was diluted to approximately 30 mg C L^{-1} with double deionized water. The $\delta^{13}C$ ratio of the beech litter extract was -28.9‰ VPDB.

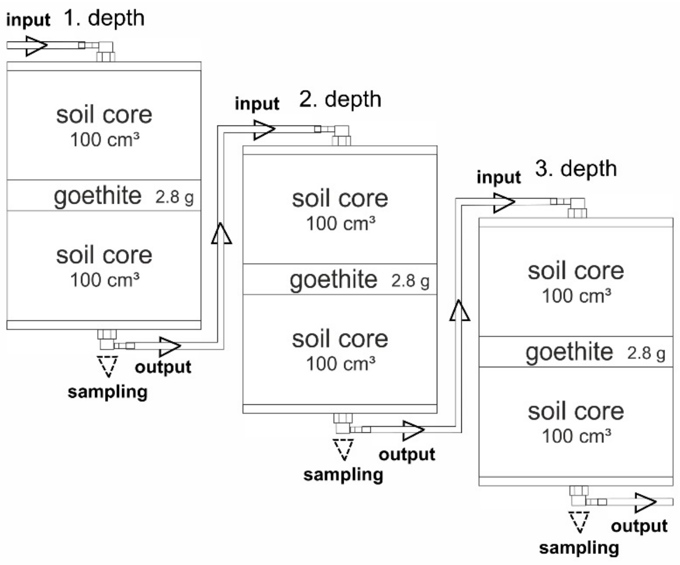
input
1. depth
soil core
100 cm³
goethite 2.8 g
soil core
100 cm³
output
sampling
input
2. depth
soil core
100 cm³
goethite 2.8 g
soil core
100 cm³
output
sampling
input
3. depth
soil core
100 cm³
goethite 2.8 g
soil core
100 cm³
output
sampling

Figure 7.1: Experimental setup of the column experiment. The arrows represent the direction of water flow. The dotted arrows represent sampling ports.

Three columns, representing soil from the different soil depths, were combined into one cascade with three replicates (Fig. 7.1). The experiments were carried out in a temperature controlled cabinet at a constant temperature of 8°C, closely approximating the mean annual temperature at the sampling sites. The prepared solution was pumped at a flux rate of 5.5 ml h^{-1} (3 mm h^{-1}) for 32 days into the first column inlet and the efflux from the first depth compartment was sequentially pumped into the second and third depth compartments. A volume of 100 ml of the outflow solution from each column and the inflow solution from the first depth column was sampled after 1, 2, 4, 8, and 16 days, and at the end of the experiment (first depth 32 days, second depth 27 days and third depth 22 days). The second and third columns had to be started after a 5 day delay with respect to their upper column because ca. 300 ml of percolation solution had to accumulate to enable secure solution supply. In total 4224 ml (2346 mm) solution were pumped through the first depth compartment, 3564 ml (1969 mm) through the second depth compartment, and 2904 ml (1604 mm) through the third depth increment, simulating the cumulative mean water flux of three years' mean precipitation. The volume reduction over depth was due to the cascade design of the experiment, as the available solution for the second and third columns declined by the withdrawn sample volume (100 ml per sampling). However, such a decrease in water flux with soil depth occurs also in the natural environment, as was recorded for the sampling site Grinderwald (Leinemann et al., 2016). After the experiment, the soil was removed from the cores, air dried, and stored for further measurements.

Measurements

DOC concentration was measured by high temperature combustion (Vario TOC cube; Elementar, Langenselbold, Germany), and the UV absorbance of DOM was determined at 280 nm on a Varian Cary 50 UV-Vis spectrophotometer (Agilent Technologies, Santa Clara, CA, USA). The $\delta^{13}C$ value of DOM ($DO^{13}C$) was analysed directly in solution using a high-temperature combustion system for direct ^{13}C measurement from liquid (Federherr et al., 2014 and Kirkels et al., 2014). For this, an isoTOC cube (Elementar group, Langenselbold, Germany) total organic carbon analyzer was coupled with a continuous flow isotope ratio mass spectrometer (IsoPrime100, Isoprime Ltd, Cheadle Hulme, UK).

All samples were manually acidified to pH ~2 by HCl (37%) in order to remove dissolved inorganic C and/or prevent (re)dissolution of atmospheric CO_2. Samples were injected 4 times and only the last three injections were used for data analyses. Injection volume ranged between 0.2 and 1 ml depending on the TOC content. Both at the beginning and at the end of each sequence a set of international standards (Caffeine IAEA-600 Sucrose IAEA-CH6; Coplen et al., 2006) dissolved in the blank water at a TOC concentration similar to the one expected for the samples were run as samples, allowing for 2 point normalisation. To be able to use a two point normalisation for labelled samples also, artificial standards were prepared by thoroughly mixing non-labelled and 99%-labelled glucose in proportions to obtain the desired label. The mixtures were then normalised vs international standard as solid using an Elemental Analyzer (vario ISOTOPE cube, Elementar group, Hanau, Germany) coupled to IRMS (IsoPrime100, Isoprime Ltd., Cheadle Hulme, UK) and then used to prepare the standard solutions as described above. The artificial solid mixtures were checked several times during the entire period of analyses to ensure the consistency of the obtained values. Blanks samples of the same water used for the preparation of the normalising standards were analysed before, after, and between samples. All calculations for corrections and normalisation were done according to those described in Kirkels et al. (2014).

After the experiment, soil columns were opened and the soil core above and below the goethite as well as the goethite layer were sampled separately, freeze dried and stored in the dark until analyses. C and N content and δ^{13}C ratios of solid samples were measured using an Elementar IsoPrime100 IRMS (IsoPrime Ltd, Cheadle Hulme, UK) coupled to an Elementar vario MICRO cube EA CN analyzer (Elementar Analysensysteme GmbH, Langenselbold, Germany). Total pedogenic Fe (dithionite-citrate-extractable Fe, Fe_d) of the soil samples before the experiment were determined according to Blakemore et al. (1987), in which 1.00 g air-dried soil in the presence of 1 g sodium dithionite was extracted with 20 ml 22% sodium citrate. After 16 hours of shaking and addition of 5 ml of 5 mM $MgSO_4$, samples were centrifuged for 20 min at 500 g and filtered. The filtrate was analyzed for Fe by inductively coupled plasma optical emission spectroscopy (ICP-OES; Varian 725-ES, Varian Australia Pty Ltd., Mulgrave, Australia). The specific surface area (SSA) and pore volumes of solid samples were analysed by N_2 adsorption-desorption at 77 K, after outgassing the samples at 232 K for 24 hours until the pressure remained constant below 9.0×10^{-4} Torr (Autosorb MP1, Quantachrome, Boynton Beach, FL, USA). SSA was determined by the multipoint BET method using 11 points in the 0.05-0.3 P/P_0 range (Brunauer et al., 1938). Total pore volume (TPV) of pores with a radius <1839.6 Å was taken at a partial pressure of 0.99. Average pore radius was calculated as $r_p = 2V_{liq}/SSA$, where V_{liq} is the volume of liquid N_2 contained in the pores.

To map the distribution of sorbed OC to the goethite surface, an aliquot of the OM-coated goethite before the experiment (G0) and an aliquot of the OM-coated goethite after the experiment from each of the three depths of the columns with the sandy soil (4 cm = G1, 30 cm = G2, 100 cm = G3) were analysed with a NanoSIMS 50L (Cameca, Gennevilliers, France). In order to facilitate adhesion to a thin layer of goethite, a small quantity of dried sample was spread on a silica wafer and placed at -20°C in a freezer for one minute. Afterwards, the sample was placed at room temperature for another minute, generating condensation water that served to adhere the samples to the wafer, which was then dried in a desiccator overnight. Loose material was removed with compressed air and the remaining sticking sample was subsequently coated with gold to avoid possible charging effects (Sputter Coater S150A, Edwards, Crawley, UK) during subsequent scanning electron microscope (SEM) imaging. Using SEM on each sample, four regions with representative single layered goethite aggregates were chosen for subsequent NanoSIMS analyses. A Cs^+ ion beam with 16 keV impact energy, ~4 pA, primary current was used and $^{12}C^-$, $^{13}C^-$, $^{16}O^-$ and $^{56}Fe^{16}O^-$ secondary ions were recorded using electron multipliers on a raster area of 30 µm × 30 µm (256 × 256 pixels) by collecting 100 planes per spot with a dwell time of 1 ms $pixel^{-1}$. Appropriate slits were used to ensure a mass resolution to solve mass interferences present between $^{13}C^-$ and $^{12}C^1H^-$. Prior to analysis the region was sputtered using a high primary beam current between 500 and 600 pA to remove contaminants, the Au layer, and to implant primary ions in the surface to enhance secondary ion emission. The images were corrected for electron multiplier dead time (44 ns) and further processed using the look@nanoSIMS software (Polerecky et al., 2012) operated with Matlab 2013b (The MathWorks Inc., Natick, MA, USA). Regions of interest (ROIs) were selected by the interactive threshold function on the basis of the $^{12}C^-$ counts of the accumulated measurements, as they represented areas of sorbed OM containing moieties rich in $^{13}C^-$ abundance as well. The areas corresponding to goethite were selected similarly on the basis of $^{56}Fe^{16}O^-$ counts. The distribution of sorbed OM to the goethite was quantified by calculating the percentage of area covered by OM on the goethite surface. The $^{13}C^{-}$ / $^{12}C^{-}$ was calculated for the OM ROIs to evaluate OC dynamics on the goethite surface over the course of the experiment. The ratio numbers were multiplied by 100 to better visualise small differences. The numbers then were in the range of atom% ^{13}C. To compare with NanoSIMS atom% ^{13}C the bulk EA-IRMS measurements were converted from the δ‰ notation to atom% ^{13}C values by taking the $^{13}C^{-}$ / $^{12}C^{-}$ ratio of the EA-IRMS standard (0.0111802) into account (Frey, 2007). For further discussion of the results the ROIs with an atom% ^{13}C of <1.40 were considered to consist mainly of newly sorbed OC as they occurred on the samples only after the column experiment (Table S7.6) and are referred to as low enriched. The ROIs with an atom%^{13}C of >1.4 and <2.4 are referred to as intermediate enriched and to possibly consist of a mixture of old and new sorbed OC. The ROIs with an atom%^{13}C of >2.40 are referred to as high enriched and were considered to consist of mainly old OC, as the they were similar to or higher than bulk EA-IRMS measurements of the OM-coated goethite before the experiment.

For *q*PCR analysis, DNA was extracted from 0.3 g sample of the experimental run with pure goethite (Table S7.2) using a FastDNA SPIN Kit for soil (BIO101, MP Biomedicals, Santa Ana, CA, USA) and quantified with a Nanodrop ND-2000 spectrophotometer (Thermo Scientific, Waltham, MA, USA), followed by dilution of the samples with ultra-pure water to a target concentration of 5 ng DNA μl^{-1}. The quantification of the abundances of total bacteria, fungi, and archaea and the abundances of the bacterial taxa *Betaproteobacteria*, *Actinobacteria*, *Acidobacteria*, *Bacteroidetes*, *Firmicutes*, *Verrucomicrobia* and *Gemmatimonadetes* via *q*PCR was carried out with an ABI prism 7500 Fast System (Applied Biosystems, Foster City, CA, USA). For each *q*PCR assay a cocktail of 0.75 µl of each forward and reverse primer, 0.375 µl T4gp32, 7.5 µl SYBR Green, 4.125 µl ultra-pure water, and 1.5 µl DNA template (for total bacteria and archaea only 1.0 µl) was mixed. Standard curves were generated in triplicate with serial dilutions of a known quantity of the respective isolated plasmid DNA. Each *q*PCR run included two no-template controls showing no or negligible values. Table S7.1 lists the selected primers, thermal cycling conditions, and PCR efficiencies. Sampling strategy as well as sample storage made it possible to measure the qPCR derived from samples of the sandy Dystric Cambisol only.

Calculations

The total amount of DOC transported at each sampling point was calculated by multiplying the measured DOC concentration with the volume of percolate passing the column over the period represented by the sample (eq. 1).

$$total\ transported\ DOC\ (\ mg\ ) = DOC\ concentration\ (\ mg\ L^{-1}\ )\ \times flux\ (\ L\ h^{-1}\ ) \times period\ (\ h\ ) \quad \text{(eq. 1)}$$

DOC exchange in the 1st depth increment was calculated by subtracting the cumulative DOC in the inflow solution (DOC_{in1}) from the cumulative outflow solution (DOC_{out1}) (eq. 2). Because of the delayed start for the second depth increment, the cumulative DOC of the 4th to the 6th samples of the outflow from the first depth compartment (DOC_{out1}) was subtracted from the sum of cumulative DOC from the second depth compartment (DOC_{out2}) (eq. 3). For the third depth compartment the cumulative DOC of the 4th to the 6th samples of the second depth compartment (DOC_{out2}) was subtracted from the sum of the cumulative DOC of the third depth compartment (DOC_{out3}) (eq. 4).

$$DOC\ exchange\ 1.depth = \sum_{i=1}^{6} DOC_{out1} - \sum_{i=1}^{6} DOC_{in1} \qquad \text{(eq. 2)}$$

$$DOC\ exchange\ 2.depth = \sum_{i=1}^{6} DOC_{out2} - \sum_{i=4}^{6} DOC_{out1} \qquad \text{(eq. 3)}$$

$$DOC\ exchange\ 3.depth = \sum_{i=1}^{6} DOC_{out3} - \sum_{i=4}^{6} DOC_{out2} \qquad \text{(eq. 4)}$$

The specific UV absorbance (SUVA) at 280 nm was calculated as the ratio of UV absorbance of the solutes and DOC concentration (L mg C^{-1} cm^{-1}). Mean values for inflow and outflow solutions were calculated for the six sampling times. For the net SUVA change in the first depth the mean SUVA of the inflow solution ($SUVA_{in1}$) was subtracted from the mean SUVA of the outflow solution from the first depth compartment ($SUVA_{out1}$) (eq. 5). For the SUVA change in the second depth compartment, the mean SUVA of the outflow solution from the first depth compartment ($SUVA_{out1}$) was subtracted from the mean SUVA of the outflow solution from the second depth compartment ($SUVA_{out2}$) (eq. 6). For the SUVA change in the third depth compartment the mean SUVA of the outflow solution from the second depth compartment ($SUVA_{out2}$) was subtracted from the mean SUVA of the outflow solution from the third depth compartment ($SUVA_{out3}$) (eq. 7).

$$SUVA\ change\ 1.depth = SUVA_{out1} - SUVA_{in1} \qquad \text{(eq. 5)}$$

$$SUVA\ change\ 2.depth = SUVA_{out2} - SUVA_{out1} \qquad \text{(eq. 6)}$$

$$SUVA\ change\ 3.depth = SUVA_{out3} - SUVA_{out2} \qquad \text{(eq. 7)}$$

The proportion of C derived from the OM-coated goethite in the outflow solution (goethite-derived OC, GDC_{DOM}) of each column was calculated relative to the $\delta^{13}C$ ratio of the respective inflow solution (eq. 8), where $\delta^{13}C_{out}$ and $\delta^{13}C_{in}$ represent the $\delta^{13}C$ ratio of the outflow and the inflow solutions and $\delta^{13}C_{CG}$ represents the $\delta^{13}C$ ratio of the OM-coated goethite. The $\delta^{13}C$ ratios were averaged over the six sampling times.

$$GDC_{DOM}\ (\%) = \frac{(\delta 13C_{out} - \delta 13C_{in})}{(\delta 13C_{CG} - \delta 13C_{in})} x\ 100 \qquad \text{(eq. 8)}$$

The proportion of C on the OM-coated goethite-derived from the solution after the experiment (solution-derived OC, $SDC_{goethite}$) was calculated relative to the $\delta^{13}C$ ratio of the inflow solution

($\delta^{13}C_{in}$), where $\delta^{13}C_{CGA}$ represents the $\delta^{13}C$ ratio of the goethite after the experiment and $\delta^{13}C_{CG}$ represents the $\delta^{13}C$ ratio of the OM-coated goethite before the experiment (eq. 9). Hence, the remaining proportion of OC on the goethite after the experiment was still derived from the OM-coating applied before the experiment.

$$SDC_{goethite}\ (\%) = \frac{(\delta 13C_{CGA} - \delta 13C_{CG})}{(\delta 13C_{in} - \delta 13C_{CG})}\ x\ 100 \qquad \text{(eq. 9)}$$

The relative change in OC concentration (ΔC) of the OM-coated goethite before (C_{before}) and after the experiment (C_{after}) was calculated by equation 10.

$$\Delta C\ (\%) = \frac{(C_{after} - C_{before})}{C_{before}}\ x\ 100 \qquad \text{(eq. 10)}$$

The previously goethite-bound OC that was mobilized during the experiment (MC) was calculated by the difference in the absolute amount of SDC and the net change in OC content of the mineral before (C_{before}) and after the experiment (C_{after}) relative to the OC content before the experiment.

$$MC\ (\%) = \frac{\left(\frac{SDC(\%) \times C_{after}}{100} - (C_{after} - C_{before})\right)}{C_{before}}\ x\ 100 \qquad \text{(eq. 11)}$$

The magnitude of change in the $\delta^{13}C$ ratios of the soil samples before and after the experiment was too small to calculate the respective GDC in the soil samples. Thus the total amount of OC retained in the soil cores that was mobilized from the OM-coated goethite (Retained MC) was calculated as the difference between the total amount of MC and the total amount of GDC in the outflow solution (eq. 12). The total amount of MC (mg) was the product of C_{before} (mg g^{-1}) and MC (%) times the weight of the goethite between the soil cores (2.8 g), divided by 100. The total amount of GDC (mg) was the product of the total DOC_{output} (mg) and the GDC (%), divided by 100.

$$Retained\ MC\ (mg) = \frac{C_{before} \times MC(\%) \times 2.8}{100} - \frac{total\ DOC_{output} \times GDC(\%)}{100} \qquad \text{(eq. 12)}$$

Statistical analysis

Effects of soil type (soil), depth (depth), position inside the column above the goethite or below the goethite (pos), OM-coating of the goethite (goethite), and interactions of these factors were analysed with linear mixed-effect (lmer) models. Due to the design with three experimental repetitions of the three–step cascade system, the soil columns were set as random factor. Comparison of means was conducted for all factors and interactions. Significance was tested at $p < 0.05$ in all cases. Homogeneity of variance was tested for all parameters by Levene’s test. All statistical analyses were carried out with R statistics version 3.2.1 (R Core Team, 2015) using the “lme4” (Bates et al., 2015) and the “lsmeans” package (Lenth, 2016).

7.3 Results

DOC transport

Mean DOC concentration in the column outflow solution decreased with increasing depth, and the columns with OM-coated goethite had higher DOC concentrations than the columns with pure goethite (Fig. 7.2). Both results were more pronounced for the soil developed from sand than for the silty soil developed from basalt (Table 7.1). Concurrent with the DOC concentration, cumulative DOC transport also decreased with depth, and more DOC was found in the effluent of columns with OM-coated goethite than in the effluent of columns with pure goethite (Fig. 7.2). With respect to cumulative DOC flux, the differences with depth were more pronounced for the sandy soil than for the silty soil (Fig. 7.3). The net OC exchange was calculated to evaluate whether, over the course of the experiment, OC was retained or released in the columns. Samples from the first depth showed a higher cumulative DOC flux in the outflow than in the inflow indicating that DOC was released over the course of the experiment (values above the 1:1 line in Fig. 7.3). The samples from the first depth compartments with silty soil and pure goethite were an exception as OC was retained. In contrast, all columns from the second and third depths retained OC, and under all experimental conditions less OC was retained for the experiments with OM-coated goethite than for those with pure goethite ($F_{1,10} = 11.98$, $p < 0.01$; Table S7.4).

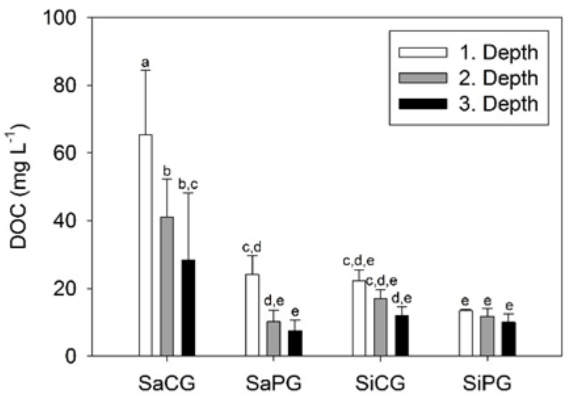

Figure 7.2 Mean DOC concentrations (mg L^{-1}) and standard deviations of the outflow solution per treatment and depth (4, 30, and 100 cm for the columns with sandy soil and 4, 12, and 26 cm for the columns with silty soil). Abbreviations: SaCG = sandy soil and OM-coated goethite, SaPG = sandy soil and pure goethite, SiCG = silty soil and OM-coated goethite, SiPG = silty soil and pure goethite. Different letters above the error bars indicate significant differences with p-values <0.05.

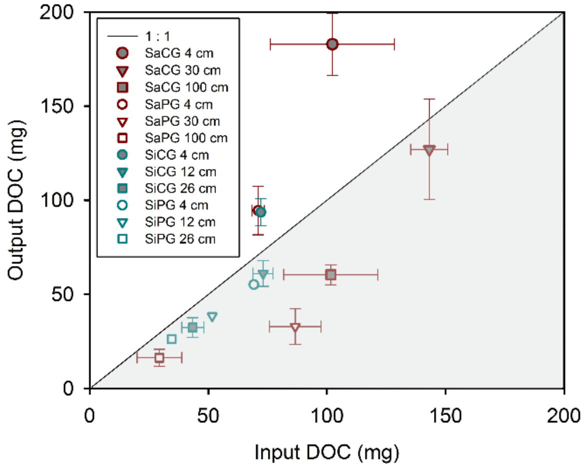

Figure 7.3 Total output DOC (mg) vs. total input DOC (mg) of all experimental treatments. Abbreviations: SaCG = sand and OM-coated goethite, SaPG = sand and pure goethite, SiCG = silt and OM-coated goethite, SiPG = silt and pure goethite. Values above the 1:1 line represent net leaching, whereas values below the 1:1 line represent net retention. Error bars indicate standard deviation. Filled symbols represent columns with OM-coated goethite whereas empty symbols represent columns with pure goethite.

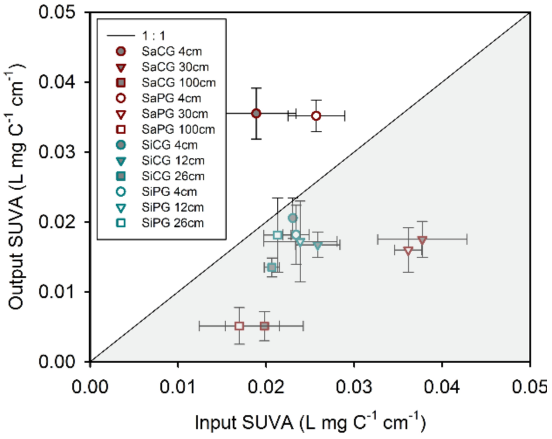

Figure 7.4 Mean values of output specific UV-Vis absorbance (SUVA) at 280 nm (L mg C^{-1} cm^{-1}) vs. input SUVA at 280 nm of all experimental variations. Abbreviations: SaCG = sand and OM-coated goethite, SaPG = sand and pure goethite, SiCG = silt and OM-coated goethite, SiPG = silt and pure goethite. Values above the 1:1 line represent increasing SUVA values as a result of sorption / desorption processes, whereas values below the 1:1 line represent decreasing SUVA values. Error bars indicate standard deviation.

Aromaticity of DOM

The outflow solution of the first depth of the sandy soil had a higher mean SUVA than the inflow solution (Fig. 7.4). But with increasing depth the mean SUVA of the column outflow decreased (depth: $F_{2,133} = 100.06$, $p < 0.01$). The effect of OM-coated or pure goethite on SUVA was less pronounced than on the DOC concentration (Fig. 7.3 and 7.4). The silty soil showed smaller differences in SUVA between the three depths than the sandy soil. A depth trend was only apparent in the columns with OM-coated goethite (significant difference between first and third depths, $p < 0.01$; Fig. 7.4; Table S7.5). The sandy soil had a higher mean SUVA in the outflow of the first depth compartments than the silty soil. The mean SUVA of the outflow of the second depth compartments with sandy soil was in the same range as in case of the silty columns, while for the third depth compartments it was lower for the sandy soil than for the silty soil.

Exchange of OC between goethite, soil and solution

Along with the sorptive exchange of unlabelled DOM from the percolation solution with the labelled goethite-bound OM, the δ^{13}C ratio of the outflow DOM solution significantly increased with soil depth (depth: $F_{2,72} = 76.7$, $p < 0.01$). This increase was less pronounced in the effluent of the silty soil columns than of the sandy soil columns (Fig. 7.5A). In the sandy soil, the proportion of labelled OM desorbed from the goethite to total DOM increased from the first to the second depth and then remained constant (Fig. 7.5B). In the silty soil, the contribution of labelled OM desorbed from the goethite to the DOM output of the columns did not change significantly with depth (Fig. 7.5B).

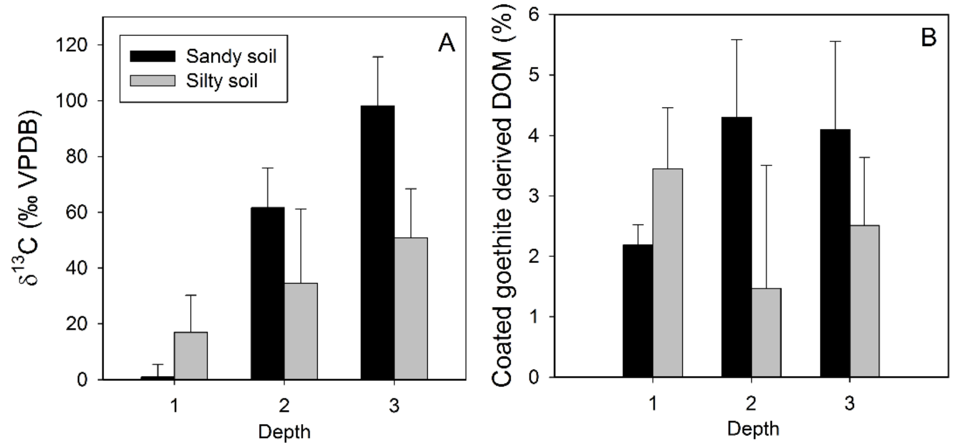

Figure 7.5 (A) $\delta^{13}C$ value of the outflow solution of the three cascade depths of the columns from both soils. (B) Mean proportion of OM derived from the coated goethite in the outflow solution of the three cascade depths of the columns from the sandy and the silty soils. Error bars indicate standard deviation. Different letters above the error bars indicate significant differences ($p < 0.05$).

Percolation of the DOM solution through all first depth compartments increased the OC content of the goethite. In the second and third depths, the OC content was in the range of the OM-coated goethite before the experiment (19.4 mg g^{-1}) or slightly decreased (Table 7.2). As an unlabelled DOM solution ($\delta^{13}C$ of –28.9‰) was used, the $\delta^{13}C$ of the goethite-associated OM decreased during the experiment (Table 7.2). In the first depth compartments of both soils the proportion of OM adsorbed to the goethite after the experiment was evenly distributed between new OM derived from the percolation solution and OM that had already been adsorbed before the experiment (Fig. 7.6). With increasing depth, the proportion of unlabelled OM newly sorbed to the goethite decreased. In the columns derived from silty soil, the goethite from the second and third depth compartments had similar percentages of goethite- and solution-derived OC (Fig. 7.6). A replacement of pre-experimentally bound OC, calculated according to equations 8-11, was evident in all columns, even where the net OC exchange (ΔC) of the goethite was negative. More OC was replaced in the columns of the silty soil than in those of the sandy soil ($F_{1,9} = 35.1$, $p < 0.01$), but the depth patterns were similar (Fig. 7.6).

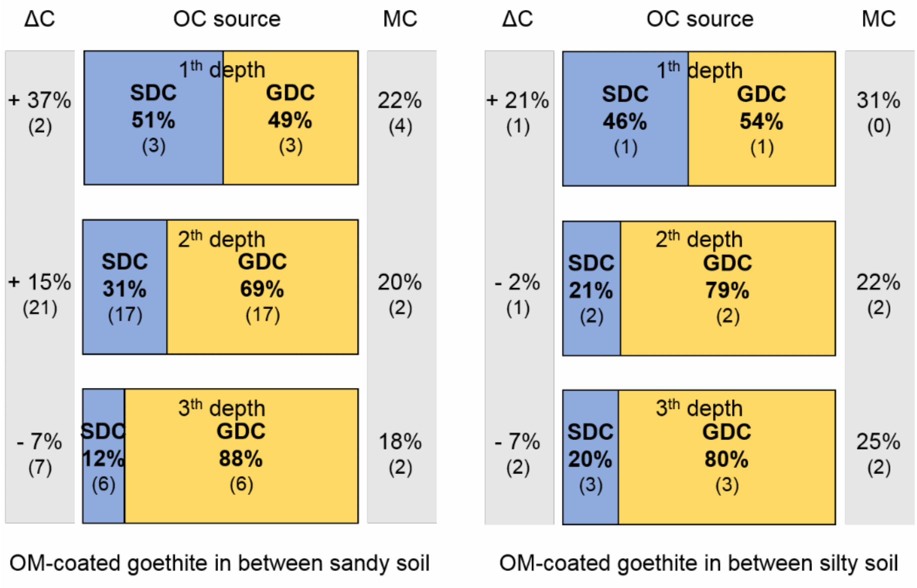
ΔC
OC source
MC
1th depth
SDC 51% (3)
GDC 49% (3)
+ 37% (2)
22% (4)
2th depth
SDC 31% (17)
GDC 69% (17)
+ 15% (21)
20% (2)
3th depth
SDC 12% (6)
GDC 88% (6)
- 7% (7)
18% (2)
OM-coated goethite in between sandy soil
ΔC
OC source
MC
1th depth
SDC 46% (1)
GDC 54% (1)
+ 21% (1)
31% (0)
2th depth
SDC 21% (2)
GDC 79% (2)
- 2% (1)
22% (2)
3th depth
SDC 20% (3)
GDC 80% (3)
- 7% (2)
25% (2)
OM-coated goethite in between silty soil

Figure 7.6 Mean fraction of the newly sorbed solution-derived carbon (SDC; eq. 9) versus the remaining carbon of the initial carbon coating (GDC; eq. 8) on the goethite samples after the column experiment for the sandy soil (4, 30, and 100 cm) and the silty soil (4, 12, and 26 cm), the net carbon exchange (ΔC; eq. 10), and the mobilized carbon (MC; eq. 11) of the respective samples. Standard deviations are given in brackets.

In the first and second depth compartments of the sandy soil, the OC adsorbed to goethite from the percolation solution (SDC) exceeded the overall increase in OC content (ΔC) over the course of the experiment. Hence, for both soil depths, around 20% of the goethite-derived OM was exchanged by OM from the percolation solution (MC), while the rest of the OC was sorbed additionally. In the third depth, both the OC content and the δ^{13}C ratio of the goethite decreased, leading to a calculated proportion of 12% of OM derived from the percolation solution and 18% of the OM adsorbed to the goethite before the experiment was mobilized. In the first depth compartments with silty soil, 31% of the OM adsorbed to the goethite before the experiment was exchanged over the course of the experiment. In the second and third depths, an overall decrease in OC concentration of the goethite as compared to the concentrations before the experiment corresponded to an adsorption of 20% OC from the solution, and about 25% of the previously bound OC was replaced (Fig. 7.6, Table 7.2).

Table 7.3: *Mean mobilized OC from the OM-coated goethite (MC), mean goethite-derived OC (GDC) in the solution and mean Retained$_{MC}$ (eq. 12), and the proportion of retained$_{MC}$ relative to the total amount of mobilized OC from the respective goethite sample (± standard deviation) in the three depths of the columns with sandy and silty soils. Retained$_{MC}$ represents the fraction of OC mobilized from the OM-coated goethite but retained in the soil core below the goethite and thus not transported out of the column.*

Texture	Depth (cm)	MC from OM-coated goethite (mg)	GDC in solution (mg)	Retained$_{MC}$ (mg)	Retained$_{MC}$ (% of MC)
Sand	4	11.94 ± 2.10	4.11 ± 0.54	7.83 ± 2.17	64.88 ± 6.86
Sand	30	10.68 ± 1.23	5.02 ± 1.20	5.66 ± 1.22	53.11 ± 9.63
Sand	100	9.61 ± 1.22	2.79 ± 0.65	6.81 ± 1.76	70.05 ± 9.47
Silt	4	17.12 ± 0.09	3.29 ± 0.78	13.83 ± 0.87	80.74 ± 4.68
Silt	12	12.23 ± 0.75	0.86 ± 0.99	11.37 ± 1.21	92.98 ± 8.09
Silt	26	13.85 ± 0.85	0.77 ± 0.14	13.08 ± 0.96	94.39 ± 1.26

The δ^{13}C ratio of the original soil increased with increasing depth (Table 7.1). After the percolation experiment, in the first and second depth compartments the δ^{13}C ratio of the soil either above or below the goethite showed major changes compared to the δ^{13}C ratio of the original soil. In the third depth the δ^{13}C ratios of the soil above and below the goethite increased by 10.4‰ and 11.7‰, respectively (Table S7.5). Based on the difference between the amount of mobilized OC from the goethite and the measured goethite-derived OC in the DOM solutions, we were able to determine the amount of OC mobilized from the goethite that was thereafter retained in the soil below the goethite layer ($\text{Retained}_{\text{MC}}$). In the first depth compartment of the sandy soil, this amounted to 7.9 mg OC, whereas 5.2 mg OC and 7.1 mg OC were calculated for the second and third depth compartments, respectively (eq. 12). In the columns with silty soil, 13.9 mg of the mobilized OC was retained under the goethite layer of the first depth and 11.3 mg OC and 13.0 mg OC were retained in the second and third depths, respectively (Table 7.3).

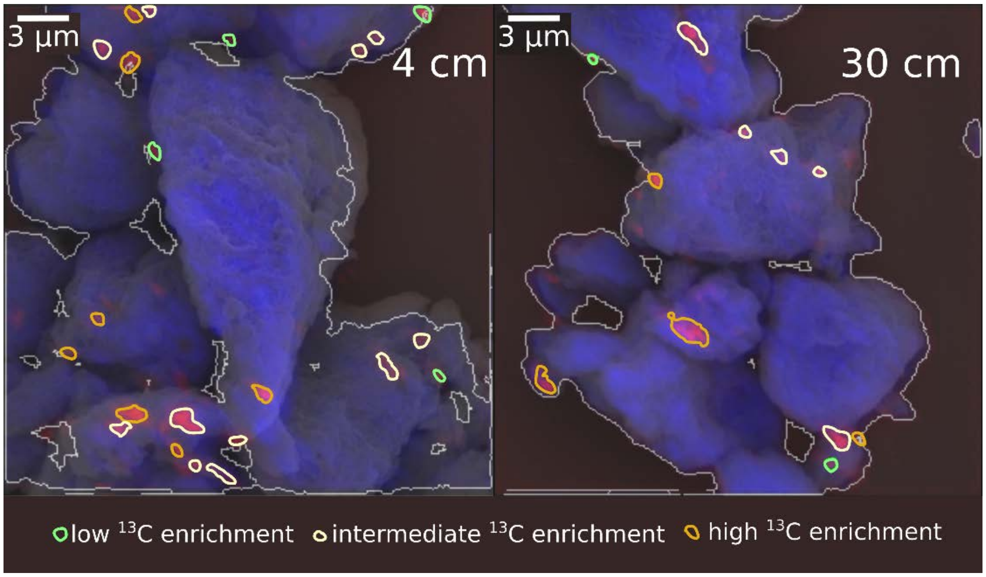

Figure 7.7 SEM image of goethite superposing the NanoSIMS image of $^{12}C^-$ in red and $^{56}Fe^{16}O^-$ in blue. A) Sample from the 4-cm depth compartment of sandy soil; B) Sample from 30-cm depth compartment of sandy soil. Regions of carbon accumulation on the goethite surface identified as regions of interest (ROI) are encircled. The color represents the range of the atom% ^{13}C for the respective ROI: green marks OM with <1.4 atom% ^{13}C (high abundance of newly adsorbed organic matter; low ^{13}C enrichment), white marks OM with 1.4-2.4 atom% ^{13}C (intermediate abundance of newly adsorbed organic matter, intermediate ^{13}C enrichment), and brown marks OM with >2.4 atom% ^{13}C (low abundance of newly adsorbed organic matter, high ^{13}C enrichment). The white line surrounds the mineral surface.

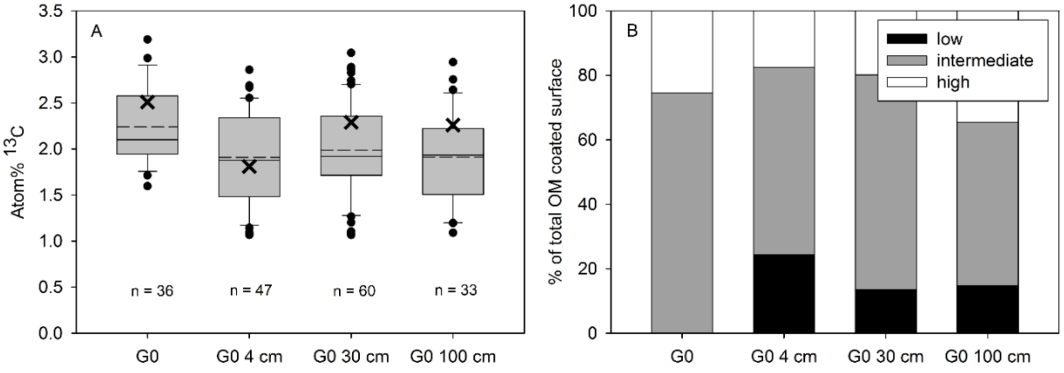

Figure 7.8 Results from NanoSIMS measurements of the OM-coated goethite samples from the columns with sandy soil. A) Atom% ^{13}C of the ROIs of the OM-coated goethite before the experiment (G0) and from the three depth compartments with sandy soil after the experiment, as determined by NanoSIMS. For comparison the respective bulk atom% ^{13}C value as calculated from the IRMS measurements is shown as a black cross. The number of ROIs is given for each boxplot (n). B) Area of high (atom% ^{13}C > 2.4), intermediate (atom% ^{13}C 1.4-2.4) and low (atom% ^{13}C < 1.4) ^{13}C enrichment, relative to the total OM covered surface, as determined by NanoSIMS.

Microbial community composition

The microbial communities in the soil and of the goethite in all depth compartments of the sandy Dystric Cambisol were dominated by bacteria with relative proportions of 69-92% (Fig. 7.9A). Post-experimental absolute abundances of bacteria increased significantly from the first to the second soil depth for both bulk soil and goethite layers, with the highest mean increase in bacterial abundance of 265% in the goethite layer at 30 cm depth compared to the respective layer at the 4 cm depth (depth: $F_{1,18} = 13.29$, $p < 0.01$). Bacterial abundances also tended to differ between sampling points within each depth compartment, with the largest differences between the soil above the goethite layer and the goethite itself (pos: $F_{2,18} = 3.18$, $p < 0.1$). Fungi and archaea showed highest relative proportions in the 4 cm soil columns of up to 13 and 19%, respectively. Archaea exhibited increasing absolute abundances with depth and showed pronounced differences within each depth compartment (Fig. 7.9A). Greatest changes were found between the goethite layers (lowest abundances) and the soil below (highest abundances, depth: $F_{1,15} = 7.40$, $p < 0.05$; pos: $F_{2,15} = 6.16$, $p < 0.05$).

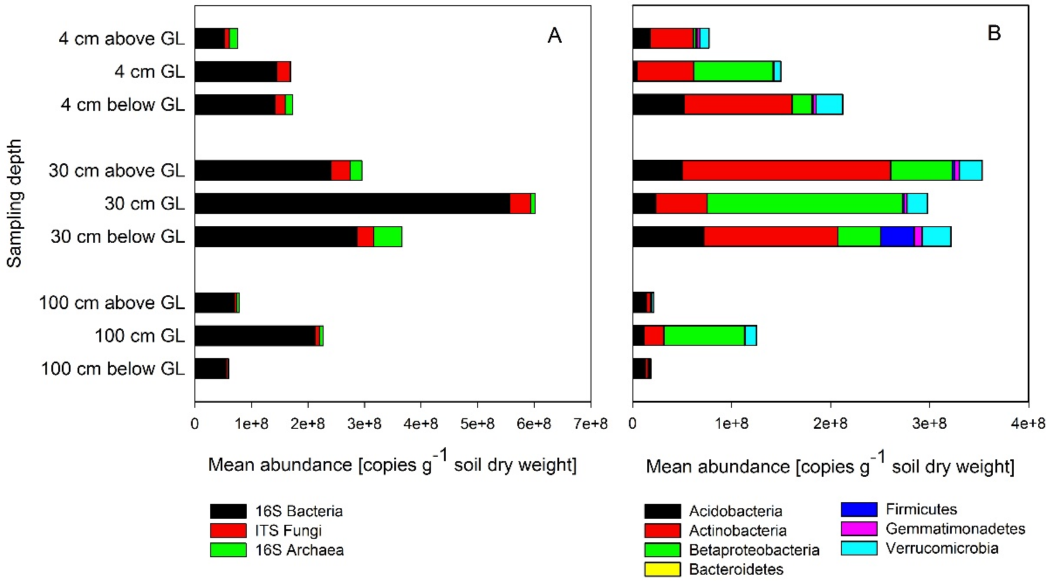

Figure 7.9 Microbial abundances of the sandy soil above and below the goethite layer (GL) as well as in the goethite itself sampled from the 4 cm, 30 cm, and 100 cm depth increments. A) Mean abundances of bacteria, fungi and archaea; B) Mean abundances of the bacterial taxa *Acidobacteria*, *Actinobacteria*, *Betaproteobacteria*, *Bacteroidetes*, *Firmicutes*, *Gemmatimonadetes*, and *Verrucomicrobia*.

Taxa-specific assays of the bacterial communities revealed that all soil depth compartments, both above and below the goethite layers, were dominated by *Actinobacteria* (up to 60%) and *Acidobacteria* (up to 25%). In contrast, goethite layers showed the highest abundances of *Betaproteobacteria*, with relative proportions ranging between 54 and 66% (Fig. 7.9B). Three of the six investigated taxa were significantly affected by soil depth or position within the column (above or below the goethite). While *Actinobacteria, Verrucomicrobia* and *Firmicutes* did not show any significant effects, the abundances of *Acidobacteria*, *Betaproteobacteria* and the generally less abundant *Gemmatimonadetes* increased with depth (Fig 9B; *Acidobacteria*: $F_{1,15} = 7.52$, $p < 0.05$; *Betaproteobacteria*: $F_{1,15} = 6.89$, $p < 0.05$; *Gemmatimonadetes*: $F_{1,15} = 8.22$, p

<0.05). Additionally, *Betaproteobacteria* were more abundant in the goethite layers than in the bulk soil compartments, while *Acidobacteria* and *Gemmatimonadetes* showed the opposite effect (*Betaproteobacteria:* $F_{2,15} = 7.90$, $p < 0.01$*; Acidobacteria*: $F_{2,15} = 10.41$, $p < 0.01$; *Gemmatimonadetes:* $F_{2,15} = 4.49$, $p < 0.05$).

Spatial distribution of OM on goethite surfaces

About 2.7 ± 0.7% of the mineral surfaces of the OM-coated goethite used in the column experiments and analysed by NanoSIMS were covered by OM (Fig. 7.7, Table S7.7). The mean atom% ^{13}C of the ROIs on all samples was 2.2 ± 0.4 with a minimum of 1.6 ± 0.3 and a maximum of 3.2 ± 0.7. The bulk EA-IRMS measurement was in the same range and translates to 2.5 atom% ^{13}C (Fig. 7.8A). As only the goethite from the columns taken in the sandy soil was analysed by NanoSIMS, the following results are restricted to this soil type. After the experiment, 3.5 ± 1.0% of the goethite surface from the first depth compartment was covered by OM, while the mean atom% ^{13}C changed to 1.9 ± 0.5. The bulk EA-IRMS measurement was in the same range (1.8 atom% ^{13}C). The samples from the second depth compartment showed slightly smaller mineral surface coverage by OC (2.7 ± 1.4%) and a slightly higher mean atom%^{13}C (2.0 ± 0.5), which mirrored the bulk EA-IRMS measurement (2.3 atom% ^{13}C). The samples from the third depth showed a mineral surface coverage (3.5 ± 2.1%) and atom% ^{13}C results (1.9 ± 0.5) comparable to the first depth samples, but the bulk EA-IRMS result was higher (2.3 atom% ^{13}C, Fig. 7.8A).

On average, 74.5 ± 33.3% of the ROI area of the OM-coated goethite before the experiment showed intermediately enriched atom% ^{13}C values (1.4-2.4 atom% ^{13}C) whereas the remainder showed high ^{13}C enrichments (>2.4 atom% ^{13}C). The ROI area of the goethite from the first depth compartment comprised the largest proportion of less enriched OM (<1.4 atom%^{13}C) and the smallest proportion with highest ^{13}C enrichment. The ROI area of the goethite from the second and third depth compartments showed comparable proportions of the low enriched category, which decreased compared to the first depth compartment. For all post-experimental goethite samples, slightly above 50% of the ROI fell into the intermediate enriched category, with the maximum area (66.5 ± 14.3% of ROI) observed for goethite from the second depth compartment (Fig. 7.8B).

7.4 Discussion

Net OC exchange at goethite surfaces

DOC concentration and DOM composition changed through interaction of soils and goethite with the percolated solutions. In the first depth compartments of all experiments, except for the columns from the basalt site with pure goethite, there was a net release of DOC, and the SUVA increased in the outflow solution relative to the inflow solution (leaf leachate). This indicated a release of plant derived aromatic compounds from the topsoil (McDowell and Likens, 1988), which was assumed to be the initial step of the cascade-like transport of DOM down the soil profile (Kaiser and Kalbitz, 2012). The inflow solutions of the second depth compartments consequently had the highest DOC concentrations in the experiments along with the highest proportion of aromatic moieties. Retention processes in the second and third depth compartments led to a decrease in DOC concentration in the effluents; declining SUVA values indicated the preferential sorption of aromatic compounds. Field experiments on DOC dynamics (Kaiser et al., 2004; Leinemann et al., 2016) found comparable results with respect to the behaviour of aromatic moieties; we conclude, therefore, that the column experiment was suitable for investigation of natural processes. The transport of DOM in the second and third depths of the column experiment can thus be characterised as the competitive retention of aromatic, mostly plant derived compounds with higher sorption affinity versus potentially labile microbially-derived compounds that remain in solution or become desorbed from mineral surfaces (Guo and Chorover, 2003). The smaller inter-depth differences in DOC concentrations and SUVA observed for the silty soil cascade were most likely due to the smaller depth gradient, resulting in smaller differences in C and N content between the samples of the different depth increments (Table 7.1). The larger quantities of released DOC in the sandy topsoil than in the silty topsoil led to the conjecture that OM is adsorbed more strongly in the more fine-grained substrate with a higher content of dithionite-extractable Fe (Table 7.1). This is in accordance with studies of the relationship between OC storage and content of pedogenic Fe (and Al) oxides (Eusterhues et al., 2005; Herold et al., 2014; Mikutta et al., 2006).

Gross OC exchange between goethite and soil solution

The use of goethite coated with ^{13}C-labelled OC enabled us to distinguish between sink and source processes on goethite surfaces. This made it possible to determine whether or not a competitive exchange of OC between the mineral phase and soil solution occurs due to the input of reactive DOM compounds as proposed in the “cascade model”. Over the whole cascade, the OM-coated goethite acted as a C source as the δ^{13}C in the columns’ output solution increased with every step (Fig. 7.5A). At the same time the OM-coated goethite also sorbed DOM at all three depths, even though its OC content decreased in the third depth compartment of the sandy soil and the second and third depth compartments of the silty soil (Fig. 7.6).

The proportion of mobilized OC from the goethite (MC) was relatively constant with depth but was higher in the OM-rich silty soil than in the OM-depleted sandy soil, at least in the first and third depth compartments (Fig. 7.6). Thus, the mobilization of goethite-associated OM was soil specific. The greater mobilization of OC from the goethite in the third depth of the silty soil can be explained by a higher reactivity of the percolating DOM, as in the second depth the aromaticity of the output solution of the silty soil columns was higher than the aromaticity in the output solution of the sandy soil columns (Fig. 7.4). The SUVA values also help to explain the comparable OC mobilization in the second depth, but not the differences between the sandy and the silty soil in the first depth, where the aromaticity of the solution percolating through the sandy soil columns was higher.

It was not possible to calculate the proportion of solution-derived OC sorbed to the soil samples because changes in $\delta^{13}C$ ratios of the soil (above and below the OM-coated goethite) during the experiment were minor. However, the assessment of changes in ^{13}C of the OM-coated goethite and of the DOM output solution enabled us to precisely calculate the retention of OC mobilized from OM-coated goethite in the subsequent soil depth. Following this approach, the shallow silty soil retained two times more OC than the sandy soil from the OM-coated goethite (Tab. 3) and was thus identified as the more reactive system. This is in accordance with a 10-fold higher dithionite-extractable Fe content (Table 7.1). Thus, the greater sorption capacity of the silty soil provides an explanation for the ambiguous results of higher proportions of mobilized OC from the goethite (Fig. 7.6) and lower proportions of goethite-derived OC in the output solution (Fig. 7.5) in comparison to the sandy soil columns. The lower sorption capacity of the sandy topsoil, in contrast, resulted in a higher proportion of solution-derived OC in the first two depths and as a consequence, more OC could be additionally sorbed to the goethite layer.

The strong decline in solution-derived OC at the goethite surfaces in the third depth of the sandy soil (Fig. 7.6) likely resulted from its interaction with less reactive DOM, as according to the “cascade model”, high-affinity aromatic compounds were already preferentially adsorbed in the second depth compartment (Fig. 7.4). The retention of aromatic compounds in the second depth most likely occurred for the most part in the soil core above the goethite, since, compared to the first depth, no stronger mobilization of OC from the goethite was found. This is in accordance with results of Hagedorn et al. (2015) who found a strong retention of percolated DOM in the uppermost 2 cm of soil cores. Mobilisation of less strongly sorbing OM components in the second depth compartment is likewise reasonable. According to adsorption experiments using in situ DOM extracts from different soil depths, the reactivity of subsoil DOM is lower than that of topsoils (Rennert and Mansfeldt 2003). Hence, the comparable proportion of solution-derived OC associated with goethite in the second and third depths of the silty soil (Fig. 7.6) is in accordance with the minor changes in SUVA of the percolating soil solution in these depth increments (Fig. 7.4).

The release of ^{13}C from the goethite into the percolation solution at every depth step confirms that the interaction of DOM with mineral-associated OM led to a re-mobilisation of previously bound OM, thus providing strong evidence for the partially stepwise transport of DOM through soil profiles (Kaiser and Kalbitz, 2012). Even though the goethite was not OM-coated to its maximum sorption capacity (Kaiser and Guggenberger, 2007) it did not further sorb OC during the experiment but rather directly participated in the cycling of OM. Despite the low OC loading of the goethite, fostering strong interactions between the mineral and OM, and careful washing of the OM-goethite associations to remove non-sorbed and easily bound OM, as much as 18 to 31% of the initially sorbed OC took part in the cascade transport. Based on other sorption experiments and using the initial mass isotherm approach, the DOC-induced desorption of OC from 48 different mineral soil samples, including topsoils and subsoils, averaged 3.2% (Moore et al., 1992). This is in accordance with the fraction of desorbable goethite-associated OM (2.7%) after treatment with DOC-free synthetic soil solution (Kaiser and Zech 2000). However, the column experiment clearly highlights that for quantification of the cycling potential of OM bound to soil minerals, *gross exchange processes* need to be considered. Batch desorption studies without extra information derived from the use of stable isotope labelling are not suitable for determination of the potential DOC source of mineral-associated OM. Absent this additional information, the importance of mineral-associated OM for soil C cycling cannot be quantified reliably. It has recently been suggested that such exchange processes occur between litter-derived DOC and organic layers (Müller et al., 2009). Using the column experiment with ^{13}C-labelled goethite-bound OM, we were able to provide evidence that DOM from different soil compartments―including mineral topsoil and subsoil horizons―is able to replace mineral-associated OM and thus the transport of DOC does occur in a cascade-like manner, in constant exchange with mineral bound OC.

Depth and substrate effects on microbial abundance and community composition

Reactive minerals such as goethite are hotspots of biochemical interactions between mineral surfaces, organics, and microbial degraders with high bioactivity (Heckman et al., 2013). Consequently, the increase in bacterial abundance by up to 265% and the altered bacterial community composition in the goethite layers in comparison to the surrounding bulk soil reflect high C processing on mineral surfaces as postulated in the “cascade model” (Fig. 7.9A and B). DOC transport within the soil profile as well as the pronounced C exchange processes on the goethite surfaces led to large amounts of bio-available OC in the goethite layers (Fig.7.3). The high availability of labile carbon compounds stimulated the growth of predominantly copiotrophic bacteria such as *Betaproteobacteria* in the goethite layers. This result is in accordance with a study of Eilers et al. (2010) characterising *Betaproteobacteria* as an important taxon under conditions of high concentrations of labile carbon. The mean fungal-to-bacteria ratio of 1:14 in the goethite layers in comparison to 1:9 in the bulk soil layers also led to the conclusion that labile carbon mainly stimulated the growth of copiotrophic bacteria in the former (Fig. 7.9B). In addition, *Betaproteobacteria* may have also benefited from higher pH values in the goethite layer (pH 5.1-6.7) in comparison to the bulk soil (pH 3.2-4.6) (Table S7.2; see also Blagodatskaya and Anderson, 1998). Especially in the two deeper soil horizons with lower OC content (Table 7.1), actual microbial C availability may have been increased in the goethite layers where OC loading was higher than in the surrounding environment. The higher C availability was reflected by the negative net decrease of OC content on the goethite in the 100 cm depth compartments and increasing ^{13}C content of the solution with every depth step (Fig. 7.6). This suggests that - despite of the high sorption capacity of goethite - sufficiently large amounts of labile C were available for microbial turnover processes and may indicate an active function of microorganisms in remobilization processes of mineral-bound OM. However, future studies using stable isotope probing need to clarify the re-mobilization potential of microorganisms in bioactive mineral-microbe systems. Nevertheless, the increased microbial access to OC in the goethite layers explains the increase in copiotrophic (r-strategists, fast growth rates) *Betaproteobacteria* and decrease in oligotrophic (K-strategists, low growth rates) *Acidobacteria*, which decreased in relative proportions in the microbial communities under increased OC availability (Fierer et al., 2007). Consequently, *Betaproteobacteria* may be initial colonizers of reactive minerals such as goethite and the relative increase in this taxon could indicate a shift from *K*- to *r*-strategist-dominated microbial communities from bulk soil to goethite layers. The dominance of *Acidobacteria* and *Actinobacteria* in the soil compartments was also found *in situ* at the field site of the Dystric Cambisol (Preusser et al., 2017). The microbiological results of this study highlight the contribution of microbial degraders to the cascade processes of DOC transport within the soil profile as well as the magnitude of C exchange processes on surfaces of reactive minerals such as goethite.

Small-scale variability of OC on mineral surfaces

To track the exchange of OC sorption at the small scale, goethite samples were analysed by NanoSIMS. The data suggested that OM occurred in randomly distributed patches over the goethite surfaces (Fig. 7.7) with a low maximum coverage of 3.5% of the goethite surfaces as detected by NanoSIMS (Table S7.6). Using comparable NanoSIMS measurements, Vogel et al. (2014) observed a fivefold higher OM coverage (19%) mainly on micro-aggregates composed of clay-sized soil minerals at an OC loading of 1.1 mg m^{-2}, which is roughly five times the OC loading of the OM-coated goethite used in our experiment (Tab. 2). However, Xiao et al. (2016) analysed extracted Fe-bearing soil colloids with C content of 15 to 25 mg C g^{-1} by NanoSIMS and found C surface coverages of 7 to 10%. The rather small surface coverages found on our samples are thus in a range comparable to other NanoSIMS studies.

In our NanoSIMS study it was possible to additionally distinguish between OC sorbed before and during the experiment based on changes in atom% ^{13}C values in selected ROIs. The approximately 25% of OC on the mineral surface residing in the highly enriched category can be considered as sorbed before the experiment and to have remained unchanged during the experiment. Evidence for this is that the proportion of OC on the goethite samples in the highly enriched category after the experiment declined only relatively in the first and second depth samples as their total carbon content increased over the course of the experiment. In the third depth sample the proportion increased relatively because of the decreasing total OC content (Table 7.2, Fig.7.8). Between 15 and 25% of the OM on the surface of the goethite after the experiment was freshly sorbed. In the first and second depths this was less than the proportion of solution-derived OC on the goethite determined by EA-IRMS measurements (Fig. 7.6), suggesting that the intermediate enriched category was involved in the interactions with the DOM to a great extent. These results provide further evidence for a mobilisation of previously bound OM. It also corroborates the findings of Vogel et al. (2014) who were able to show a rapid accrual of fresh C and N on micro-aggregate surfaces with a specific sorption to inherited OM. Our study highlights the importance of microscale OM patches for the cycling of OC at microscale mineral interfaces as indicated by the dilution of the ^{13}C signals. This interaction of previously sorbed OC and DOC as indicated by declining ^{13}C enrichment at certain spots on the goethite surface supports the “cascade model” (Kaiser and Kalbitz 2012) and thus the exchange of inherited OM by percolating DOC.

7.5 Conclusion

Undisturbed soil column experiments with ^{13}C-labelled goethite-associated OM were conducted to verify the “cascade model” of DOM transport through soil profiles and to quantify the *net* and *gross* exchange processes on mineral surfaces as well as associated shifts in microbial communities. We found that, during the transport of DOM through soil columns, aromatic DOM moieties were preferentially retained, similar to natural conditions. Variable *gross* OC exchange rates of up to 31% showed that fresh OM inputs can replace a significant fraction of mineral-associated OM. Exchange processes at mineral surfaces due to simultaneous adsorption and desorption of OM thus play a crucial role in DOM transport, as well as in the fate and properties of mineral-associated OM. Comparably high microbial abundances in goethite layers highlight the role of secondary minerals as hotspots for OM transformation and decomposition. The high concentrations of copiotrophic bacteria such as *Betaproteobacteria* in the goethite layers provided evidence that large quantities of labile carbon are processed on the surfaces of reactive minerals. Nevertheless the roles of different microbial taxa and phyla in re-mobilization need further study, for example by using different stable isotope probing techniques. In conclusion, sorbed OM can be mobilized and replaced by DOC over an entire soil profile even at depth, thus confirming the validity of the “cascade model”.

7.6 Acknowledgements

Funding of the research was provided by the Deutsche Forschungsgemeinschaft DFG within the research unit FOR 1806 ‘‘The Forgotten Part of Carbon Cycling: Organic Matter Storage and Turnover in Subsoils (SUBSOM)’’. The funding for NanoSIMS analyses was provided by MU 3021/4-1. We would like to thank Dr. Stefanie Heinze and Prof. Dr. Bernd Marschner for project coordination and Petra Kuner and numerous student helpers for support in the laboratory.

7.7 Supplementary materials

Table S7.1: *qPCR primers and conditions.*

Gene	Primer*	Thermal profile**	No. of Cycles	Efficiency mean (%)	Reference
16S rRNA genes	341F 515R	95°C – 10 m, 95°C – 15 s, 60°C – 30 s, 72°C – 30 s, 75°C – 30 s	1 35	99%	(Lopez-Gutierrez et al., 2004)
Fungal ITS fragment	ITS3F ITS4R	95°C – 10 m95°C – 15 s, 55°C – 30 s, 72°C – 30 s, 76°C – 30 s	1 35	93%	(White et al., 1990; Manerkar et al.,2008)
16S Archaea	Ar912R Ar109F	95°C – 10 m, 95°C – 30 s, 52°C – 60 s, 72°C – 60 s, 75°C – 30 s	1 40	92%	(Lueders and Friedrich, 2000)
Acidobacteria	Acid31 Eub518	95°C – 10 m, 95°C – 15 s, 55°C – 30 s, 72°C – 30 s, 81°C – 30 s	1 35	92%	(Fierer et al., 2005)
Actinobacteria	Act920F3 Act1200R	95°C – 10 m, 95°C – 15 s, 61.5°C – 30 s, 72°C – 30 s, 78°C – 30 s	1 35	92%	(Bacchetti De Gregoris et al., 2011)
β-Proteobacteria	Eub338 Bet680	95°C – 10 m, 95°C – 15 s, 55°C – 30 s, 72°C – 30 s, 80°C – 30 s	1 35	92%	(Fierer et al., 2005)
Firmicutes	Lgc353 Eub518	95°C – 10 m, 95°C – 15 s, 60°C – 30 s, 72°C – 30 s, 79°C – 30 s	1 35	97%	(Fierer et al., 2005)
Verrucomicrobia	Verr 349 Eub 518	95°C – 10 m 95°C – 15 s, 60°C – 30 s, 72°C – 30 s, 77°C – 30 s	1 35	90%	(Philippot et al., 2009)
Gemmatimonadetes	Gem440 Eub518	95°C – 10 m, 95°C – 15 s, 58°C – 30 s, 72°C – 30 s, 78°C – 30 s	1 35	95%	(Philippot et al., 2009)
Bacteroidetes	Cfb798F Cfb967R	95°C – 10 m, 95°C – 15 s, 61.5°C – 30 s, 72°C – 30 s, 75°C – 30 s	1 35	96%	(Bacchetti De Gregoris et al., 2011)

*Primer concentration was 10 pmol μl^{-1}

**Additionally, a 60°C to 95°C step was added to each run to obtain the denaturation curve specific for each amplified sequence.

Table S7.2: *Selected soil and goethite parameters of the samples from the experimental run with pure goethite used for the qPCR analyses.*

Depth column	Sample type	pH ($CaCl_2$)	C (mg g^{-1})	N (mg g^{-1})	C/N	Sand (%)	Silt (%)	Clay (%)
4	Soil	3.2	58.22	2.42	24	54	41	5
4	Goethite	5.1	15.54	1.13	14	-	-	-
30	Soil	4.1	8.72	0.37	23	56	39	5
30	Goethite	6.3	4.96	0.66	8	-	-	-
100	Soil	4.6	1.00	0.19	5	76	23	1
100	Goethite	6.7	1.94	0.57	3	-	-	-

Table S7.3: *Mean DOC concentrations (mg L^{-1}) of the outflow solutions of all experimental variations at the three respective depths (cm).*

Depth (cm)	4	30	100
Sandy soil OM-coated goethite	65.35 ± 19.17	41.17 ± 11.11	28.41 ± 19.73
Sandy soil pure goethite	24.07 ± 5.64	10.22 ± 3.42	7.53 ± 3.17
Depth (cm)	4	12	26
Silty soil OM-coated goethite	22.21 ± 3.28	16.95 ± 2.60	12.01 ± 2.52
Silty soil pure goethite	13.42 ± 0.36	11.73 ± 2.32	10.00 ± 2.39

Table S7.4: *Cumulative mean DOC inflow (mg), and outflow (mg) as well as the gross balance of both (± standard deviation). Negative values represent adsorption processes from the solution, whereas positive values represent desorption processes into the solution. The balance in percent is calculated relative to the inflow solution.*

Sandy soil and OM-coated goethite*			
Depth (cm)	4	30	100
DOC in	102.34 ± 26.13	143.77 ± 7.85	101.64 ± 19.84
DOC out	182.79 ± 16.53	127.04 ± 26.62	60.44 ± 5.26
Balance	80.45 ± 12.40	-16.73 ± 18.86	-41.19 ± 20.08
Balance (%)	85.04 ± 38.18	-11.24 ± 12.51	-38.99 ± 12.44
Sandy soil and pure goethite*			
Depth (cm)	4	30	100
DOC in	71.04 ± 2.63	86.62 ± 10.87	29.40 ± 9.40
DOC out	94.51 ± 12.88	32.92 ± 9.40	16.37 ± 4.57
Balance	23.47 ± 10.25	-53.71 ± 20.28	-13.03 ± 13.97
Balance (%)	32.80 ± 13.21	-61.01 ± 15.75	-38.70 ± 35.15
Silty soil and OM-coated goethite*			
Depth (cm)	4	12	26
DOC in	72.17 ± 0.00	73.10 ± 4.21	43.43 ± 4.64
DOC out	93.62 ± 7.16	61.17 ± 6.89	32.49 ± 5.19
Balance	21.45 ± 7.16	-11.92 ± 5.30	-10.95 ± 3.40
Balance (%)	29.73 ± 9.92	-16.36 ± 7.51	-25.31 ± 7.49
Silty soil and pure goethite*			
Depth (cm)	4	12	26
DOC in	69.18	51.64	34.60
DOC out	55.24	38.61	26.35
Balance	-13.94	-13.03	-8.25
Balance (%)	-20.15	-25.23	-23.86

* Differences in output concentration and the consecutive input concentration of the next depth compartment are caused by the delayed start of the next column leaching as some solution was used for sampling.

Table S7.5: *Mean values of total specific UV absorbance (SUVA) at 280 nm (L mg C^{-1} cm^{-1}) of DOM in the inflow and in the outflow as well as the balance of both (± standard deviation). Negative values represent decreasing SUVA in the outflow whereas positive values represent increasing SUVA in the outflow. The balance in percent is calculated relative to the inflow solution.*

Sandy soil and OM-coated goethite*			
depth (cm)	4	30	100
SUVA in	0.019 ± 0.005	0.038 ± 0.005	0.020 ± 0.004
SUVA out	0.035 ± 0.004	0.018 ± 0.003	0.005 ± 0.002
Balance	0.017 ± 0.006	-0.020 ± 0.005	-0.015 ± 0.004
Balance (%)	97.63 ± 53.94	-53.3 ± 8.14	-73.53 ± 11.05

Sandy soil and pure goethite*			
depth (cm)	4	30	100
SUVA in	0.026 ± 0.003	0.036 ± 0.002	0.017 ± 0.005
SUVA out	0.035 ± 0.002	0.016 ± 0.003	0.005 ± 0.003
Balance	0.009 ± 0.001	-0.020 ± 0.005	-0.012 ± 0.007
Balance (%)	37.40 ± 8.46	-55.56 ± 10.72	-66.56 ± 24.43

Silty soil and OM-coated goethite*			
depth (cm)	4	12	26
SUVA in	0.023 ± 0.000	0.026 ± 0.003	0.021 ±0.001
SUVA out	0.021 ± 0.003	0.017 ± 0.002	0.014 ± 0.001
Balance	-0.002 ± 0.003	-0.009 ± 0.004	-0.007 ± 0.002
Balance (%)	-10.85 ± 12.67	-34.47 ± 13.29	-34.45 ± 9.07

Silty soil and pure goethite*			
depth (cm)	4	12	26
SUVA in	0.023 ± 0.001	0.024 ± 0.004	0.021 ± 0.002
SUVA out	0.018 ± 0.004	0.017 ± 0.006	0.018 ± 0.005
Balance	-0.005 ± 0.006	-0.005 ± 0.004	-0.002 ± 0.003
Balance (%)	-19.65 ± 25.77	-25.22 ± 20.32	-9.03 ± 15.66

* Differences in the output SUVA and the consecutive input SUVA of the next depth compartment are caused by the delayed start of the next column leaching as some solution was used for sampling.

Table S7.6: *Mean OC concentration and δ^{13}C ratio of the soil samples before and after the experiment and the respective change of both, per depth increment and used soil, on basis of bulk EA-IRMS measurements.*

Texture	Depth	Position*	OC after the experiment (mg g^{-1})	OC before the experiment (mg g^{-1})	C change (mg g^{-1})	$\delta^{13}C_{AE}$ (‰)	$\delta^{13}C_{BE}$ (‰)	$\delta^{13}C_{change}$ (‰)
sand	4	above	83.21 ± 30.05	56.31	26.90 ± 30.04	-28.53 ± 0.13	-28.32	-0.21 ± 0.13
sand	4	below	109.38 ± 8.01	56.31	53.07 ± 8.01	-28.34 ± 0.33	-28.32	-0.25 ± 0.33
sand	30	above	10.36 ± 1.63	5.99	4.37 ± 1.63	-27.12 ± 0.17	-26.62	-0.50 ± 0.17
sand	30	below	10.60 ± 1.62	5.99	4.60 ± 1.62	-26.28 ± 0.04	-26.62	0.34 ± 0.04
sand	100	above	1.17 ± 0.04	0.20	0.97 ± 0.04	-16.06 ± 4.83	-26.41	10.35 ± 4.83
sand	100	below	0.95 ± 0.35	0.20	0.75 ± 0.34	-14.71 ± 1.00	-26.41	11.70 ± 1.00
silt	4	above	47.29 ± 5.36	48.79	-1.50 ± 5.36	-26.31 ± 0.36	-26.54	-0.23 ± 0.36
silt	4	below	47.94 ± 8.27	48.79	-0.85 ± 8.27	-26.97 ± 0.59	-26.54	-0.43 ± 0.59
silt	12	above	45.16 ± 5.93	44.80	0.36 ± 5.93	-26.33 ± 0.26	-26.28	-0.05 ± 0.26
silt	12	below	44.45 ± 6.82	44.80	-0.35 ± 6.82	-26.29 ± 0.42	-26.28	-0.01 ± 0.42
silt	26	above	32.47 ± 4.59	30.25	2.22 ± 4.59	-25.52 ± 0.14	-25.96	0.44 ± 0.14
silt	26	below	33.59 ± 3.97	30.25	3.34 ± 3.97	-25.89 ± 1.34	-25.96	0.07 ± 1.34

* Above and below the goethite layer.

Table S7.7: *Surface coverage and isotopic data based on NanoSIMS images of OM-coated goethite before (G0) and after the experiment (G0 4 cm, G0 30 cm, G0 100 cm). We report mean atom% ^{13}C values of regions of interest (ROIs) that represented regions with OM coating and the respective bulk IRMS measurements for the whole sample. The ROIs with an atom% ^{13}C of <1.40 were considered to be related to newly sorbed OC (low ^{13}C enrichment), the ROIs with an atom% ^{13}C of >1.40 and <2.40 were considered to consist of a mixture of old and new sorbed OC (intermediate ^{13}C enrichment), and ROIs with an atom% ^{13}C of >2.40 were assumed to consist of mainly old OC (high ^{13}C enrichment). The table shows the relative proportion of the surface covered by OC of each category and the number of ROIs (n) in each category.*

Sample	Surface covered by OM (% ± SD)	Mean atom% ^{13}C of ROI (± SD)	Bulk IRMS (atom% ^{13}C)	low ^{13}C (% of total OC ± SD)	n	intermediate ^{13}C (% of total OC ± SD)	n	high ^{13}C (% of total OC ± SD)	n
G0	2.68 ± 0.71	2.24 ± 0.41	2.51	0.00 ± 0.00	0	74.55 ± 33.26	18	25.45 ± 33.26	8
G0 4 cm	3.45 ± 0.99	1.91 ± 0.50	1.81	24.54 ± 19.36	11	57.96 ± 22.33	25	17.51 ± 12.26	11
G0 30 cm	2.72 ± 1.43	1.99 ± 0.49	2.29	13.65 ± 10.95	7	66.50 ± 14.32	42	19.85 ± 19.05	11
G0 100 cm	3.52 ± 2.09	1.91 ± 0.50	2.26	14.87 ± 29.74	6	50.56 ± 19.58	21	34.57 ± 29.49	6

8 General Discussion

Microbial decomposer communities and their regulatory function in C-cycling are decisively influenced by depth-specific habitat conditions within soil profiles. The objectives of this thesis were to evaluate the effects of specific factors (substrate, micro-environment) and their interplay on microbial characteristics, and to identify potential implications for the microbial regulatory function in C turnover and storage in subsoil. In order to achieve these objectives, two reciprocal soil translocation experiments under *in situ* conditions (chapters 5 and 6) and one laboratory flow cascade experiment (chapter 7) have been conducted.

Effects of substrate and environment on microbial biomass and function in subsoil

Availability of C has been described as the key determinant for microbial abundance within soil profiles (Fierer et al., 2003; Ekblad and Nordgren, 2002). In line with this, we expected microbial biomass response according to the altered C availability in the translocation and cellulose addition treatments of the first reciprocal soil translocation experiment (chapter 5) with upper (10-20 cm soil depth; Bsw-Bw horizon) and lower (110-120 cm; C horizon) subsoil. However, neither the translocation and the ensuing changes in substrate availability in different soil depths nor the addition of cellulose influenced the microbial biomass (Fig. 5.3 a and c), although cellulose-derived C accumulated up to 15% in the microbial biomass (Fig. 5.3 b and d). We could explain this inhibition of microbial growth with a subsequent N limitation following the alleviation (via cellulose addition) of the primary C limitation as previously observed in other studies (e.g. Kamble et al., 2013) (Table S5.4). Moreover, we concluded that the detected low water content - as a result of scarce precipitation and high water uptake by trees - in interplay with the highly sandy texture of the two subsoil layers may have caused an enhanced spatial (micro-scale) fragmentation of the subsoil environment and thus a spatial separation between microorganisms and their substrates (see Chapter 5.4.3). Under low soil moisture conditions, substrate-induced limitation of microbial activity is more likely in the investigated subsoil than in the topsoil due to the coarser soil structure of mineral soil and the related lower pore connectivity and stronger decline in solute diffusion as water content decreases (Manzoni et al., 2012). As enzyme production is an energy and nutrient demanding process (Schimel and Weintraub, 2003; De Nobili et al., 2001), the detected low enzymatic activity with no or only minor response to cellulose addition (Table S5.2 and S5.3) mirrored the impact of soil moisture and nutrient limitations on microbial growth and activity in subsoil, where a largely dormant microbial community might have been largely incapable to efficiently exploit newly emerging resources. Accordingly, several studies investigating SOM decomposition found a strong dependence of enzyme production and activity on soil moisture and nutrient availability (e.g. Baldrian et al., 2010; Allison and Vitousek, 2005). This inefficiency in microbial substrate utilization due to spatial separation between microorganisms and substrates may therefore be of high relevance for C accumulation in subsoil.

In contrast to the first translocation experiment, increases in absolute microbial abundance due to enhanced substrate availability were not masked by nutrient-induced growth limitations in the second reciprocal soil translocation experiment (chapter 6) with topsoil (5-10 cm soil depth; Bsw horizon) and subsoil (105-110 cm; C horizon). Therefore, this experiment demonstrated the beneficial effect of higher substrate availability on soil microorganisms, both in shallower soil depth (microbial biomass increase of up to 605%), via root addition (up to 91%) and through the interplay of both (up to 847%; see also Table 6.1). In this context, the enormous increase in microbial biomass due to translocation of subsoil to shallower soil depth and the concurrently decreasing relative importance of root litter as microbial C source emphasized the higher diversity of microbial C sources in topsoil (Fig. 6.3 a and c). Moreover, we concluded from the constant absolute microbial root-C utilization capacities in translocated topsoil as well as subsoil samples that the functional groups of root decomposers remained at a similar abundance level within the entire soil profile and that the increase in microbial biomass in the topsoil environment was largely due to growth of microorganisms using newly available C from e.g. fresh leaf litter-derived DOC inputs or root exudation (Fig. 6.3 b and d). Decrease in microbial biomass with soil depth is therefore a consequence of both decrease in quantitative C availability and in potential C sources.

Comparing the results of the two translocation experiments allowed us to clarify the impact of environmental conditions on soil microorganisms and their substrate utilization capacities within soil profiles. Although root litter was of higher importance as microbial C source in non-translocated subsoil than in non-translocated topsoil samples (Fig. 6.3 a and c), absolute microbial root-C utilization capacities were generally lower in the comparatively dry subsoil than in the more moist topsoil of the second translocation experiment (Fig. 6.3 b and d; Fig. S6.3). Between the two subsoil layers with comparable soil texture and similarly low water content (generally < 30% water holding capacity; WHC) of the first translocation experiment, however, no decreases in absolute microbial cellulose-C utilization capacities with increasing soil depth were detected (Fig. S5.1). This confirmed our finding of the first translocation experiment that soil moisture was crucial for maintaining microbial activity and thus greatly affected microbial substrate utilization capacities within the soil profiles as also described in a study by Gill and Burke (2002). However, other previous studies investigating root decomposition dynamics in topsoil and subsoil detected no differences within soil profiles under non-limiting water conditions (Sanaullah et al., 2011, Solly et al., 2015). Consequently, the comparison with these previous studies emphasized the discrepancy between potential and actual microbial substrate utilization and the enormous influence of soil moisture on these processes. Our results implied that especially in very sandy soils like the Dystric Cambisol at the experimental site of the two field experiments (Table 5.1), moisture content of the soil respectively of the different soil horizons is the most critical environmental factor controlling microbial C turnover with soil depth.

While non-translocated soil samples allowed us to compare microbial C processing under different moisture regimes with soil depth, the translocation of soil samples enabled us to study the specific influence of different temperature regimes within soil profiles. However, the temperature differences within the soil profile were rather small, which is explained both by the coarse and thus well aerated soil structure and further by the mitigating effect of tree stands on local temperature patterns (lower diurnal temperature amplitude in forest compared to e.g. pasture) (Fig. 6.1 a). We concluded that the detected minor temperature differences had no or only minor influence on microbial abundance, since soil temperatures were well within the physiological limits of soil microbial communities of temperate climate zones (Fierer et al., 2003). It also emerged that the microbial C utilization capacities were not negatively affected by the slightly differing temperature regimes with soil depth, as seen in both translocation experiments (Fig. 6.3 b; Fig. S5.1). Contrary, other studies described soil temperature to be of high relevance for microbial abundance and functioning (Waldrop and Firestone, 2006; Treseder et al., 2016); and this applies in particular for microbial degradation processes (Frey et al., 2013). Therefore, it could not be excluded that during the two field experiments temperature effects have been masked by the enormous impact of the generally low soil moisture and will be present under (occasionally occurring) more favourable soil moisture conditions within the soil profile.

Specific responses of bacterial and fungal abundance and function to substrate and environment in subsoil

One of the most striking results of the second translocation experiment was the steeply increasing fungal abundance under enhanced availability of root-C in subsoil demonstrating substrate limitation as key factor for low fungal abundance in deeper soil layers (Fig. 6.4 c and f). In line with the results of the first translocations experiment, highest relative substrate-derived C incorporation rates were determined in fungal PLFA with incorporation rates of up to 100% in subsoil samples within their home field soil depth (Fig. 5.5; Fig. 6.5 a – f). The generally high substrate-C incorporation rates (%) into fungi in both translocation experiments demonstrated the role of (saprotrophic) fungi as the primary degraders of structural components of recent plant-derived substrates due to their pronounced ability to decompose complex OM compounds (e.g. cellulose and lignin) as also recently described by Baldrian (2017) and Hicks Pries et al. (2018). However, the decreasing relative importance of root litter as fungal C source (Fig. 6.5 c and f) concurrently with steeply increasing fungal abundance (Fig. 6.4 c and f) from subsoil to topsoil in the second translocation experiment suggested that pronounced alterations in fungal communities occurred, and that these alterations were driven by the availability of more diverse C resources with shallower soil depth as shown in a study by Moll et al. (2015).

Another important finding could be obtained through the differences in bacterial and fungal root-C utilization capacities revealing a fungal competitive advantage in decomposition processes under the prevailing environmental conditions in subsoil during the second field experiment. The added roots had a higher relative importance as C source for both bacteria and fungi in subsoil than in topsoil samples as C inputs from other sources decreased with soil depth (Fig. 6.5). However, while the absolute bacterial root-C incorporation showed a similar pattern as for the total microbial community, with less incorporation in subsoil than in topsoil, fungi were able to incorporate higher amounts of root-derived C in subsoil (Fig. 6.5 g – l). We explained this by the lower moisture sensitivity of fungi and by the fungal ability to bridge air-filled pores via hyphal growth enabling fungi to exploit resources more efficiently and to maintain their metabolic activity under unfavourable conditions for longer time periods than bacteria (Manzoni et al., 2012; Drenovsky et al., 2004). Conversely, this implied that the bacterial decomposition activity was more negatively affected by low water content in the subsoil environment. Beside a generally weaker bacterial affinity to use recent plant-derived C (Kramer and Gleixner, 2006), this decrease in root decomposition activity with soil depth was largely caused by the drought-induced spatial fragmentation of the subsoil environment restricting bacteria to remaining water-filled pore spaces disconnected from the surrounding soil volume and thus largely impeding bacterial utilization of the potentially available substrate. Consequently, we found bacterial responses to hot spots of substrate availability to be considerably lower than fungal responses, showing no or only marginal, and by soil depth negatively affected increases in abundance in both translocation experiments (Fig. 5.4; Fig. 6.4). The largely restriction of bacterial growth and activity in deeper soil was in particular shown in the bacterial community composition of the first translocation experiment showing generally no response to cellulose addition, supporting our assumption of a largely dormant bacterial decomposer community in subsoil (Fig. 5.7). Among the investigated bacterial phyla, in particular *Betaproteobacteria* and *Acidobacteria* have been identified as potentially important cellulose degraders in previous studies (e.g. Stursová et al., 2012).

In contrast to this extensive inhibition of bacterial growth and activity in subsoil, the increase in microbial abundance in the topsoil layer of the second translocation experiment indicated an enhanced microbial activity in this near-surface environment (Fig. 6.4). However, the increase in abundance was accompanied by substantial decreases in relative microbial root-C incorporation and thus a greater microbial utilization of other C sources (Fig. 6.5 a – f). Among these different potential C sources, in particular DOM is of major importance. The laboratory flow cascade experiment (chapter 7) allowed us to investigate the development of the quality and quantity of DOM with passage through the soil profile, with particular consideration of exchange processes on goethite as reactive soil mineral. As mineral surfaces are hot spots of biochemical interactions with high OC processing (Heckman et al., 2013), this experiment further provided important information about microbial characteristics in this soil micro-environment.

An outstanding result of this experiment under non-limiting water conditions (see chapter 7.2.3) was the greater dominance of bacteria in the microbial communities of goethite layers (fungi-to-bacteria ratio: 1:14) compared to bulk soil layers (1:9) at the end of the 32-day experimental period (Fig. 7.9 a). This community shift revealed the beneficial effect of high labile C availability due to extensive C exchange processes on mineral surfaces on bacterial growth with, in particular, rapid increases of copiotrophic bacteria (r-strategists, fast growth rates) such as *Betaproteobacteria* (Fig. 7.6; Fig. 7.9 b). This finding is in accordance with other studies investigating the relationship between soil properties and bacterial community composition describing *Betaproteobacteria* as important taxon under conditions of high labile C availability (Eilers et al., 2010; Fierer et al., 2007). The column experiment further allowed comparing the bacterial community composition of soil minerals as micro-habitats within soil profiles with the overall bacterial community composition of larger bulk soil volumes. This comparison revealed that the dominance of *Betaproteobacteria* in the bacterial communities on mineral surfaces was in clear contrast to the community composition of the bulk soil compartments with high relative proportions of oligotrophic bacteria (K-strategists, low growth rates) such as *Acidobacteria* and *Actinobacteria* (Fig. 7.9 b). A predominantly oligotrophic bacterial community dominated by *Acidobacteria* and *Actinobacteria* was also detected under *in* *situ* conditions in the first translocation experiment (Fig. 5.7). Both bacterial phyla have been characterized to be adapted to resource- and moisture-limited conditions in previous studies (e.g. Barnard et al., 2013; Naether et al., 2012; Castro et al., 2010), Therefore, we concluded that their high abundance reflected the low C availability in the bulk soil layers compared to the goethite layers of the column experiment as well as in the subsoil environment of the first translocation experiment (Fig. 7.2; Fig.5.2 a and c). As postulated in the “cascade model” (Kaiser and Kalbitz, 2012), the flow cascade experiment further demonstrated that the quality and quantity of DOM substantially changed with passage through the soil profile (Fig. 7.2; Fig. 7.6). However, despite these preceding alterations of DOM, we found mineral surfaces in the subsoil environment to be hot spots of microbial abundance with a comparable community composition as on those minerals in shallower soil depth (Fig. 7.9 b). This indicated that despite the high proportions of mineral-bound C (Angst et al., 2016) subsoil-C was at least partly bioavailable and that the microbial C availability on mineral surfaces in the subsoil was significantly increased compared to the surrounding soil environment. However, microbial C availability in subsoil strongly depends on OC transport with the soil solution from upper soil layers, whereas the total extent and the spatial and seasonal patterns of soil water fluxes were found to be highly variable under field conditions (Leinemann et al., 2016). Therefore, a synthesis of the results of the soil translocation experiments and the column experiment allowed conclusions on the microbially regulated C dynamics with increasing soil depth. The column experiment clearly demonstrated the high potential of extensive C processing on mineral surfaces in deeper soil environments with distinct influence on especially bacterial properties and C turnover. However, the results of the translocation experiments suggested that the extent of microbial C processing in deeper soil under *in situ* conditions is temporary and spatially restricted. In this regard, especially bacteria as key players of mineral-associated C turnover were found to be inhibited in growth and decomposition activity by soil moisture limitations. Consequently, intense bacterial activity in the sandy subsoil might largely be limited to preferential flow paths or to rainfall events with pronounced DOM fluxes down to deeper soil layers (Bundt et al., 2001). Contrary, fungi – primarily involved in the decomposition of recent plant-derived substrates as well as complex plant compounds such as cellulose and lignin – were rather restricted by substrate limitation in deeper soil than by micro-climatic conditions. The resistance of specific fungal strains against micro-climatic fluctuations might be an important fungal characteristic in decomposition processes under future warmer climatic conditions, where soils might dry out for longer time periods and to greater extent.

9 Final Conclusions and Perspectives

Carbon dynamics in subsoil have gained increasing attention in recent years due to the high proportion of total SOC stored for long timescales in deeper soil layers and the relevance of subsoil as potential source or sink of C in the global C-cycle. However, to date, there is still insufficient understanding of the mechanisms of OC storage and turnover in subsoil and of the biological, chemical and physical factors influencing these processes. The aim of the SUBSOM research group was to comprehensively investigate these complex processes in subsoil C-cycling. Within the framework of this research group, the studies presented in this thesis have investigated the effects of various factors and their interactions on the abundance and regulatory function of microorganisms in C-cycling in deeper soil layers. This thesis provides novel knowledge about the microbial community structure in subsoil habitats, the function of different microbial groups in SOM decomposition within soil profiles, and the effects of changing habitat conditions with soil depth on microbial characteristics.

The results of this thesis demonstrated that deep soil layers exhibit a substantial potential for microbial C turnover. Under field conditions, however, this potential was found to be limited by the predominant environmental conditions, so that the actual microbial C turnover was generally low during the investigation period. Beside the coarse soil texture of the Dystric Cambisol at the experimental site, the nearly perpetually occurring low soil water content and the interaction of these factors led to a spatial separation between microorganisms and potentially available substrates. This applied in particular for the subsoil horizons of the site causing a pronounced inhibition of microbial C turnover in deeper soil. Spatial separation might consequently be a key determinant for the accumulation of OC in subsoil. The extent of spatial separation decisively depends on the texture and water holding capacity of the soil as well as on the amount and temporal pattern of precipitation and the resulting soil moisture. Based on the results of this thesis, soils/soil horizons with a high sand content and thus a rather coarse soil structure appear to be more susceptible to micro-scale fragmentation and thus to spatial separation between microorganisms and substrates under low soil moisture conditions. Moreover, this thesis demonstrated that bacteria and their C turnover were more negatively influenced by these habitat conditions than fungi suggesting that bacterial characteristics were predominantly affected by micro-climatic conditions, in particular low soil moisture, whereas fungi exhibited a clear dependence on preferential substrates. This finding indicated that the fungal role in SOM turnover could be of increasing importance under future climatic conditions, where soils might dry out for longer time periods and to greater extent. Fungi were found to maintain their metabolic activity under low soil moisture for longer time periods than bacteria due to their ability to bridge air-filled pores via hyphal growth and their generally lower soil moisture sensitivity. Nevertheless, the laboratory flow cascade experiment revealed that also increased bacterial growth and activity could occur in subsoil. Here, high C processing on mineral surfaces and favorable water conditions led to an increased growth of in particular copiotrophic bacteria indicating high labile C availability in this micro-environment. Consequently, this thesis reveals that microbial C turnover in subsoil largely depends on spatial C availability for microorganisms in a heterogeneous environment. The microbial C availability, in turn, strongly depends on direct and indirect effects of soil water content and fluxes on C transport, interconnection of the soil pore space, as well as on microbial metabolism and mobility. In the context of subsoil as source or sink of C this means that increasing OC input due to climate change (e.g. higher net primary production; NPP) or human impact may not necessarily lead to an increased C sequestration in deeper soil (Lorenz and Lal, 2005), but rather to enhanced microbial C turnover and thus to an accelerated C release (e.g. via positive priming effects) from subsoil C pools.

The newly gained knowledge from this thesis provides the basis for further investigations on the regulatory function of microorganisms in subsoil C-cycling. However, more studies are required on taxa-specific C utilization in response to different habitat conditions in order to obtain a more detailed picture of the different actors in subsoil C-cycling and their development under future climate change scenarios. This can be achieved by analyzing nucleic acids in labelling experiments (DNA-SIP, RNA-SIP) and the taxonomic and functional characterization of the microbial communities and their metabolic function (functional genes) in subsoil. Fungal decomposition communities might be of particular interest due to their increased importance in C-cycling under dry soil conditions, as demonstrated in this thesis. Moreover, the microbial communities of different soil types and their response to different habitat conditions should be integrated into investigations in order to assess the development of microbial regulation of subsoil C pools on larger spatial scales.

10 References

Agnelli, A., Ascher, J., Corti, G., Ceccherini, M.T., Nannipieri, P., Pietramellara, G., 2004. Distribution of microbial communities in a forest soil profile investigated by microbial biomass, soil respiration and DGGE of total and extracellular DNA. Soil Biology and Biochemistry 36, 859-868.

Ali, R.S., Ingwersen, J., Demyan, M.S., Funkuin, Y.N., Wizemann, H.D., Kandeler, E., Poll, C., 2015. Modelling *in situ* activities of enzymes as a tool to explain seasonal variation of soil respiration from agro-ecosystems. Soil Biology and Biochemistry 81, 291–303.

Allison, S.D., Vitousek, P.M., 2005. Responses of extracellular enzymes to simple and complex nutrient inputs. Soil Biology and Biochemistry 37, 937-944.

Allison, S.D., Lu, Y., Weihe, C., Goulden, M.L., Martiny, A.C., Treseder, K.K., Martiny, J.B.H., 2013. Microbial abundance and composition influence litter decomposition response to environmental change. Ecology 94, 714-725.

Anderson, J., Domsch, K.H., 1978. A physiological method for the quantitative measurement of microbial biomass in soils. Soil Biology and Biochemistry 10, 215–221.

Anderson, J., Domsch, K.H., 1980. Quantities of plant nutrients in the microbial biomass of selected soils. Soil Science Society of America Journal 130, 211-216.

Angst, G., Kögel-Knabner, I., Kirfel, K., Hertel, D., Mueller, C.W., 2016a. Spatial distribution and chemical composition of soil organic matter fractions in rhizosphere and non-rhizosphere soil under European beech (*Fagus sylvatica* L.). Geoderma 264, 179–187.

Angst, G., Heinrich, L., Kögel-Knabner, I., Mueller, C. W, 2016b. The fate of cutin and suberin of decaying leaves, needles and roots – inferences from the initial decomposition of bound fatty acids. Organic Geochemistry 95, 81-92.

Angst, G., John, S., Mueller, C.W., Kögel-Knabner, I., Rethemeyer, J., 2016c. Tracing the sources and spatial distribution of organic carbon in subsoils using a multi-biomarker approach. Nature Scientific Reports 6, 29478

Angst, G., Messinger, J., Greiner, M., Häusler, W., Hertel, D., Kirfel, K., Kögel-Knabner, I., Leuschner, C., Rethemeyer, J., Mueller, C.W., 2018. Soil organic carbon stocks in topsoil and subsoil controlled by parent material, carbon input in the rhizosphere, and microbial-derived compounds. Soil Biology and Biochemistry 122, 19-30.

Austin, A.T., Yahdjian, L., Stark, J.M., Belnap, J., Porporato, A., Norton, U., Ravetta, D.A., Schaeffer, S.M., 2004. Water pulses and biogeochemical cycles in arid and semiarid ecosystems. Oecologia 141, 221–235.

Bacchetti De Gregoris, T., Aldred, N., Clare, A.S., Burgess, J.G., 2011. Improvement of phylum- and class-specific primers for real-time PCR quantification of bacterial taxa. Journal of Microbiological Methods 86, 351–356.

Baldrian, P., Merhautová, V., Petránková, M., Cajthaml, T., Snajdr, J., 2010. Distribution of microbial biomass and activity of extracellular enzymes in a hardwood forest soil reflect soil moisture content. Applied Soil Ecology 46, 177-182.

Baldrian, P., 2017. Microbial activity and the dynamics of ecosystem processes in forest soils. Current Opinion in Microbiology 37, 128-134.

Balesdent, J., Wagner, G.H., Mariotti, A., 1988. Soil Organic Matter Turnover in Long-term Field Experiments as Revealed by Carbon-13 Natural Abundance. Soil Science Society of America Journal 52, 118-124.

Balser, T.C., Firestone, M.K., 2005. Linking Microbial Community Composition and Soil Processes in a California Annual Grassland and Mixed-Conifer Forest. Biogeochemistry 73, 395-415.

Bardgett, R.D., Freeman, C., Ostle, N.J., 2008. Microbial contributions to climate change through carbon cycle feedbacks. The ISME Journal 2, 805-814.

Baritz, R., Seufert, G., Montanarella, L., Van Ranst, E., 2010. Carbon concentrations and stocks in forest soils of Europe. Forest Ecology and Management 260, 262-277.

Barnard, R.L., Osborne, C.A., Firestone, M.K., 2013. Responses of soil bacterial and fungal communities to extreme desiccation and rewetting. The ISME Journal 7, 2229–2241.

Bates, D., Maechler, M., Bolker, B., Walker, S., 2015. Fitting Linear Mixed-Effects Models Using lme4. Journal of Statistical Software 67(1), 1-48.

Batjes, N.H., 1996. Total carbon and nitrogen in the soils of the world. European Journal of Soil Science 47, 151–163.

Bernal, B., McKinley, D.C., Hungate, B.A., White, P.M., Mozder, T.J., Megonigal, J.P., 2016. Limits to soil carbon stability; Deep, ancient soil carbon decomposition stimulated by new labile organic inputs. Soil Biology and Biochemistry 98, 85-94.

Blagodatskaya, E.V., Anderson, T.-H., 1998. Interactive effects of pH and substrate quality on the fungal-to-bacterial ratio and qCO_2 of microbial communities in forest soils. Soil Biology and Biochemistry 30, 1269-1274.

Blakemore L.C., Searle P.L. and Daly B.K., 1987. Methods for Chemical Analysis of Soils. New Zealand Soil Bureau Scientific Report 80. Lower Hutt, New Zealand, Department of Scientific and Industrial Research.

Blume, E., Bischoff, M., Reichert, J.M., Moorman, T., Konopka, A., Turco, R.F., 2002. Surface and subsurface microbial biomass, community structure and metabolic activity as a function of soil depth and season. Applied Soil Ecology 20, 171–181.

Boberg, J.B., Finlay, R.D., Stenlid, J., Lindahl, B.D., 2010. Fungal C translocation restricts N-mineralization in heterogeneous environments. Functional Ecology 24, 454–459.

Boberg, J.B., Finlay, R.D., Stenlid, J., Ekblad, A., Lindahl, B.D., 2014. Nitrogen and carbon reallocation in fungal mycelia during decomposition of boreal forest litter. PloS One 9, e92897.

Boschker, H.T.S., Middelburg, J.J., 2002. Stable isotopes and biomarkers in microbial ecology. FEMS Microbiology Ecology 40, 85–95.

Boyle, S.A., Rich, J.J., Bottomley, P.J., Cromack Jr., K., Myrold, D.D., 2006. Reciprocal transfer effects on denitrifying community composition and activity at forest and meadow sites in the Cascade Mountains of Oregon. Soil Biology and Biochemistry 38, 870-878.

Bradford, M.A., 2013. Thermal adaptation of decomposer communities in arming soils. Frontiers in Microbiology 4, 1-16.

Brockett, B.F., Prescott, C.E., Grayston, S.J., 2012. Soil moisture is the major factor influencing microbial community structure and enzyme activities across seven biogeoclimatic zones in western Canada. Soil Biology and Biochemistry 44, 9–20.

Brunauer S., Emmett P. H. and Teller E. 1938. Adsorption of gases in multimolecular layers. Journal of the American Chemical Society 60, 309–319.

Bull, I.D., Parekh, N.R., Hall, G.H., Ineson, P., Evershed, R.P., 2000. Detection and classification of atmospheric methane oxidizing bacteria in soil. Nature 405, 175-178.

Bundt, M., Widmer, F., Pesaro, M., Zeyer, J., Blaser, P., 2001. Preferential flow paths: biological `hot spots' in soils. Soil Biology and Biochemistry 33, 729–738.

Castro, H.F., Classen, A.T., Austin, E.E., Norby, R.J., Schadt, C.W., 2010. Soil microbial community responses to multiple experimental climate change drivers. Applied and Environmental Microbiology 76, 999–1007.

Chabbi, A., Kögel-Knabner, I., Rumpel, C., 2009. Stabilised carbon in subsoil horizons is located in spatially distinct parts of the soil profile. Soil Biology and Biochemistry 41, 256–261.

Chirinda, N., Elsgaard, L., Thomsen, I.K., Heckrath, G., Olesen, J.E., 2014. Carbon dynamics in topsoil and subsoil along a cultivated toposequence. Catena 120, 20–28.

Chorover, J., Amistadi M.K., 2001. Reaction of forest floor organic matter and goethite, birnessite and smectite surfaces. Geochimica et Cosmochimica Acta 65, 95-109.

Conant, R.T., Ryan, M.G., Agren, G.I., Birge, H.E., Davidson, E.A., Eliasson, P.E., Evans, S.E., Frey, S.D., Giardina, C.P., Hopkins, F.M., Hyvönen, R., Kirschbaum, M.U.F., Lavallee, J.M., Leifeld, J., Parton, W.J., Steinweg, J.M., Wallenstein, M.D., Wetterstedt, J.A.M., Bradford, M.A., 2011. Temperature and soil organic matter decomposition rates – synthesis of current knowledge and a way forward. Global Change Biology 17, 3392–3404.

Coplen, T.B., Brand, W.A., Gehre, M., Groning, M., Meijer, H.A.J., Toman, B., Verkouteren, R.M., 2006. New guidelines for $\delta^{13}C$ measurements. Analytical Chemistry 78, 2439-2441.

Davidsons, E.A., Janssens, I.A., 2006. Temperature sensitivity of soil carbon decomposition and feedbacks to climate change. Nature 440, 165-173.

DeAngelis, K.M., Pold, G., Topcuoglu, B.D., van Diepen, L.T.A., Varney, R.M., Blanchard, J.L., Melillo, J., Frey, S.D., 2015. Long-term forest soil warming alters microbial communities in temperate forest soils. Frontiers in Microbiology 6, 1-13.

De Nobili, M., Contin, M., Mondini, C., Brookes, P.C., 2001. Soil microbial biomass is triggered into activity by trace amounts of substrate. Soil Biology and Biochemistry 33, 1163-1170.

Demoling, F., Figueroa, D., Bååth, E., 2007. Comparison of factors limiting bacterial growth in different soils. Soil Biology and Biochemistry 39, 2485–2495.

Djajakirana, G., Joergensen, R.G., Meyer, B., 1996. Ergosterol and microbial biomass relationship in soil. Biology and Fertility of Soils 22, 299–304.

Drenovsky, R.E., Vo, D., Graham, K.J., Scow, K.M., 2004. Soil Water Content and Organic Carbon Availability Are Major Determinants of Soil Microbial Community Composition. Microbial Ecology 48, 424-430.

Dumont, M.G., Murrell, J.C., 2005. Stable isotope probing — linking microbial identity to function. Nature Reviews 3, 499-504.

Dungait, J.A.J., Hopkins, D.W., Gregory, A.S., Whitmore, A.P., 2012. Soil organic matter turnover is governed by accessibility not recalcitrance. Global Change Biology 18, 1781–1796.

Edwards, I.P., Upchurch, R.A., Zak, D.R., 2008. Isolation of fungal cellobiohydrolase I genes from sporocarps and forest soils by PCR. Applied and Environmental Microbiology 74, 3481–3489.

Eichorst, S.A., Kuske, C.R., Schmidt, T.M., 2011. Influence of Plant Polymers on the Distribution and Cultivation of Bacteria in the Phylum Acidobacteria. Applied and Environmental Microbiology 77, 586–596.

Eilers, K.G., Lauber, C.L., Knight, R., Fierer, N., 2010. Shifts in bacterial community structure associated with inputs of low molecular weight carbon compounds to soil. Soil Biology and Biochemistry 42, 896-903.

Eilers, K.G., Debenport, S., Anderson, S., Fierer, N., 2012. Digging deeper to find unique microbial communities: The strong effect of depth on the structure of bacterial and archaeal communities in soil. Soil Biology and Biochemistry 50, 58–65.

Ekblad, A., Nordgren, A., 2002. Is growth of soil microorganisms in boreal forests limited by carbon or nitrogen availability? Plant and Soil 242, 115–122.

Ekelund, F., Ronn, R., Christensen, S., 2001. Distribution with depth of protozoa, bacteria and fungi in soil profiles from three Danish forest sites. Soil Biology and Biochemistry 33, 475–481.

Eusterhues, K., Rumpel, C., Kögel-Knabner, I., 2005. Organo-mineral associations in sandy acid forest soils: importance of specific surface area, iron oxides and micropores. European Journal of Soil Science 56, 753-763.

Eusterhues, K., Rumpel, C., Kögel-Knabner, I., 2005. Stabilization of soil organic matter isolated via oxidative degradation. Organic Geochemistry 36, 1567–1575.

Evans, S.E., Wallenstein, M.D., Burke, I.C., 2014. Is bacterial moisture niche a good predictor of shifts in community composition under long-term drought? Ecology 95, 110-122.

Evershed, R.P., Crossman, Z.M., Bull, I.D., Mottram, H., Dungait, J., Maxfield, P.J., Brennand, E.L., 2006. ^{13}C-Labelling of lipids to investigate microbial communities in the environment. Current Opinion in Biotechnology 17, 72–82.

Fang, C., Moncrieff, J.B., 2005. The variation of soil microbial respiration with depth in relation to soil carbon composition. Plant and Soil 268, 243–253.

Federherr E., Cerli C., Kirkels F.M., Kalbitz K., Kupka H.J., Dunsbach R., Lange L., Schmidt T.C., 2014. A novel high-temperature combustion based system for stable isotope analysis of dissolved organic carbon in aqueous samples. I: development and validation. Rapid Communication in Mass Spectrometry 28, 2559-73.

Feng, X., Simpson, M.J., 2009. Temperature and substrate controls on microbial phospholipid fatty acid composition during incubation of grassland soils contrasting in organic matter quality. Soil Biology and Biochemistry 41, 804–812.

Fierer, N., Schimel, J.P., 2002. Effects of drying-rewetting frequency on soil carbon and nitrogen transformations. Soil Biology and Biochemistry 34, 777-787.

Fierer, N., Schimel, J.P., Holden, P.A., 2003. Variations in microbial community composition through two soil depth profiles. Soil Biology and Biochemistry 35, 167–176.

Fierer, N., Allen, A.S., Schimel, J.P., Holden, P.A., 2003a. Controls on microbial CO_2 production: a comparison of surface and subsurface soil horizons. Global Change Biology 9, 1322-1332.

Fierer, N., Jackson, J.A., Vilgalys, R., Jackson R.B., 2005. Assessment of soil microbial community structure by use of taxon-specific quantitative PCR assays. Applied and Environmental Microbiology 71, 4117–4120.

Fierer, N., Bradford, M.A., Jackson, R.B., 2007. Toward an ecological classification of soil bacteria. Ecology 88, 1354-1364.

Fontaine, S., Barot, S., Barré, P., Bdioui, N., Mary, B., Rumpel, C., 2007. Stability of organic carbon in deep soil layers controlled by fresh carbon supply. Nature 450, 277–280.

Frey, S.D., Elliott, E.T., Paustian, K., Peterson, G.A., 2000. Fungal translocation as a mechanism for soil nitrogen inputs to surface residue decomposition in a no-tillage agroecosystem. Soil Biology and Biochemistry 32, 689–698.

Frey, S.D., Drijber, R., Smith, H., Melillo, J., 2008. Microbial biomass, functional capacity, and community structure after 12 years of soil warming. Soil Biology and Biochemistry 40, 2904–2907.

Frey, S.D., Lee, J., Melillo, J.M., Six, J., 2013. The temperature response of soil microbial efficiency and its feedback to climate. Nature Climate Change, 1-4.

Fröberg, M., Jardine, P.M., Hanson, P.J., Swanston, C.W., Todd, D.E., Tarver, J.R., Garten Jr., C.T., 2007. Low Dissolved Organic Carbon Input from Fresh Litter to Deep Mineral Soils. Soil Science Society of America Journal 71, 347-354.

Frostegård, A., Tunlid, A., Bååth, E., 1991. Microbial biomass measured as total lipid phosphate in soils of different organic content. Journal of Microbiological Methods 14, 151–163.

Frostegård, A., Tunlid, A., Bååth, E., 1993. Phospholipid fatty acid composition, biomass, and activity of microbial communities from two soil types experimentally exposed to different heavy metals. Applied and Environmental Microbiology 59, 3605–3617.

Frostegård, A., Bååth, E., 1996. The use of phospholipid fatty acid analysis to estimate bacterial and fungal biomass in soil. Biology and Fertility of Soils, 59–65.

Fry, B., 2007. Stable Isotope Ecology. Springer Science+Business Media, New York.

Gaudinski, J.B., Trumbore, S.E., Davidson, E.A., Zheng, S., 2000. Soil Carbon Cycling in a Temperate Forest: Radiocarbon-Based Estimates of Residence Times, Sequestration Rates and Partitioning of Fluxes. Biogeochemistry 51, 33-69.

Gill, R.A., Burke, I.C., 2002. Influence of soil depth on the decomposition of Bouteloua gracilis roots in the shortgrass steppe. Plant and Soil 241, 233-242.

Goberna, M., Insam, H., Klammer, S., Pascual, J.A., Sanchez, J., 2005. Microbial Community Structure at Different Depths in Disturbed and Undisturbed Semiarid Mediterranean Forest Soils. Microbial Ecology 50, 315-326.

Göransson, H., Olde Venterink, H., Bååth, E., 2011. Soil bacterial growth and nutrient limitation along a chronosequence from a glacier forefield. Soil Biology and Biochemistry 43, 1333–1340.

Gordon, H., Haygarth, P.M., Bardgett, R.D., 2008. Drying and rewetting effects on soil microbial community composition and nutrient leaching. Soil Biology and Biochemistry 40, 302–311.

Grüneberg, E., Schöning, I., Kalko, E.K.V., Weisser, W.W., 2010. Regional organic carbon stock variability: A comparison between depth increments and soil horizons. Geoderma 155, 426-433.

Gu, B., Schmitt, J., Chen, Z., Liang, L., McCarthy, J.F., 1994. Adsorption and desorption of natural organic matter on iron oxide: Mechanisms and Models. Environmental Science and Technology 28, 38-46.

Guenet, B., Juarez, S., Bardoux, G., Abbadie, L., Chenu, C., 2012. Evidence that stable C is as vulnerable to priming effect as is more labile C in soil. Soil Biology and Biochemistry 52, 43-48.

Guo, M., Chorover, J., 2003. Transport and fractionation of dissolved organic matter in soil columns. Soil Science 168, 108-118.

Hagedorn, F., Saurer, M., Blaser, P., 2004. A ^{13}C tracer study to identify the origin of dissolved organic carbon in forested mineral soils. European Journal of Soil Science 55, 91-100.

Hagedorn, F., Bruderhofer, N., Ferrari, A., Niklaus, P.A., 2015. Tracing litter-derived dissolved organic matter along a soil chronosequence using ^{14}C imaging: Biodegradation, physic-chemical retention or preferential flow? Soil Biology and Biochemistry 88, 333-343.

Hansel, C.M., Fendorf, S., Jardine, P.M., Francis, C.A., 2008. Changes in bacterial and archaeal community structure and functional diversity along a geochemically variable soil profile. Applied and Environmental Microbiology 74, 1620–1633.

Hanson, C.A., Allison, S.D., Bradford, M.A., Wallenstein, M.D., Treseder, K.K., 2008. Fungal Taxa Target Different Carbon Sources in Forest Soil. Ecosystems 11, 1157-1167.

Harrell Jr, F.E., with contributions from Charles Dupont and many others, 2015. Hmisc: Harrell Miscellaneous R package version 3.15-0. http://cran.r-project.org/package=Hmisc Cambridge University Press, Cambridge and New York.

Harrison, Robert B., Footen, P.W., Strahm, B.D., 2011. Deep soil horizons: Contribution and importance to soil carbon pools and in assessing whole-ecosystem response to management and global change. Forest Science 57, 67–76.

Hartmann, M., Lee, S., Hallam, S.J., Mohn, W.W., 2009. Bacterial, archaeal and eukaryal community structures throughout soil horizons of harvested and naturally disturbed forest stands. Environmental Microbiology 11, 3045–3062.

Heckman, K., Welty-Bernard, A., Vasquez-Ortega, A., Schwartz, E., Chorover, J., Rasmussen, C., 2013. The influence of goethite and gibbsite on soluble nutrient dynamics and microbial community composition. Biogeochemistry 112, 179-195.

Heitkötter, J., Heinze, S., Marschner, B., 2017. Relevance of substrate quality and nutrients for microbial C-turnover in top- and subsoil of a Dystric Cambisol. Geoderma 302, 89–99.

Herold, N., Schöning, I., Berner, D., Haslwimmer, H., Kandeler, E., Michalzik, B., Schrumpf, M., 2014. Vertical gradients of potential enzyme activities in soil profiles of European beech, Norway spruce and Scots pine dominated forest sites. Pedobiologia 57, 181–189.

Herold, N., Schöning, I., Michalzik, B., Trumbore, S., Schrumpf, M., 2014a. Controls on soil carbon storage and turnover in German landscapes. Biogeochemistry 119, 435-451.

Hicks Pries, C.E., Sulman, B.N., West, C., O`Neill, C., Poppleton, E., Porras, R.C., Castana, C., Zhu, B., Wiedemeier, D.B., Torn, M.S., 2018. Soil Biology and Biochemistry 125, 103-114.

Holden, P., Fierer, N., 2005. Microbial Processes in the Vadose zone. Vadose Zone Journal 4, 1-21.

IUSS Working Group WRB, 2014. World Reference Base for Soil Resources 2014. International soil classification system for naming soils and creating legends for soil maps. World Soil Resources Reports No. 106. FAO, Rome.

Jansen, B., Nierop, K.G.J., Kotte, M.C., de Voogt, P., Verstraten, J.M., 2006. The applicability of accelerated solvent extraction (ASE) to extract lipid biomarkers from soils. Applied Geochemistry 21, 1006–1015.

Jobbagy, E.G., Jackson, R.B., 2000. The vertical distribution of soil organic carbon and its relation to climate and vegetation. Ecological Applications 10, 423–436.

Joergensen, R.G., Mueller, T., 1996. The fumigation-extraction method to estimate soil microbial biomass: Calibration of the k_{en} value. Soil Biology and Biochemistry 28, 33–37.

Joergensen, R.G., Scheu, S., 1999. Response of soil microorganisms to the addition of carbon, nitrogen and phosphorus in a forest Rendzina. Soil Biology and Biochemistry 31, 859-866.

Johnsen, A.R., Jacobsen, O.S., 2008. A quick and sensitive method for the quantification of peroxidase activity of organic surface soil from forests. Soil Biology and Biochemistry 40, 814-821.

Jones, D.L., Nguyen, C., Finlay, R.D., 2009. Carbon flow in the rhizosphere: carbon trading at the soil–root interface. Plant and Soil 321, 5-33.

Jumpponen, A., Jones, K.L., Blair, J., 2010. Vertical distribution of fungal communities in tallgrass prairie soil. Mycologia 102, 1027-1041.

Kaiser, C., Kilburn, M.R., Clode, P.L., Fuchslueger, L., Koranda, M., Cliff, J.B., Solaiman, Z.M., Murphy, D.V., 2015. Exploring the transfer of recent plant photosynthates to soil microbes: mycorrhizal pathway vs direct root exudation. New Phytologist 205, 1537–1551.

Kaiser, K., Guggenberger, G., Haumaier, L., Zech, W., 1997. Dissolved organic matter sorption on subsoils and soil minerals studied by ^{13}C NMR and DRIFT spectroscopy. European Journal of Soil Science 48, 301-310.

Kaiser, K., Zech, W., 2000. Sorption of dissolved organic nitrogen by acid subsoil horizons and individual mineral phases. European Journal of Soil Science 51, 403-411.

Kaiser, K., Guggenberger, G., 2000. The role of DOM sorption to mineral surfaces in the preservation of organic matter in soils. Organic Geochemistry 31, 711–725.

Kaiser, K., 2003. Sorption of natural organic matter fractions to goethite (α-FeOOH): effect of chemical composition as revealed by liquid-state ^{13}C NMR and wet-chemical analysis. Organic Geochemistry 34, 1569-1579.

Kaiser, K., Guggenberger, G., Haumaier L., 2004. Changes in dissolved lignin-derived phenols, neutral sugars, uronic acids, and amino sugars with depth in forested Haplic Anenosols and Rendzic Leptosols. Biogeochemistry 70, 135-151.

Kaiser, K., Guggenberger, G., 2007. Sorptive stabilization of organic matter by microporous goethite: sorption into small pores vs. surface complexation. European Journal of Soil Science 58, 45-59.

Kaiser, K., Kalbitz, K., 2012. Cycling downwards - dissolved organic matter in soil. Soil Biology and Biochemistry 52, 29-32.

Kalbitz, K., Kaiser, K., 2008. Contribution of dissolved organic matter to carbon storage in forest mineral soils. Journal of Plant Nutrition and Soil Science 171, 52-60.

Kamble, P.N., Rousk, J., Frey, S.D., Bååth, E., 2013. Bacterial growth and growth-limiting nutrients following chronic nitrogen additions to a hardwood forest soil. Soil Biology and Biochemistry 59, 32–37.

Kandeler, E., Stemmer, M., Gerzabek, M.H., 2005. Role of microorganisms in carbon cycling in soils. In: Varma, A., Buscot, F. (Eds.), Microorganisms in Soils: Roles in Genesis and Functions. Springer, Berlin Heidelberg, pp. 139-157.

Kandeler, E., Mosier, A.R., Morgan, J.A., Milchunas, D.G., King, J.Y., Rudolph, S., Tscherko, D., 2008. Transient elevation of carbon dioxide modifies the microbial community composition in a semi-arid grassland. Soil Biology and Biochemistry 40, 162–171.

Karhu, K., Hilasvuori, E., Fritze, H., Biasi, C., Nykänen, H., Liski, J., Vanhala, P., Heinonsalo, J., Pumpanen, J., 2016. Priming effect increases with depth in a boreal forest soil. Soil Biology and Biochemistry 99, 104-107.

Kätterer, T., Börjesson, G., Kirchmann, H., 2014. Changes in organic carbon in topsoil and subsoil and microbial community composition caused by repeated additions of organic amendments and N fertilisation in a long-term field experiment in Sweden. Agriculture, Ecosystems and Environment 189, 110-118.

Kirkels, F.M.S.A., Cerli, C., Fedeherr, E., Gao, J., Kalbitz, K., 2014. A novel high-temperature combustion based system for stable isotope analysis of dissolved organic carbon in aqueous samples. II: optimization and assessment of analytical performance. Rapid Communications in Mass Spectrometry 28, 2574-2586.

Koranda, M., Kaiser, C., Fuchslueger, L., Kitzler, B., Sessitsch, A., Zechmeister-Boltenstern, S., Richter, A., 2014. Fungal and bacterial utilization of organic substrates depends on substrate complexity and N availability. FEMS Microbiology Ecology 87, 142-152.

Kramer, C., Gleixner, G., 2006. Variable use of plant- and soil-derived carbon by microorganisms in agricultural soils. Soil Biology and Biochemistry 38, 3267-3278.

Kramer, C., Gleixner, G., 2008. Soil organic matter in soil depth profiles: Distinct carbon preferences of microbial groups during carbon transformation. Soil Biology and Biochemistry 40, 425-433.

Kramer, S., Marhan, S., Haslwimmer, H., Ruess, L., Kandeler, E., 2013. Temporal variation in surface and subsoil abundance and function of the soil microbial community in an arable soil. Soil Biology and Biochemistry 61, 76-85.

Krull, E.S., Baldock, J.A., Skjemstad, J.O., 2003. Importance of mechanisms and processes of the stabilization of soil organic matter for modelling carbon turnover. Functional Plant Biology 30, 207-222.

Kuzyakov, Y., Blagodatskaya, E., 2015. Microbial hotspots and hot moments in soil: Concept & review. Soil Biology and Biochemistry 83, 184-199.

Lal, R., 2004. Soil carbon sequestration impacts on global climate change and food security. Science 304, 1623-1627.

Lal, R., 2005. Forest soils and carbon sequestration. Forest Ecology and Management 220, 242-258.

LaMontagne, M.G., Schimel, J.P., Holden, P.A., 2003. Comparison of subsurface and surface soil bacterial communities in California grassland as assessed by terminal restriction fragment length polymorphisms of PCR-amplified 16S rRNA genes. Microbial Ecology 46, 216–227.

Lauber, C.L., Hamady, M., Knight, R., Fierer, N., 2009. Pyrosequencing-based assessment of soil pH as a predictor of soil bacterial community structure at the continental scale. Applied and Environmental Microbiology 75, 5111–5120.

Leinemann, T., Mikutta, R., Kalbitz, K., Schaarschmidt, F., Guggenberger, G., 2016. Small scale variability of vertical water and dissolved organic matter fluxes in sandy Cambisol subsoils as revealed by segmented suction plates. Biogeochemistry 131, 1-15.

Leinemann, T., Preusser, S., Mikutta, R., Kalbitz, K., Cerli, C., Höschen, C., Mueller, C.W., Kandeler, E., Guggenberger, G., 2018. Multiple exchange processes on mineral surfaces control the transport of dissolved organic matter through soil profiles. Soil Biology and Biochemistry 118, 79-90.

Lenth, R.V., 2016. Least-Squares Means: The R Package lsmeans. Journal of Statistical Software 69, 1-33.

Liang, C., Balser, T.C., 2008. Preferential sequestration of microbial carbon in subsoils of a glacial-landscape toposequence, Dane County, WI, USA. Geoderma 148, 113-119.

Lorenz, K., Lal, R., 2005. Soil organic carbon sequestration in agroforestry systems. A review. Agronomy for Sustainable Development 34, 443-454.

Lueders, T., Kindler, R., Miltner, A., Friedrich, M.W., Kaestner, M., 2006. Identification of Bacterial Micropredators Distinctively Active in a Soil Microbial Food Web. Applied and Environmental Microbiology 72, 5342–5348

Lützow, M.v., Kögel-Knabner, I., Ekschmitt, K., Matzner, E., Guggenberger, G., Marschner, B., Flessa, H., 2006. Stabilization of organic matter in temperate soils. Mechanisms and their relevance under different soil conditions - a review. European Journal of Soil Science 57, 426–445.

Manerkar, M.A., Seena, S., Bärlocher, F., 2008. Q-RT-PCR for Assessing Archaea, Bacteria, and Fungi during Leaf Decomposition in a Stream. Microbial Ecology 56, 467–473.

Manzoni, S., Schimel, J.P., Porporato, A., 2012. Responses of soil microbial communities to water stress: results from a meta-analysis. Ecology 93, 930-938.

Marhan, S., Kandeler, E., Rein, S., Fangmeier, A., Niklaus, A., 2010. Indirect effects of soil moisture reverse soil C sequestration responses of a spring wheat agroecosystem to elevated CO_2. Global Change Biology 16, 469–483.

Marschner, P., Marhan, S., Kandeler, E., 2012. Microscale distribution and function of soil microorganisms in the interface between rhizosphere and detritusphere. Soil Biology and Biochemistry 49, 174–183.

Marx, M.-C., Wood, M., Jarvis, S., 2001. A microplate fluorimetric assay for the study of enzyme diversity in soils. Soil Biology and Biochemistry 33, 1633–1640.

Mathieu, J.A., Hatte, C., Balesdent, J., Parent, E., 2015. Deep soil carbon dynamics are driven more by soil type than by climate: a worldwide meta-analysis of radiocarbon profiles. Global Change Biology 21, 4278-4292.

McCarthy J. F., Gu B., Liang J., Mas-Pla T. M., Williams T. M., Yeh T.-C. J., 1996. Field tracer tests on mobility of natural organic matter in a sandy aquifer. Water Resources Research 32, 1223-1238.

McDowell, W.H., Likens, G.E., 1988. Origin, composition, and flux of dissolved organic carbon in the Hubbard Brook valley. Ecological Monograph 58, 177-195.

Melillo, J.M., Frey, S.D., DeAngelis, K.M., Werner, W.J., Bernard, M.J., Bowles, F.P., Pold, G., Knorr, M.A., Grandy, A.S., 2017. Long-term pattern and magnitude of soil carbon feedback to the climate system in a warming world. Science 358, 101-105.

Mendez-Millan, M., Dignac, M.-F., Rumpel, C., Derenne, S., 2011. Can cutin and suberin biomarkers be used to trace shoot and root-derived organic matter? A molecular and isotopic approach. Biogeochemistry 106, 23-38.

Michalzik, B., Kalbitz, K., Park, J-H., Solinger, S., Matzner, E., 2001. Fluxes and concentrations of dissolved organic carbon and nitrogen – a synthesis for temperate forests. Biogeochemistry 52, 173-205.

Mikutta, R., Kleber, M., Torn, M.S., Jahn, R., 2006. Stabilization of soil organic matter: association with minerals or chemical recalcitrance? Biogeochemistry 77, 25-56.

Mikutta, R., Lorenz, D., Guggenberger, G., Haumeier, L., Freund, A., 2014. Properties and reactivity of Fe-organic matter associations formed by coprecipitation versus adsorption: Clues from arsenate batch adsorption. Geochimica et Cosmochimica Acta 144, 258-276.

Moll, J., Goldmann, K., Kramer, S., Hempel, S., Kandeler, E., Marhan, S., Ruess, L., Krüger, D., Buscot, F., 2015. Resource Type and Availability Regulate Fungal Communities Along Arable Soil Profiles. Microbial Ecology 70, 390-399.

Moni, C., Rumpel, C., Virto, I., Chabbi, A., Chenu, C., 2010. Relative importance of sorption versus aggregation for organic matter storage in subsoil horizons of two contrasting soils. European Journal of Soil Science 61, 958-969.

Moore, T.R., de Douza, W., Koprivnjak, J-F., 1992. Controls on the sorption of dissolved organic carbon by soils. Soil Science 154, 120-129.

Moore-Kucera, J., Dick, R.P., 2008. Application of ^{13}C-labeled litter and root materials for in situ decomposition studies using phospholipid fatty acids. Soil Biology and Biochemistry 40, 2485–2493.

Müller, K., Kramer, S., Haslwimmer, H., Marhan, S., Scheunemann, N., Butenschön, O., Scheu, S., Kandeler, E., 2016. Carbon transfer from maize roots and litter into bacteria and fungi depends on soil depth and time. Soil Biology and Biochemistry 93, 79–89.

Müller, M., Alewell, C., Hagedorn, F., 2009. Effective retention of litter-derived dissolved organic carbon in organic layers. Soil Biology and Biochemistry 41, 1066-1074.

Naether, A., Foesel, B.U., Naegele, V., Wust, P.K., Weinert, J., Bonkowski, M., Alt, F., Oelmann, Y., Polle, A., Lohaus, G., Gockel, S., Hemp, A., Kalko, E.K.V., Linsenmair, K.E., Pfeiffer, S., Renner, S., Schoning, I., Weisser, W.W., Wells, K., Fischer, M., Overmann, J., Friedrich, M.W., 2012. Environmental factors effect acidobacterial communities below the subgroup level in grassland and forest soils. Applied and Environmental Microbiology 78, 7398–7406.

Nunan, N., Wu, K., Young, I.M., Crawford, J.W., Ritz, K., 2003. Spatial distribution of bacterial communities and their relationships with the micro-architecture of soil. FEMS Microbiology Ecology 44, 203–215.

Pankratov, T.A., Ivanova, A.O., Dedysh, S.N., Liesack, W., 2011. Bacterial populations and environmental factors controlling cellulose degradation in an acidic Sphagnum peat. Environmental Microbiology 13, 1800–1814.

Paul, E.A., 2016. The nature and dynamics of soil organic matter: Plant inputs, microbial transformations, and organic matter stabilization. Soil Biology and Biochemistry 98, 109-126.

Philippot, L., Bru, D., Saby, N.P.A., Čuhel, J., Arrouays, D., Šimek, M., Hallin, S., 2009. Spatial patterns of bacterial taxa in nature reflect ecological traits of deep branches of the 16S rRNA bacterial tree. Environmental Microbiology 11, 3096–3104.

Pinheiro, J., Bates, D., DebRoy, S., Sarkar, D. and R Core Team, 2015. nlme: Linear and nonlinear mixed effects models. R package version 3.1-120, <URL: http://CRAN.R-project.org/package=nlme>.

Polerecky, L., Adam, B., Milucka, J., Musat, N., Vagner, T., Kuypers, M.M.M., 2012. Look@NanoSIMS – a tool for the analysis of nanoSIMS data in environmental microbiology. Environmental Microbiology 14, 1009–1023.

Preusser, S., Marhan, S., Poll, C., Kandeler, E., 2017. Microbial community response to changes in substrate availability and habitat conditions in a reciprocal subsoil transfer experiment. Soil Biology and Biochemistry 105, 138-152.

R Core Team, 2015. R: A language and environment for statistical computing. R Foundation for Statistical Computing, Vienna, Austria. URL http://www.R-project.org/.

Radajewski, S., Ineson, P., Parekh, N.R., Murrell, J.C., 2000. Stable-isotope probing as a tool in microbial ecology. Nature 403, 646-649.

Rasse, D.P., Rumpel, C., Dignac, M.-F., 2005. Is soil carbon mostly root carbon? Mechanisms for a specific stabilisation. Plant and Soil 269, 341-356.

Rawat, S.R., Männistö, M.K., Bromberg, Y., Häggblom, M.M., 2012. Comparative genomic and physiological analysis provides insights into the role of Acidobacteria in organic carbon utilization in Arctic tundra soils. FEMS Microbiology Ecology 82, 341–355.

Rennert, T.; Mansfeldt, T., 2003. Adsorption of “real” dissolved organic matter on the clay and fine silt fractions of forested Stagnic Gelysol. Journal of Plant nutrition and Soil Science 166, 204-209.

Rousk, J., Bååth, E., Brookes, P.C., Lauber, C.L., Lozupone, C., Caporaso, J.G., Knight, R., Fierer, N., 2010. Soil bacterial and fungal communities across a pH gradient in an arable soil. The ISME Journal 4, 1340–1351.

Rumpel, C., Kögel-Knabner, I., Bruhn, F., 2002. Vertical distribution, age, and chemical composition of organic carbon in two forest soils of different pedogenesis. Organic Geochemistry 33, 1131-1142.

Rumpel, C., Eusterhues, K., Kögel-Knabner, I., 2004. Location and chemical composition of stabilized organic carbon in topsoil and subsoil horizons of two acid forest soils. Soil Biology and Biochemistry 36, 177-190.

Rumpel, C., Kögel-Knabner, I., 2011. Deep soil organic matter – a key but poorly understood component of terrestrial C cycle. Plant and Soil 338, 143-158.

Saidy, A.R., Smernik, R.J., Baldock, J.A., Kaiser, K., Sanderman, J., 2013. The sorption of organic carbon onto differing clay minerals in the presence and absence of hydrous iron oxide. Geoderma 209-210, 15-21.

Salomé, C., Nunan, N., Pouteau, V., Lerch, T.Z., Chenu, C., 2010. Carbon dynamics in topsoil and in subsoil may be controlled by different regulatory mechanisms. Global Change Biology 16, 416–426.

Sanaullah, M., Chabbi, A., Leifeld, J., Bardoux, G., Billou, D., Rumpel, C., 2011. Decomposition and stabilization of root litter in top- and subsoil horizons: what is the difference? Plant and Soil 338, 127-141.

Sanaullah, M., Chabbi, A., Maron, P.-A., Baumann, K., Tardy, V., Blagodatskaya, E., Kuzyakov, Y., Rumpel, C., 2016. How do microbial communities in top- and subsoil respond to root litter addition under field conditions? Soil Biology and Biochemistry 103, 28-38.

Sanderman, J., Baldock, J.F., Amundson, R., 2008. Dissolved organic carbon chemistry and dynamics in contrasting forest and grassland soils. Biogeochemistry 89, 181-191.

Scheel, T., Haumaier, L., Ellerbrock, R.H., Rühlmann, J., Kalbitz, K., 2008. Properties of organic matter precipitated from acidic forest soil solutions. Organic Geochemistry 39, 1439-1453.

Scheu, S., 1992. Automated measurement of the respiratory response of soil microcompartments: active microbial biomass in earthworm faeces. Soil Biology and Biochemistry 24, 1113–1118.

Scheu, S., 1993. Analysis of the microbial nutrient status in soil microcompartments: earthworm faeces from a basalt—limestone gradient. In: Soil Structure/Soil Biota Interrelationships. Elsevier, pp. 575–586.

Schimel, J., Weintraub, M.N., 2003. The implications of exoenzyme activity on microbial carbon and nitrogen limitation in soil: a theoretical model. Soil Biology and Biochemistry 35, 549-563.

Schinner, F., von Mersi, W., 1990. Xylanase-, CM-cellulase- and Invertase activity in soil: an improved method. Soil Biology and Biochemistry 22, 511–515.

Schmidt, M.W.I., Torn, M.S., Abiven, S., Dittmar, T., Guggenberger, G., Jannsens, I.A., Kleber, M., Kögel-Knabner, I., Lehmann, J., Manning, D.A.C., Nannipieri, P., Rasse, D.P., Weiner, S., Trumbore, S.E., 2011. Persistence of soil organic matter as an ecosystem property. Nature 478, 49-56.

Schwertmann, U., Cornell, R.M., 2000. Iron Oxides in the Laboratory: Preparation and Characterization. Second ed. Wiley-VCH. Weinheim. Germany.

Shah, F., Nicolás, C., Bentzer, J., Ellström, M., Smits, M., Rineau, F., Canbäck, B., Floudas, D., Carleer, R., Lackner, G., Braesel, J., Hoffmeister, D., Henrissat, B., Ahrén, D., Johansson, T., Hibbett, D.S., Martin, F., Persson, P., Tunlid, A., 2016. Ectomycorrhizal fungi decompose soil organic matter using oxidative mechanisms adapted from saprotrophic ancestors. New Phytologist 20, 1705–1719.

Silver, W.L., Miya, R.K., 2001. Global patterns in root decomposition: comparisons of climate and litter quality effects. Oecologia 129, 407–419.

Sollins, P., Homann, P., Caldwell, B.A., 1996. Stabilization and destabilization of soil organic matter: mechanisms and controls. Geoderma 74, 65-105.

Solly, E.F., Schöning, I., Herold, N., Trumbore, S.E., Schrumpf, M., 2015. No depth-dependence of fine root litter decomposition in temperate beech forest soils. Plant and Soil 393, 273-282.

Spohn, M., Klaus, K., Wanek, W., Richter, A., 2016. Microbial carbon use efficiency and biomass turnover times depending on soil depth – Implications for carbon cycling. Soil Biology and Biochemistry 96, 74-81.

Staddon, P.L., 2004. Carbon isotopes in functional soil ecology. Trends in Ecology and Evolution 19, 148-154.

Stockmann, U., Adams, M.A., Crawford, J.W., Field, D.J., Henakaarchchi, N., Jenkins, M., Minasny, B., McBratney, A.B., de Remy de Courcelles, V., Singh, K., Wheeler, I., Abbott, L., Angers, D.A., Baldock, J., Bird, M., Brookes, P.C., Chenu, C., Jastrow, J.D., Lal, R., Lehmann, J., O`Donnell, A.G., Parton, W.J., Whitehead, D., Zimmermann, M., 2013. The knowns, known unknowns and unknowns of sequestration of soil organic carbon. Agriculture, Ecosystems and Environment 164, 80– 99.

Stone, M.M., DeForest, J.L., Plante, A.F., 2014. Changes in extracellular enzyme activity and microbial community structure with soil depth at the Luquillo Critical Zone Observatory. Soil Biology and Biochemistry 75, 237-247.

Stursová, M., Zifčáková, L., Leigh, M.B., Burgess, R., Baldrian, P., 2012. Cellulose utilization in forest litter and soil: identification of bacterial and fungal decomposers. FEMS Microbiology Ecology 80, 735–746.

Talbot, J.M., Martin, F., Kohler, A., Henrissat, B., Peay, K.G., 2013. Independent roles of ectomycorrhizal and saprotrophic communities in soil organic matter decomposition. Soil Biology and Biochemistry 57, 282-291.

Talbot, J.M., Martin, F., Kohler, A., Henrissat, B., Peay, K.G., 2015. Functional guild classification predicts the enzymatic role of fungi in litter and soil biogeochemistry. Soil Biology and Biochemistry 88, 441-456.

Taylor, J., Wilson, B., Mills, M., Burns, R., 2002. Comparison of microbial numbers and enzymatic activities in surface soils and subsoils using various techniques. Soil Biology and Biochemistry 34, 387–401.

Treseder, K.K., Marusenko, Y., Romero-Olivares, A.L., Maltz, M.R., 2016. Experimental warming alters potential function of the fungal community in boreal forest. Global Change Biology 22, 3395-3404.

Tückmantel, T., Leuschner, C., Preusser, S., Kandeler, E., Angst, G., Mueller, C.W., Meier, I.C., 2017. Root exudation patterns in a beech forest: Dependence on soil depth, root morphology, and environment. Soil Biology and Biochemistry 107, 188-197.

Uksa, M., Schloter, M., Kautz, T., Athmann, M., Köpke, U., Fischer, D., 2015. Spatial variability of hydrolytic and oxidative potential enzyme activities in different subsoil compartments. Biology and Fertility of Soils 51, 517–521.

Vance, E.D., Brookes, P.C., Jenkinson, D.S., 1987. An extraction method for measuring soil microbial biomass C. Soil Biology and Biochemistry 19, 703–707.

Van der Heijden, M.G.A., Bardgett, R.D., van Straalen, N.M., 2008. The unseen majority: soil microbes as drivers of plant diversity and productivity in terrestrial ecosystems. Ecology Letters 11, 296–310.

Větrovský, T., Steffen, K.T., Baldrian, P., 2014. Potential of cometabolic transformation of polysaccharides and lignin in lignocellulose by soil Actinobacteria. PloS one 9, e89108.

Vogel, C., Müller, C.W., Höschen, C., Buegger, F., Heister, K., Schulz, S., Schloter, M., Kögel-Knabner, I., 2014. Submicron structures provide preferential spots for carbon and nitrogen sequestration in soils. Nature Communications 5, 29-47.

Waldrop, M.P., Balser, T.C., Firestone, M.K., 2000. Linking microbial community composition to function in a tropical soil. Soil Biology and Biochemistry 32, 1837–1846.

Waldrop, M.P., Firestone, M.K., 2004. Altered utilization patterns of young and old soil C by microorganisms caused by temperature shifts and N additions. Biogeochemistry 67, 235-248.

Waldrop, M.P., Firestone, M.K., 2006. Response of Microbial Community Composition and Function to Soil Climate Change. Microbial Ecology 52, 716-724.

Wiesenberg, G.L.B., Schwark, L., Schmidt, M.W.I., 2004. Improved automated extraction and separation procedure for soil lipid analyses. European Journal of Soil Science 55, 349–356.

Will, C., Thürmer, A., Wollherr, A., Nacke, H., Herold, N., Schrumpf, M., Gutknecht, J., Wubet, T., Buscot, F., Daniel, R., 2010. Horizon-specific bacterial community composition of German grassland soils, as revealed by pyrosequencing-based analysis of 16S rRNA genes. Applied and Environmental Microbiology 76, 6751–6759.

Xiao J., He X., Hao, J., Zhou Y., Zheng L., Ran W., Shen Q. and Yu G. 2016. New strategies for submicron characterization the carbon binding of reactive minerals in long-term contrasting fertilized soils: implications for soil carbon storage. Biogeosciences 13, 3607-2618.

Zelles, L., 1999. Fatty acid patterns of phospholipids and lipopolysaccharides in the characterisation of microbial communities in soil: a review. Biology and Fertility of Soils 29, 111–129.

Zumsteg, A., Bååth, E., Stierli, B., Zeyer, J., Frey, B., 2013. Bacterial and fungal community responses to reciprocal soil transfer along a temperature and soil moisture gradient in a glacier forefield. Soil Biology and Biochemistry 61, 121–132.

Curriculum vitae

Sebastian Preußer

Personal information

Name: Sebastian Preußer

Date of birth: 14.07.1981

Place of birth: Duisburg, North Rhine-Westphalia, Germany

Marital status: Married

Nationality: German

Studies

Since 04/2013	PhD student, Institute of Soil Science and Land Evaluation, Soil Biology Section, University of Hohenheim, Stuttgart, Baden-Wuerttemberg, Germany Thesis title: “Biological Regulation of Subsoil C-cycling”
10/2005-09/2012	Studies of Biogeography (Diploma), University of Trier, Trier, Rhineland-Palatinate, Germany Thesis title: “Auswirkungen des regionalen Klimawandels auf bodenbiologische Eigenschaften“
10/2002-09/2005	Studies of Economics, University of Duisburg-Essen, North Rhine-Westphalia, Germany

Professional experience

Since 04/2013	Scientific assistant, Institute of Soil Science and Land Evaluation, Soil Biology Section, University of Hohenheim, Stuttgart, Baden-Wuerttemberg, Germany
01/2013-03/2013	Student assistant, Institute of Soil Science and Land Evaluation, Soil Biology Section, University of Hohenheim, Stuttgart, Baden-Wuerttemberg, Germany

01/2012-06/2012	Student assistant, Institute of Soil Science, University of Trier, Trier, Rhineland-Palatinate, Germany
10/2009-12/2009	Internship, Biological laboratory, Cheminova A/S, Thyborøn, Midtjylland, Denmark
09/2010-10/2010	Internship, District Government (Bezirksregierung) Düsseldorf, Department of Nature and Landscape Protection and Fisheries (Dezernat 51 Natur- und Landschaftsschutz, Fischerei), Düsseldorf, North Rhine-Westphalia, Germany
03/2009-09/2009	Student assistant, Institute of Soil Science, University of Trier, Trier, Rhineland-Palatinate, Germany
07/2001-05/2002	Military Service, German Army Base Essen, North Rhine-Westphalia, Germany

School education

2001	Higher education entrance qualification (Abitur)
08/1992-06/2001	Krupp-Gymnasium, Duisburg, North Rhine-Westphalia, Germany
08/1988-07/1992	Primary school, Duisburg, North Rhine-Westphalia, Germany

Trier, 19.11.2018

S. Preußer

(Sebastian Preußer)

Publications, Presentations and Supervisions

This PhD thesis has been prepared cumulative. Parts of this PhD thesis are published or otherwise presented as follows.

Publications and Manuscripts

Sebastian Preusser, Sven Marhan, Christian Poll, Ellen Kandeler, 2017. Microbial community response to changes in substrate availability and habitat conditions in a reciprocal subsoil transfer experiment. Soil Biology & Biochemistry 105, 138-152.

Timo Tückmantel, Christoph Leuschner, **Sebastian Preusser**, Ellen Kandeler, Gerrit Angst, Carsten W. Mueller, Ina Christin Meier, 2017. Root exudation patterns in a beech forest: Dependence on soil depth, root morphology and environment. Soil Biology & Biochemistry 107, 188-197.

Stefanie Heinze, Bernard Ludwig, Hans-Peter Piepho, Robert Mikutta, Axel Don, Patrick Wordell-Dietrich, Mirjam Helfrich, Dietrich Hertel, Christoph Leuschner, Kristina Kirfel, Ellen Kandeler, **Sebastian Preusser**, Georg Guggenberger, Timo Leinemann, Bernd Marschner, 2018. Factors controlling the variability of organic matter in the top- and subsoil of a sandy Dystric Cambisol under beech forest. Geoderma 311, 37-44.

Timo Leinemann, **Sebastian Preusser**, Robert Mikutta, Karsten Kalbitz, Chiara Cerli, Carmen Höschen, Carsten W. Mueller, Ellen Kandeler, Georg Guggenberger, 2018. Multiple exchange processes on mineral surfaces control the transport of dissolved organic matter through soil profiles. Soil Biology & Biochemistry 118, 79-90.

Sebastian Preusser, Christian Poll, Sven Marhan, Gerrit Angst, Carsten W. Mueller, Jörg Bachmann, Ellen Kandeler, 2019. Fungi and bacteria respond differently to changing habitat conditions within a soil profile. Soil Biology & Biochemistry 137, 107543.

Presentations

2014

Sebastian Preusser, Jana Niebuhr, Gerrit Angst, Stefanie Heinze, Carsten Müller, Ingrid Kögel-Knabner, Bernd Marschner, Ellen Kandeler. Depth-dependent abundance and distribution of microorganisms in forest soil. Poster presentation, European Geosciences Union General Assembly, Vienna, Austria.

Jana Niebuhr, Stefanie Heinze, Robert Mikutta, Carsten W. Mueller, **Sebastian Preusser**, Bernd Marschner. Spatial variability of microbial activity and substrate utilization patterns in top- and subsoils under European beech. Poster presentation, European Geosciences Union General Assembly, Vienna, Austria.

Stefanie Heinze, Stephan John, Kristina Kirfel, Robert Mikutta, Jana Niebuhr, **Sebastian Preusser**, Bernd Marschner. Spatial variability of soil parameters - subsoils as heterogenic environments. Oral presentation, European Geosciences Union General Assembly, Vienna, Austria.

Sebastian Preusser, Jana Niebuhr, Gerrit Angst, Stefanie Heinze, Carsten Müller, Ingrid Kögel-Knabner, Bernd Marschner, Ellen Kandeler. Depth-dependent abundance and distribution of microorganisms in forest soil. Poster presentation, Workshop on "Soil processes – is the whole system regulated at ‘hot spots’? From micro-scales to the pedon" of the German Soil Science Society, Freising, Germany.

2015

Sebastian Preusser, Christian Poll, Sven Marhan, Ellen Kandeler. Influence of substrate availability and environmental conditions on microbial communities and enzyme activities in topsoil and subsoil habitats. Oral presentation, Symposium of the SUBSOM research group, Raesfeld, Germany.

Sebastian Preusser, Sven Marhan, Christian Poll and Ellen Kandeler. Influence of substrate availability and environmental conditions on microbial communities and enzyme activities in topsoil and subsoil habitats. Oral presentation, International Conference on Soil interfaces for sustainable development (ISMOM), Montréal, Canada.

Sebastian Preusser, Jana Niebuhr, Gerrit Angst, Patrick Dietrich, Stefanie Heinze, Ellen Kandeler. Einfluss von Substratverfügbarkeit und Umweltbedingungen auf Mikroorganismengemeinschaften im Ober- und Unterboden. Oral presentation, Annual meeting of the German Soil Science Society, Munich, Germany.

Sebastian Preusser, Kristina Kirfel, Jana Niebuhr, Stefanie Heinze, Sven Marhan, Christian Poll, Ellen Kandeler. Reciprocal Soil Transfer Experiments Improve the Understanding of Biological Regulation of Subsoil C-cycling. Poster presentation, 2nd International Conference on the Ecology of Soil Microorganisms, Prague, Czech Republic.

2016

Sebastian Preusser, Christian Poll, Sven Marhan, Ellen Kandeler. Reciprocal Soil Transfer Experiments with ^{13}C-labelled Cellulose and Roots. Poster presentation, 5th International Conference on Enzymes in the Environment: Activity, Ecology, & Applications, Bangor, Wales, United Kingdom.

Sebastian Preusser, Sven Marhan, Christian Poll and Ellen Kandeler. Influence of substrate availability and environmental conditions on microbial communities and enzyme activities in subsoil habitats. Oral presentation, Workshop on Soil food webs: Linking structure, energy flux and function, Berlin, Germany

2017

Sebastian Preusser, Christian Poll, Sven Marhan, Ellen Kandeler. Carbon turnover in topsoil and subsoil: The microbial response to root litter addition and different environmental conditions in a reciprocal soil translocation experiment. Poster presentation, European Geosciences Union General Assembly, Vienna, Austria.

Ellen Kandeler, Runa Boeddinghaus, Dinah Nassal, **Sebastian Preusser**, Sven Marhan, Christian Poll. Spatial distribution of enzyme driven reactions at micro-scales. Oral presentation, European Geosciences Union General Assembly, Vienna, Austria.

Timo Tückmantel, Christoph Leuschner, **Sebastian Preusser**, Ellen Kandeler, Gerrit Angst, Carsten W. Mueller, Ina Christin Meier. Root exudation depends on soil depth, root morphology, and environment. Oral Presentation, 7th International Symposium on Physiological Processes in Roots of Woody Plants, Tartu, Estonia.

Sebastian Preusser, Christian Poll, Sven Marhan, Jörg Bachmann, Ellen Kandeler. Microbial regulation of carbon cycling in topsoil and subsoil: A reciprocal soil translocation experiment separated the response of root addition from environmental conditions. Poster presentation, 6th International Symposium on Soil Organic Matter, Harpenden, England, United Kingdom.

Sebastian Preusser, Christian Poll, Sven Marhan, Bernd Marschner, Robert Mikutta, Georg Guggenberger, Jörg Bachmann, Axel Don, Karsten Kalbitz, Ellen Kandeler. Microbial turnover of litter-derived DOC in topsoil and subsoil – Insights from a DO^{13}C switch off experiment. Poster presentation, 6th International Symposium on Soil Organic Matter, Harpenden, England, United Kingdom.

2018

Sebastian Preusser, Johannes Wirsching, Karolin Müller, Christian Poll, Sven Marhan, Bernd Marschner, Robert Mikutta, Georg Guggenberger, Jörg Bachmann, Axel Don, Karsten Kalbitz, Ellen Kandeler. Bacterial and fungal turnover of litter-derived DOC in top- and subsoil of a beech forest. Oral Presentation, 3rd International Conference on the Ecology of Soil Microorganisms, Helsinki, Finland.

Supervised Master theses

„Einfluss von Substratverfügbarkeit auf die mikrobielle Gemeinschaft im Unterboden“ (M.Sc., Mathias Bischoff)

„Untersuchung der mikrobiell angetriebenen Kohlenstoffdynamik im Unterboden eines Dystric Cambisols“ (M.Sc., Johannes Wirsching)

„The long-term development of microbial utilization of litter-derived C in a soil profile” (M.Sc., Andres Stucke)

Other student projects

Project in soil science:

„Einfluss von Substratverfügbarkeit und Umweltbedingungen auf Pilze im Ober- und Unterboden“ (Andreas Lieb)

„The long-term use of litter-derived C by the microbial biomass in a soil profile (Andres Stucke)

Acknowledgements

I would first like to thank Prof. Dr. Ellen Kandeler for her great support and guidance throughout the PhD process and the opportunity to work in the SUBSOM research group. She always found time for helpful discussions and her commitment for the Soil Biology group is outstanding. Thank you to Prof. Dr. Georg Guggenberger for co-reviewing my PhD thesis and the successful cooperation in the research group.

Special thanks to Dr. Christian Poll and Dr. Sven Marhan for their great support in data interpretation and statistical analyses as well as constructive criticism of my manuscripts. Further they created an enjoyable working environment and kept the Soil Biology group “running” (on and off the badminton court).

I would like to thank Sabine Rudolph, Heike Haslwimmer and Wolfgang Armbruster for their support in the laboratory and performing the isotopic analyses, Karolin Müller for keeping the project running during my parental leave, and the many student helpers for their help during the establishment of the field experiments and many soil samplings throughout the last years.

A big thank you goes to all my current and former colleagues at the Soil Biology group, especially Rana Shahbaz Ali, Chris Bamminger, Moritz Hallama and Robert Kahle. It always was and still is a pleasure to work with you! Many thanks also to Kathy Regan for English corrections of my manuscripts and to my colleagues at the SUBSOM group for great collaboration. Special thanks to Prof. Dr. Bernd Marschner, Dr. Stefanie Heinze, Dr. Nils Borchard and Dr. Julian Heitkötter for the coordination of the research group.

Most of all I want to thank my beloved wife Anne, my lovely daughter Ada and my parents. Anne supported me with her love and patience over all the years and made it possible for me to fulfil my dream. Ada may never know how much she supported me with her good sleep every night in writing my doctoral thesis. She makes my life complete. My parents always supported me unconditionally in my plans. I owe them everything.

Finally, thank you to the Deutsche Forschungsgemeinschaft (DFG) for funding the SUBSOM research group. The financial support made a great project possible.

Eidesstattliche Erklärung

Ich erkläre hiermit an Eides statt, dass ich die vorliegende Dissertation selbstständig angefertigt, nur die angegebenen Quellen und Hilfsmittel benutzt und inhaltlich oder wörtlich übernommene Stellen als solche gekennzeichnet habe. Ich habe noch keinen weiteren Promotionsversuch unternommen.

S. Preußer

Stuttgart, den 19.11.2018
Sebastian Preußer